

NOAA Technical Report, NWS 43



A Methodology for Updating a Conceptual Snow Model With Snow Measurements

Silver Spring, Md.

March 1990.

U.S. DEPARTMENT OF COMMERCE
National Oceanic and Atmospheric Administration
National Weather Service

NOAA TECHNICAL REPORTS
National Weather Service Series

The National Weather Service (NWS) observes and measures atmospheric phenomena; develops and distributes forecasts of weather conditions and warnings of adverse weather; collects and disseminates weather information to meet the needs of the public and specialized users. The NWS develops the national meteorological service system and improves procedures, techniques, and dissemination for weather and hydrologic measurements, and forecasts.

NWS series of NOAA Technical Reports is a continuation of the former series, ESSA Technical Report Weather Bureau (WB).

Reports listed below are available from the National Technical Information Service, U.S. Department of Commerce, Sills Bldg., 5285 Port Royal Road, Springfield, VA 22161. Prices vary. Order by accession number (given in parentheses).

ESSA Technical Reports

- WB 1 Monthly Mean 100-, 50-, 30-, and 10-Millibar Charts January 1964 through December 1965 of the IQSY Period. Staff, Upper Air Branch, National Meteorological Center, February 1967, 7 p, 96 charts. (AD 651 101)
- WB 2 Weekly Synoptic Analyses, 5-, 2-, and 0.4-Mb Surfaces for 1964 (based on observations of the Meteorological Rocket Network during the IQSY). Staff, Upper Air Branch, National Meteorological Center, April 1967, 16 p, 160 charts. (AD 652 696)
- WB 3 Weekly Synoptic Analyses, 5-, 2-, and 0.4-Mb Surfaces for 1965 (based on observations of the Meteorological Rocket Network during the IQSY). Staff, Upper Air Branch, National Meteorological Center, August 1967, 173 p. (AD 662 053)
- WB 4 The March-May 1965 Floods in the Upper Mississippi, Missouri, and Red River of the North Basins. J. L. H. Paulhus and E. R. Nelson, Office of Hydrology, August 1967, 100 p.
- WB 5 Climatological Probabilities of Precipitation for the Conterminous United States. Donald L. Jorgenson, Techniques Development Laboratory, December 1967, 60 p.
- WB 6 Climatology of Atlantic Tropical Storms and Hurricanes. M. A. Alaka, Techniques Development Laboratory, May 1968, 18 p.
- WB 7 Frequency and Areal Distributions of Tropical Storm Rainfall in the United States Coastal Region on the Gulf of Mexico. Hugo V. Goodyear, Office of Hydrology, July 1968, 33 p.
- WB 8 Critical Fire Weather Patterns in the Conterminous United States. Mark J. Schroeder, Weather Bureau, January 1969, 31 p.
- WB 9 Weekly Synoptic Analyses, 5-, 2-, and 0.4-Mb Surfaces for 1966 (based on meteorological rocket-sonde and high-level rawinsonde observations). Staff, Upper Air Branch, National Meteorological Center, January 1969, 169 p.
- WB 10 Hemispheric Teleconnections of Mean Circulation Anomalies at 700 Millibars. James F. O'Connor, National Meteorological Center, February 1969, 103 p.
- WB 11 Monthly Mean 100-, 50-, 30-, and 10-Millibar Charts and Standard Deviation Maps, 1966-1967. Staff, Upper Air Branch, National Meteorological Center, April 1969, 124 p.
- WB 12 Weekly Synoptic Analyses, 5-, 2-, and 0.4-Millibar Surfaces for 1967. Staff, Upper Air Branch, National Meteorological Center, January 1970, 169 p.

NOAA Technical Reports

- NWS 13 The March-April 1969 Snowmelt Floods in the Red River of the North, Upper Mississippi, and Missouri Basins. Joseph L. H. Paulhus, Office of Hydrology, October 1970, 92 p.
- NWS 14 Weekly Synoptic Analyses, 5-, 2-, and 0.4-Millibar Surfaces for 1968. Staff, Upper Air Branch, National Meteorological Center, May 1971, 169 p. (COM-71-50383)
- NWS 15 Some Climatological Characteristics of Hurricanes and Tropical Storms, Gulf and East Coasts of the United States. Francis P. Ho, Richard W. Schwerdt, and Hugo V. Goodyear, May 1975, 87 p. (COM-75-11088)
- NWS 16 Storm Tide Frequencies on the South Carolina Coast. Vance A. Myers, June 1975, 79 p. (COM-75-11335)
- NWS 17 Estimation of Hurricane Storm Surge in Apalachicola Bay, Florida. James E. Overland, June 1975. 66 p. (COM-75-111332)

(Continued on last page)

NOAA Technical Report, NWS 43



A Methodology for Updating a Conceptual Snow Model With Snow Measurements

Gerald N. Day

Office of Hydrology
National Weather Service
Silver Spring, Md.
March 1990.

U.S. DEPARTMENT OF COMMERCE

Robert A. Mosbacher, Sr.; Secretary

National Oceanic and Atmospheric Administration

John A. Knauss, Under Secretary

National Weather Service

Elbert W. Friday, Jr.; Assistant Administrator

PREFACE

This report is essentially a reproduction of the author's Ph.D. dissertation. The degree was obtained through the Department of Geography and Environmental Engineering, The Johns Hopkins University, Baltimore, Maryland, in October 1989.

ACKNOWLEDGEMENTS

This study was conducted at the National Weather Service Hydrologic Research Laboratory. The Colorado River Forecast Service provided partial support for the study as part of a project to improve streamflow forecasts for the Upper Colorado Basin.

The author's colleagues at the National Weather Service deserve special acknowledgement. Dr. Michael Hudlow, Dr. Danny Fread, and Dr. Richard Farnsworth, as managers in the Office of Hydrology, provided the support needed to complete the study. Dr. John Schaake and Dr. Eric Anderson provided insight that significantly influenced the direction of this research. Mr. Michael Kane gave valuable assistance and suggestions. Dr. George Smith, Dr. James Smith, and Mr. Mark Walton provided advice and encouragement. Ms. Annette Cardona performed the word processing for the dissertation, and Mrs. Virginia Radcliffe converted the dissertation into technical report format.

Dr. J. Hugh Ellis, and Dr. Jared Cohon served as dissertation advisors at The Johns Hopkins University. Their critical reviews of the research and the report are appreciated.

Other colleagues in private industry, other agencies, and universities contributed to this study. In particular, Dr. Larry Brazil provided advice and comments which, undoubtedly, improved the quality of the work.

Finally, my family provided the moral support and encouragement that was necessary to complete the study.

TABLE OF CONTENTS

	<u>Page</u>
ACKNOWLEDGEMENTS.....	iii
TABLE OF CONTENTS.....	iv
INDEX OF TABLES.....	vi
INDEX OF FIGURES.....	vii
ABSTRACT	x
 CHAPTER 1	
INTRODUCTION.....	1
Background.....	1
Research Objectives.....	2
Thesis Organization.....	3
 CHAPTER 2	
LITERATURE REVIEW.....	5
Snow Measurements.....	5
Snowmelt Models.....	6
Model Updating.....	8
Areal Estimation.....	10
Summary.....	12
 CHAPTER 3	
METHODOLOGY.....	13
Overview.....	13
Model Selection.....	15
Kalman Filter Formulation.....	20
Development of the Measurement Equation.....	25
Summary.....	31
 CHAPTER 4	
PROCEDURE DEVELOPMENT.....	33
Introduction.....	33
State-Space Model.....	33
Kalman Filter Formulation.....	42
Test Basin.....	43
Regression Approach.....	55
Regression Approach - Other Months.....	62
Regression Approach - Summary.....	66
Spatial Interpolation Approach.....	73
Spatial Interpolation Approach - Other Months.....	85
Spatial Interpolation Approach - Summary.....	104
Summary.....	110

CHAPTER 5

SUMMARY, CONCLUSIONS, AND RECOMMENDATIONS.....	111
Summary.....	111
Conclusions.....	111
Recommendations for Future Research.....	113
APPENDIX	115
REFEREMCES.....	125

INDEX OF TABLES

<u>Table</u>	<u>Page</u>
3.1 NWS Snow Model Parameters.....	16
4.1 State-Space Model Parameters.....	35
4.2 State-Space Model Variable Definitions.....	36
4.3 State-Space Model Zero-One Integer Variables.....	37
4.4 Comparison Statistics.....	40
4.5 State-Space Model Verification Statistics.....	41
4.6 Streamflow Error Statistics for the Animas (1949-1983).....	48
4.7 Snow Courses Used for the Animas Basin Analysis.....	52
4.8 Effects of Updating on the State Error Variance.....	53
4.9 Upper Subarea Regression Coefficients for April 1.....	59
4.10 Streamflow Error Statistics - Updated with Regression.....	65
4.11 Statistics for Regression Pseudo-Observed Estimates.....	67
4.12 Streamflow Error Statistics - Updated with Regression - Other Months.....	68
4.13 Station Interpolation Test Results (April 1).....	80
4.14 Streamflow Error Statistics - Updated with Interpolation...	90
4.15 Animas Basin Characteristics.....	93
4.16 Comparison for Spatial Model to Lumped Model.....	98
4.17 Statistics for Interpolated Regression Pseudo-Observed Estimates.....	106
4.18 Streamflow Error Statistics - Updated with Interpolation - Other Months.....	107

INDEX OF FIGURES

<u>Figure</u>	<u>Page</u>
3.1 Schematic for the Updating Methodology.....	14
3.2 Flowchart for the Snow Accumulation and Ablation Model.....	17
3.3 Sample Snow Cover Areal Depletion Curve.....	19
3.4 Schematic for the Sacramento Soil Moisture Accounting Model.....	21
3.5 Schematic for the Filtering Procedure.....	24
4.1(a) Upper Colorado Basin Map (b) Animas Basin with Snow Courses.....	44
4.2 Animas Basin Elevation Contours (Ft-MSL) - 1000 Ft. Contours.....	45
4.3 Animas Basin October-April Precipitation Map - 10 In. Isolines.....	46
4.4 1952 Observed and Simulated Hydrographs.....	49
4.5 1960 Observed and Simulated Hydrographs.....	50
4.6 1981 Observed and Simulated Hydrographs.....	51
4.7 Pseudo-Observed vs. Simulated Snow-Water-Equivalent (Upper Area - April 1).....	57
4.8 Pseudo-Observed vs. Simulated Snow-Water-Equivalent (Lower Area - April 1).....	58
4.9 Pseudo-Observed vs. Regression Estimated Snow-Water- Equivalent (Upper Area - April 1).....	60
4.10 Pseudo-Observed vs. Regression Estimated Snow-Water- Equivalent (Lower Area - April 1).....	61
4.11 Observed vs. Simulated Seasonal Streamflow Volumes.....	63
4.12 Observed vs. April 1 Updated (Regression) Seasonal Streamflow Volumes.....	64
4.13 1971 Frozen-Water-Equivalent <u>+</u> Standard Deviation.....	69
4.14 1980 Frozen-Water-Equivalent <u>+</u> Standard Deviation.....	70

<u>Figure</u>	<u>Page</u>
4.15	1971 Hydrographs (Regression Updated - all months).....71
4.16	1980 Hydrographs (Regression Updated - all months).....72
4.17	Function Used to Calculate Mean April 1 Snow-Water- Equivalent Map.....75
4.18	Mean April 1 Snow-Water-Equivalent Map (From Function) - 10 In. Isolines.....76
4.19	Standard Deviation Function - April 1.....78
4.20	Correlation Function - April 1.....79
4.21	1971 Standardized Deviate Field.....81
4.22	1980 Standardized Deviate Field.....82
4.23	1971 Interpolated Snow-Water-Equivalent Map - 5 In. Isolines.....83
4.24	1980 Interpolated Snow-Water-Equivalent Map - 10 In. Isolines.....84
4.25	Pseudo-Observed vs. Interpolated Snow-Water-Equivalent (Upper Area - April 1).....86
4.26	Pseudo-Observed vs. Interpolated Snow-Water-Equivalent (Lower Area - April 1).....87
4.27	Pseudo-Observed vs. Regressed Spatial Interpolated Snow-Water-Equivalent (Upper Area - April 1).....88
4.28	Pseudo-Observed vs. Regressed Spatial Interpolated Snow-Water-Equivalent (Lower Area - April 1).....89
4.29	Observed vs. April 1 Updated (Interpolation) Seasonal Streamflow Volumes.....91
4.30	Mean February 1 Snow-Water-Equivalent Map (From Spatial Melt Analysis) - 10 In. Isolines.....94
4.31	Mean March 1 Snow-Water-Equivalent Map (From Spatial Melt Analysis) - 10 In. Isolines.....95
4.32	Mean April 1 Snow-Water-Equivalent Map (From Spatial Melt Analysis) - 10 In. Isolines.....96

<u>Figure</u>	<u>Page</u>
4.33 Mean May 1 Snow-Water-Equivalent Map (From Spatial Melt Analysis) - 10 In. Isolines.....	97
4.34 Standard Deviation Function - February 1.....	99
4.35 Standard Deviation Function - March 1.....	100
4.36 Standard Deviation Function - May 1.....	101
4.37 Correlation Function - February 1.....	102
4.38 Correlation Function - March 1.....	103
4.39 Correlation Function - May 1.....	105
4.40 1971 Hydrographs (Interpolation Updated - all months).....	108
4.41 1980 Hydrographs (Interpolation Updated - all months).....	109

ABSTRACT

A Methodology for Updating a Conceptual Snow Model With Snow Measurements

Conceptual hydrologic models are used to simulate basin snow cover and to forecast streamflow in the Western U.S. Seasonal forecasts are generated months in advance to provide critical information for the efficient management of scarce water resources.

The conceptual models account for the detailed water balance of a basin and require accurate estimates of basin precipitation and temperature. The high spatial variability of precipitation in the mountains and the relatively sparse data network can lead to large uncertainties in modeling precipitation and current snow cover conditions. Snow-water-equivalent data provide information that might be used to adjust simulated snow cover conditions, in order to improve streamflow forecasts.

A methodology was developed for updating the states of a snow model with observations of point snow-water-equivalent, and it was applied using the National Weather Service snow accumulation and ablation model. A Kalman filter was used to combine estimates of the states from the model simulation with estimates from observations based on their relative uncertainties. Two approaches were tested for relating the model states to the observations using an estimate of the model state, which has been conditioned on the historical streamflow. The first approach is based on regression, whereas the second approach uses optimal interpolation to estimate snow-water-equivalent throughout the basin.

The methodology produced significant improvements in daily, monthly, and seasonal streamflow simulation. The improvements in the seasonal values were particularly dramatic, because of their magnitude and the importance of seasonal forecasts to water management. Once the methodology is incorporated into an operational forecast system, enormous benefits could be realized through more efficient water use.

Chapter 1

INTRODUCTION

Hydrologic models are used in streamflow forecasting to model snow cover states and to predict snowmelt runoff. These models are often applied on a lumped basis over areas with a wide range of snow accumulation and melt characteristics. Observations of snow-water-equivalent, i.e., the total frozen and liquid-water content of the snow cover expressed as a depth of liquid water, provide additional information about the state of the snow cover at selected points. The purpose of this research is to develop an objective methodology for extracting areal information from the point snow observations and using this information to update the states of a conceptual snow model. Improving the estimates of the model snow cover states should result in more accurate streamflow forecasts.

Background

In the Western United States, more than 70 percent of the annual water supply results from snowmelt (Barton, 1977). Forecasts of water supply are critical for reservoir flood control operations, agricultural and industrial planning, irrigation scheduling, hydropower planning, municipal water supply operations, water quality management, riverine navigation, and wildlife and recreation planning. These forecasts are needed months in advance to make decisions concerning reservoir releases, water allocation, hydropower projections, planting strategies, and manufacturing production levels. Forecasts of water supply are particularly valuable for reservoir operations. Most reservoirs are operated with the conflicting objectives of flood control and water conservation. Valuable reservoir space is left empty so that it will be available to control possible future flood waters. Reservoir operators use water supply forecasts to determine which reservoir releases must be made so as to reduce the risk of flooding to an acceptable level. If releases are not large enough, severe flooding may occur later and the potential exists for damage to spillways and possible dam failures. On the other hand, excessive releases produce unnecessary flooding, decrease hydropower benefits, and waste water that might otherwise have been conserved. Accurate forecasts and their associated uncertainties are needed to ensure proper operation of reservoirs and efficient use of the available water. Castruccio et al., (1981) estimated that a 6 percent improvement in forecasting accuracy would produce \$36.5 million in annual benefits to agriculture and hydropower in the West.

Historically, regression models have been used to predict seasonal water supply from snowmelt. This practice dates back to early in this century when Mt. Rose snow course data were used to forecast the level of Lake Tahoe. Regression procedures in use today may include baseflow, precipitation, and snow-water-equivalent as independent variables. The procedures are used from January to May to forecast seasonal water

supply. More recently, conceptual hydrologic models have been used for streamflow forecasting in the mountainous West. These models are typically applied on a lumped-area basis, and they attempt to model the processes of snow accumulation and melt and to perform soil-moisture accounting. The conceptual models provide detailed streamflow information and have the potential to produce accurate forecasts under a wide range of hydrologic conditions.

The conceptual snow models use inputs of precipitation and temperature to simulate the snow accumulation and melt processes. These models keep continuous account of variables needed to describe the snow cover e.g., snow-water-equivalent, areal cover of snow, and snow cover heat storage. The variables used by a particular model to describe conditions at some point in time are called model states. The snow cover states provide advance information about snowmelt runoff that will occur months later. Since the mid-seventies, conceptual models have been used within the National Weather Service (NWS) Extended Streamflow Prediction (ESP) procedure (Twedt et al., 1978; Curtis and Schaake, 1979; Day, 1985) to produce probabilistic snowmelt runoff forecasts. The ESP procedure depends upon reliable parameter estimates for the conceptual models, representative historical time series of mean areal precipitation and temperature, and accurate estimates of the current model states.

Model and data errors both contribute to poor estimates of model states. Model error is introduced because of our inability to represent perfectly the physical processes integrated over a basin. Even with perfect knowledge of the current states of the hydrologic system and its future inputs, our forecasts would contain errors due to our inability to describe accurately how the system evolves in time. Data errors are introduced due to measurement errors and our inability to adequately estimate meteorological inputs on an areal basis.

Observations of snow-water-equivalent are another source of information about the water balance in mountainous areas. Peck and Schaake (1989) showed that the seasonal deviation from the long-term mean winter precipitation can be highly correlated over large distances in the mountains. These snow-water-equivalent observations, which are a measure of winter precipitation, provide information about the snow-water-equivalent throughout the basin that could be used to improve the estimates of snow model states (Colbeck et al., 1979). Objective procedures are presently lacking, however, to incorporate these snow data into the conceptual snow models.

Research Objectives

The purpose of this research is to develop a methodology for incorporating snow-water-equivalent measurements into a conceptual snow model to improve snowmelt forecasts. The specific objectives of the study are:

1. To provide a review of the literature on snowmelt simulation, updating of hydrologic model states, and spatial interpolation of hydrometeorologic variables.

2. To develop an approach for extracting areal information from point snow-water-equivalent observations.
3. To use estimation theory to develop an objective methodology for updating the snow model states based on the relative uncertainties of the model simulated states and the states estimated from snow observations.
4. To demonstrate the methodology by assessing its effect on streamflow simulation on a test basin.

Thesis Organization

The remainder of the thesis is organized into four chapters. Chapter 2 is a review of the relevant literature on snowmelt models, updating, and spatial interpolation. The methodology is presented in Chapter 3. This presentation includes a discussion of the theoretical basis of the methodology and an outline of how it is applied. Chapter 4 develops the details of the approach and presents the results from an application to a test basin. A summary of the work, conclusions, and recommendations for future research are included in Chapter 5.

Chapter 2

LITERATURE REVIEW

Snow Measurements

Circa 1909, Dr. James E. Church of the University of Nevada developed the Mt. Rose sampler for collecting snow data (State of California, 1971). Church was interested in gathering information on the effects of mountains and forests on the accumulation of snow. His technique consists of inserting a hollow tube into the snow cover, removing the tube and its contents, and weighing the contents to determine the water-equivalent of the snow. Ten to fifteen measurements are taken at 50 to 100 foot intervals along a line called a snow course, and the measurements are averaged to produce a single snow-water-equivalent value for the snow course. Estimates based on the Mt. Rose sampler consistently overestimate the actual water-equivalent by 7 to 12 percent (Linsley et al., 1975). Snow courses are clearly marked, so that measurements can be taken along the same line each year. A discussion of the factors to be considered in locating snow courses is given by Codd and Work (1955). It is important to note that snow courses provide a measure of snow accumulation, but they were not intended to provide an accurate estimate of actual basin snow-water-equivalent.

Snow courses were first formally measured in 1910 near Lake Tahoe (California, 1971). Interest by power companies, irrigation authorities, and municipalities in the rise of Lake Tahoe due to snowmelt led to the use of snow survey data in forecasting the lake level. The water-equivalent of the snow cover on Mt. Rose was found to be significantly correlated with the rise of Lake Tahoe. Lake level forecasts improved when additional snow courses were added to the forecast relationship. Other techniques for collecting snow data have been developed, but the Mt. Rose sampler developed by Church is still commonly used to measure snow course snow-water-equivalent. The Soil Conservation Service (SCS) of the U.S. Department of Agriculture has the responsibility for coordinating the Cooperative Snow Survey Program in the Western U.S., excluding California. As part of this program, snow-water-equivalent is measured at over 1800 snow courses each month during the late winter and early spring (Palmer, 1988). These snow course measurements are used as an index of the water-equivalent of the snow cover and to help to predict runoff.

In an attempt to provide more timely and more frequent data, the SCS began a program in the mid-1960's to develop and test new sensors. In 1978, the SCS began receiving hydrometeorological data from remote sensors through the SNOTEL (snowpack telemetry) system (Schaefer, 1982), which now consists of almost 600 sites. The system uses meteorburst communication to relay sensor measurements to master polling stations, which relay the data across land lines to a central site. The primary

sensors at the remote sites measure snow-water-equivalent, temperature, and precipitation. Pressure pillows are used to estimate snow-water-equivalent. As snow accumulates, the pressure inside the pillow increases, and pressure transducers are used to determine the weight on the pillow. In addition to problems related to malfunctions of the pressure transducer and telemetry, snow pillows sometimes underestimate the snowpack water-equivalent because of ice lenses which bridge across the pillow (Linsley et al., 1975). Non-vertical loading of the snow on the pillow can cause overestimates or underestimates of snow-water-equivalent. The major advantage of the SNOTEL system is that it provides daily data from a network of remote sensors in areas that are not easily accessible.

The National Weather Service (NWS) of the U.S. Department of Commerce began research in 1969 to develop a technique using natural terrestrial gamma radiation attenuation to measure snow-water-equivalent and soil moisture from a low flying aircraft (Carroll et al., 1985b). The NWS currently maintains an operational Airborne Gamma Radiation Snow Survey Program that includes over 1400 flight lines (Carroll and Allen, 1988). The program was designed to provide real-time snow-water-equivalent data to the NWS Forecast Offices and River Forecast Centers for use in issuing spring snowmelt flood outlooks and river and flood forecasts for the midwestern portion of the U.S. The data are also used for selected water supply forecasts issued by the NWS and for Lake Superior water supply forecasts issued by the U.S. Army Corps of Engineers. Flight lines range from 15 to 20 km long, and data are collected over a path approximately 300 m wide (Carroll et al., 1985b). The data are reported as mean areal measurements over this area.

In the Midwest, snow accumulates more uniformly than in the mountainous West because of the absence of pronounced orographic effects. In some areas, the flight lines are dense enough that snow-water-equivalent can be contoured (Carroll and Marshall, 1985a). Provided the snow accumulation is relatively homogeneous and the measurements are dense enough, a simple averaging process may give adequate estimates of basin mean areal snow-water-equivalent. Although the technique was developed for use in the Midwest, gamma data are now being collected over flight lines in the West (Carroll and Allen, 1988). Utilizing these data from mountainous areas will present the same difficulties as using point data, since the gamma data provide estimates of snow-water-equivalent over areas that are small in comparison to the total basin area.

Research is currently being conducted on the estimation of areal snow-water-equivalent from satellite data (Hall et al., 1984; and Rango, 1986). This research is very preliminary and thus far, reliable estimates of areal snow-water-equivalent from satellite data are not available.

Snowmelt Models

Regression-type models have been used to forecast water supply from snowmelt since the first Lake Tahoe forecast was made using snow-water-

equivalent measured at Mt. Rose. Kohler (1957) provides an annotated bibliography of the significant papers published from 1951 to 1956 dealing with water supply forecasting. He states that almost all of the papers reviewed used some form of correlation analysis to relate various indices of basin water storage to seasonal water supply runoff. Sufficient data are not available on an areal basis to directly determine water supply runoff from a basin water balance relationship. Regression is one way to use the available point measurements of precipitation and snow-water-equivalent, which may not adequately represent basin water balance components. Independent variables in the regression procedures may include streamflow, fall precipitation, spring precipitation, winter precipitation, and snow-water-equivalent. The dependent variable is seasonal runoff volume, typically April through July or April through September. Regression procedures are currently used throughout the forecast season, January to May, to produce seasonal water supply forecasts. The regression procedures work very well in average years, but have difficulty in forecasting years very dissimilar from the years used to develop the regression equation (Curtis and Schaake, 1979). Attempts have been made to adapt the procedures to real-time data (Huber, 1984), but the regression procedures used by operational water supply forecasting agencies have changed very little in the last 30 years.

As an alternative to the regression procedures, simulation models have been developed to attempt to model the processes of snow accumulation and ablation. The simulation models explicitly account for the magnitude and timing of the important water balance components. Snowmelt models fit into three general categories: 1) empirical temperature-driven melt factor models, which do not keep account of snow cover state variables (i.e., water-equivalent, heat deficit, liquid water, and areal coverage); 2) models that use index methods to represent heat exchange relationships, but also keep account of snow cover state variables; and 3) actual energy budget snow models that also keep account of snow cover state variables.

Models which fall into the first category are typically based on the generalized relationship:

$$M = K (T_a - T_m) \quad (2.1)$$

where, M = calculated snowmelt,

K = melt factor,

T_a = average daily air temperature, and

T_m = average daily air temperature above which melt occurs.

Numerous models based on this simple relationship appear in the literature (Linsley, 1943; U.S. Army Corps of Engineers, 1972; Bergstrom, 1975; Martinec, 1975; Charbonneau et al., 1977; Quick and Pipes, 1977; Hannaford et al., 1979; Turcan, 1981; and Sugawara, 1984). These models are strictly empirical, but they may have some parameters that can be related to watershed characteristics. Many of

the models include additional features which account for specific complexities of the snowmelt and runoff processes. Both the Martinec and Hannaford models have incorporated snow covered area into the snowmelt calculation. The Hannaford model calculates an elevation above which the watershed area is not effective in producing melt. Below this elevation, it is assumed that the snowpack is primed, i.e., isothermal at 0°C, and ready to transmit and discharge water. The Martinec model, referred to as the Snowmelt-Runoff Model (SRM), was designed to accept satellite snow covered area observations as input. SRM calculates melt over the snow covered area and uses a simple routing procedure to improve daily runoff simulation. The model by Quick and Pipes (UBC) modifies temperature in an attempt to account separately for melt due to convective heat transfer, radiant energy input, and latent heat changes. The CEQUEAU model, developed by Charbonneau et al., accounts for melt differently in forested and non-forested areas.

Models in the second and third categories are considered conceptual because they attempt to simulate individual processes. In the second category, most of the models use air temperature as an index of heat exchange at the surface of the snow cover. When the temperature is above some base temperature, surface melt is assumed to occur. Negative heat storage is retained as a model state, so that heat losses and gains can be calculated during non-melt periods. Examples of models which fit into this category are contained in Eggleston (1971), Willen et al. (1971), Anderson (1973), Leavesley (1973), and Speers et al. (1978). Air temperature has been found to be a reasonable index to heat exchange at the snow-air interface. In addition, air temperature is usually available, and generally reliable assumptions can be made about its areal variability. These models become deficient when air temperature is not a good index to the energy exchange. This occurs: 1) under clear skies with very cold temperatures (melt is underestimated); 2) with very warm temperatures and little or no wind (melt is overestimated); and 3) with high dewpoints and high winds (melt is underestimated), (Peck and Anderson, 1977).

The last category includes models which explicitly calculate the basic energy transfers of radiation, sensible heat transfer, latent heat content, and the heat content of precipitation (Anderson, 1972). Anderson (1976) describes a point energy budget snowmelt model. Other examples of models which fit into this category are NAM-II (Nielsen and Hansen, 1973) and SHE/IHDM (Morris and Godfrey, 1978). The disadvantages of models in this category are the additional data inputs required, since the data are not readily available, not easily estimated, often of poor quality, and not easily extrapolated to an areal basis.

Model Updating

The procedure of adjusting a model's states so that the model simulation reflects observations is referred to as updating. Updating techniques range from relatively simple empirically based procedures to much more complex optimal estimation techniques. An example of an empirical technique is the NWS Computed Hydrograph Adjustment Technique (CHAT) (Sittner and Krouse, 1979). In CHAT, precipitation input to a

soil-moisture accounting model is varied until the observed runoff volume matches the simulated runoff volume. The ordinates of the unit hydrograph are "warped" until the shapes of the simulated and observed hydrographs agree within some prespecified tolerance.

An optimal estimator processes measurements to produce a minimum error estimate of the state of a system by utilizing knowledge of system errors, measurement errors, and initial condition information (Gelb et al., 1974). The Kalman filter, for example, is an optimal estimator which provides a linear unbiased minimum variance estimate of a model state. The theory is developed in detail in Kalman (1960), and Kalman and Bucy (1961). The technique has been applied to problems in satellite orbit determination, submarine and aircraft navigation, and space flight (Jazwinski, 1970). In the 1970's, the Kalman filter became popular in the field of hydrology. Hino (1973) was one of the first to apply the Kalman filter to hydrologic problems, when he used it to update the parameters of a linear discharge model. Since then, many applications of the Kalman filter to water resources have appeared in the literature, e.g., Bras and Rodriguez-Iturbe (1976), Lettenmaier and Burges (1976), Szollosi-Nagy (1976), Chiu (1978), Wood and Szollosi-Nagy (1978), Bolzern et al. (1980), Kitanidis and Bras (1980a), O'Connell (1980), Cooper and Wood (1982), Bergman and Delleur (1985), Burn and McBean (1985), Mizumura and Chiu (1985), Brazil (1988), and Georgakakos et al. (1988).

Most of the hydrologic applications of the Kalman filter have dealt with the state and/or parameter estimation of linear transfer function models, e.g. unit hydrograph, autoregressive (AR) models, autoregressive moving average (ARMA) models, or autoregressive moving average models with exogenous inputs (ARMAX). These models are easily put into an adaptive framework, but because of their inability to model nonlinear processes adequately, they often require frequent updating to maintain accurate estimates of the states. The adaptive linear models are most useful when the forecast lead times are short in comparison to the response time of the watershed, the hydrologic conditions are changing slowly, and the error in the measurement of the inputs is large relative to the error in the measurement of the outputs (Kitanidis and Bras, 1980a). As the forecast lead time increases and the error in the measurement of the inputs decreases, the ability of the model to correctly simulate the natural processes becomes more important.

Kitanidis and Bras (1980a) applied the extended Kalman filter to the Sacramento soil-moisture accounting model, which is an extremely nonlinear, lumped-parameter, conceptual rainfall-runoff model. In the extended Kalman filter, nonlinear models are linearized using Taylor series expansion or statistical linearization (Bras and Rodriguez-Iturbe, 1985). The filter was used to update the Sacramento model states based on streamflow observations. The model was then used with the updated states to forecast streamflow at various lead times, and these forecasts were compared to those obtained with one of the linear adaptive models. Forecast errors were similar for very short forecast lead times, but the forecasts from the Sacramento model became increasingly more accurate than the forecasts from the linear model as the lead time increased.

Kalman filtering applications to hydrology have concentrated primarily on updating rainfall-runoff models for short-term forecasts of streamflow. In the references cited previously, only Burn and McBean (1985) and Mizumura and Chiu (1985) included snowmelt in their models. Both of these models were designed to forecast streamflow with only one day of lead time. Though the Burn and McBean model requires basin snow covered area as an input, neither model is designed to use snow-water-equivalent measurements. Leu (1988) applied a Kalman filter to a point temperature index snow model, and he updated with snow-water-equivalent, snow depth, and snow cover temperature observations. He used pattern recognition techniques to estimate the spatial distribution of snow, but the procedure has not been applied to large areas with large-scale variability.

Some attempts have been made to improve long-term streamflow forecasting accuracy in snowmelt areas using updating. One example of updating for longer-term forecasts is given by Tangborn (1978), in which a linear regression model based on the water balance concept is used. The unique aspect of Tangborn's approach is the use of part of his forecast period as a test season and the subsequent use of the streamflow forecast error in the test season to adjust the streamflow forecast for the entire forecast period.

Carroll (1978) developed a procedure to objectively incorporate snow-water-equivalent data into a conceptual snowmelt simulation model. In this procedure, a linear regression is performed between historical point snow-water-equivalent observations and the model simulated areal snow-water-equivalent state. In the updating step, a water-equivalent is calculated from the regression equation and, using an empirical relationship, weighted against the model simulated water-equivalent to determine an updated water-equivalent estimate. Limited testing indicated that the procedure improved forecasts (Carroll and Peck, 1979), but verification is difficult, since the procedure is empirical with very little statistical or conceptual basis.

Areal Estimation

A central difficulty in updating a model's states with point snow-water-equivalent observations is that most models perform snowmelt calculations on a lumped rather than on a distributed basis. The states of a lumped model represent averages over an area, so the snow-water-equivalent observations must somehow be related to the model's lumped areal snow-water-equivalent state. Conceptually, this can be viewed as two distinct transformations. The first transformation derives an estimate of the true areal snow-water-equivalent from the point observations, and the second transformation relates the areal estimate to the model areal snow-water-equivalent state. The second transformation is required because there may not be a one-to-one correspondence between the model state and the true areal snow-water-equivalent, due to inadequacies in model structure, inputs, and/or parameter estimates. A model may compensate for inadequacies by introducing a bias into one or more of its states. There is, however, no way of verifying that a model-estimated areal snow-water-equivalent

state accurately represents the true areal snow-water-equivalent, since observed areal water-equivalent data are not available.

The first transformation, converting point observations of snow-water-equivalent to an areal estimate of snow-water-equivalent, has received little attention. Johnson et al. (1982) developed a correlation area weighting scheme for combining point, line, and areal estimates of a variable, e.g., snow-water-equivalent. Each measurement is weighted based on the portion of the watershed that is correlated more highly with it than any other measurement. Correlations are partially based on judgement, since the data are usually not available to make an objective estimate. The technique has not been extended to areas where the underlying process is not homogeneous.

Although the transformation from point to areal snow-water-equivalent has received little attention, the transformation from point to areal precipitation has been researched extensively. Thiessen (1911) developed a technique that is still used today to calculate average precipitation over large areas. The technique weights each precipitation observation based on the fraction of the basin that is closer to this observation point than any other. Spatial interpolation techniques have been used to estimate point precipitation at ungaged points (Tabios and Salas, 1985). Estimated point precipitation is then integrated (or summed) to produce an estimate of the basin areal precipitation. A polynomial interpolation technique estimates the precipitation at a point as a polynomial function of the point's coordinates. The polynomial coefficients are estimated by minimizing the sum of the squared errors between the observed precipitation and the predicted precipitation. Inverse weighting represents another spatial interpolation technique commonly used to estimate mean areal precipitation. When inverse weighting is used, the rainfall at a point is interpolated as a linear combination of the observed values. The observations are weighted as an inverse function of the distance to the interpolated point. A major disadvantage of this technique is that it does not recognize potentially redundant information, e.g., when two observations are situated close together.

Another set of techniques falls under the category of optimal interpolation. This set includes the objective analysis technique developed by Gandin (1965) and the kriging technique developed by Matheron (1971). These techniques also assume that the interpolated values are linear combinations of the observations, but the coefficients are determined by minimizing the expected value of the squared difference between the interpolated value and the true value (mean squared error criterion). In order to use these methods, the spatial variability of the process, which is usually estimated from the observations, must be described. Gandin uses the spatial correlation function, and Matheron uses variograms to describe this spatial variability. Though these techniques assume the underlying process is stationary in space, an extension of kriging (universal kriging) allows a trend to be accounted for in the mean (Bras and Rodriguez-Iturbe, 1985). These techniques have been used by many researchers for the analysis of rainfall fields (Creutin and Obled, 1982; Chua and Bras, 1982; and Bastin et al., 1982).

The concepts of optimal error criteria have been extended for rainfall analysis and network design. Rodriguez-Iturbe and Mejia (1974b) showed the relationship between point and areal rainfall based on the correlation structure of the point rainfall. A multivariate point rainfall model, developed by Mejia and Rodriguez-Iturbe (1974), is able to simulate point processes with the appropriate temporal and spatial variability. A multidimensional model which was developed by Lenton and Rodriguez-Iturbe (1977a) as an extension of the point model is able to synthesize areal rainfall that preserves the correct areal covariance structure using the point covariance relationship as input. Models such as these have been used for rainfall network design (Rodriguez-Iturbe and Mejia, 1974a; Bras and Rodriguez-Iturbe, 1976a; and Lenton and Rodriguez-Iturbe, 1977b). Bras and Rodriguez-Iturbe (1976b) used a rainfall-runoff model in conjunction with a multivariate rainfall model for rainfall network design. This methodology used streamflow forecast accuracy as a criterion. Smith and Karr (1985) present a physically based space-time rainfall model intended for management and design applications. Schaake and Peck (1986) developed a methodology for analyzing data networks in mountainous areas, that accounts for the spatial variability of the long-term mean precipitation and the spatial correlation of the seasonal deviations from the long term-mean precipitation. A simple runoff model is incorporated into the methodology, so that the effect of the network configuration on streamflow forecast errors can be assessed.

The interpolation/estimation procedures that have been applied to areal precipitation estimation generally rely upon one of two fundamental criteria: 1) a network which is dense in relation to the spatial variability of the precipitation process so that the interpolation does not produce excessive errors; or 2) the ability to estimate the mean and spatial covariance of the precipitation process.

Summary

The theory and application of snow accumulation and ablation models is well documented in the literature. In addition, estimation theory has been used extensively in the updating of hydrologic models and in the analysis of precipitation data networks. Some of this work has addressed the problems encountered in applying these techniques in mountainous areas, however, very little work has been done in the spatial analysis of snow-water-equivalent data and in the incorporation of these data into snow models for large-scale basin application. This research partially fills this void by developing an objective methodology for extracting areal information from point snow-water-equivalent observations and using this information to update the states of a large-scale conceptual snow model.

Chapter 3

METHODOLOGY

Overview

When conceptual snowmelt simulation models are used in conjunction with a rainfall runoff model, they provide detailed streamflow information and have the potential of producing accurate forecasts under a wide range of hydrologic conditions. There are obstacles, however, to applying the conceptual snowmelt simulation models. They require estimates of basin precipitation and temperature, which are typically calculated from relatively sparse networks of point measurements. The interaction of atmospheric dynamics with the topography complicates the spatial variability of precipitation in mountainous areas. Furthermore, high elevation precipitation data are scarce because of the difficulty in locating and servicing gages at high elevations. These data are often a source of error because of the high winds in these areas and the effects of wind on obtaining accurate precipitation measurements (Larson and Peck, 1974). The errors in estimating precipitation at high elevations are particularly important from a water balance standpoint, since the majority of the precipitation in a basin falls at the higher elevations. Additionally, errors in temperature affect the determination of the form of precipitation, i.e., rain or snow, and the calculation of snowmelt. A reasonable estimate of the spatial distribution of temperature can be made based on a local temperature versus elevation relationship, but lapse rates may vary significantly during individual events.

Errors in model inputs, model formulation, and parameter estimates contribute to inaccurate estimates of snowmelt and snow cover states. Estimation theory provides a logical framework within which an estimate of a state variable from a model simulation can be objectively combined with one from observations, based on the relative accuracy of the estimates. The methodology described herein applies a Kalman filter to a conceptual snow model so that the snow model states can be updated based on observations of snow-water-equivalent.

Figure 3.1 shows a schematic for the updating methodology. Areal precipitation and temperature estimates are computed from the meteorological observations and input to the snow model filter, which then computes estimates of the current snow model states and their uncertainties. Similarly, snow-water-equivalent observations are processed through an objective analysis procedure to produce an estimate of the model areal snow-water-equivalent from these snow data. This estimate and its uncertainty are also input to the snow model filter and used to update the current estimates of the model states. Melt is computed using the updated states and input to rainfall-runoff and routing models, which then predict streamflow.

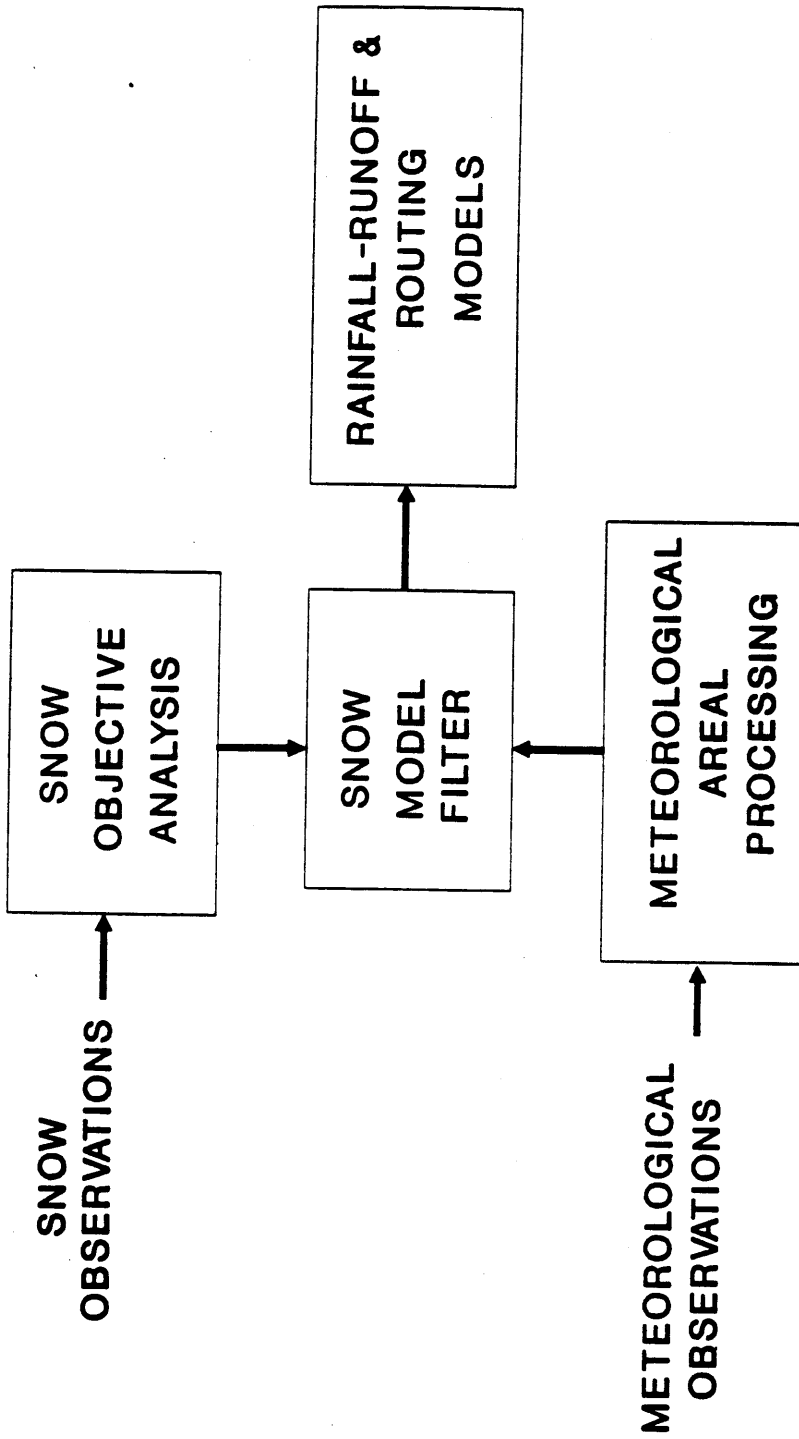


Figure 3.1 Schematic for the Updating Methodology

Model Selection

The methodology requires a snow model that keeps continuous account of the snow cover states. The National Weather Service (NWS) snow model developed by Anderson (1973) was selected for this research, because it is used operationally by the NWS in most of the West, it has been tested extensively, and it is well accepted by snow hydrologists. It was included as part of a World Meteorological Organization (WMO) snowmelt model intercomparison study (WMO, 1986). The model is conceptual and typically applied on a lumped area basis, but basins may be subdivided to minimize the effect of lumping inputs, parameters, and states over large non-homogeneous areas.

The model parameters are defined in Table 3.1, and Figure 3.2 presents a flowchart for the Anderson snow model. Precipitation and temperature are required as inputs. Air temperature is compared against the parameter PXTEMP to determine whether precipitation falls as rain or snow. Melt is calculated when the air temperature is greater than the parameter MBASE. During non-rain periods, melt is assumed to be a linear function of the difference between the air temperature and MBASE:

$$M = M_f(T_a - \text{MBASE}) \quad (3.1)$$

where, M = amount of melt (mm/6 hr),
 M_f = melt factor ($\text{mm} \cdot ^\circ\text{C}^{-1} \cdot 6 \text{ hr}^{-1}$), and
 T_a = air temperature ($^\circ\text{C}$).

M_f varies as a function of the time of year and the parameters MFMIN and MFMAX. This variation accounts for the seasonal change in incoming solar radiation and albedo.

During rain periods, several assumptions can be made that allow melt to be calculated through simplification of the energy balance equation:

$$\text{Energy available for melt} = Q_n + Q_e + Q_h + Q_g + Q_m \quad (3.2)$$

where, Q_n = net radiation transfer,
 Q_e = latent heat transfer,
 Q_h = sensible heat transfer,
 Q_g = heat transfer across the snow-soil interface, and
 Q_m = heat transfer by mass changes (advected heat)

If it is assumed that: 1) the incoming solar radiation is negligible because of overcast conditions; 2) the incoming longwave radiation is equal to blackbody radiation at air temperature; and 3) the relative humidity is 90 percent, equation (3.2) can be expressed as:

$$M = 3.67 \cdot 10^{-9} (T_a + 273)^4 - 20.4 + 0.0125 P_x T_a + \quad (3.3)$$

$$8.5 f(u^a) [(0.9e^s - 6.11) + 0.00057 P_a T_a]$$

Table 3.1

NWS Snow Model Parameters

PXTEMP	Temperature above which precipitation is assumed to be rain (°C).
SCF	Multiplying factor to correct for precipitation gage catch deficiency during periods of snowfall.
MBASE	Base temperature for melt computations during non-rain periods (°C).
UADJ	Average six-hour wind function during rain on snow events (mm/mb).
MFMAX	Maximum non-rain melt factor which occurs on June 21 ($\text{mm} \cdot ^\circ\text{C}^{-1} \cdot 6 \text{ hr}^{-1}$).
MFMIN	Minimum non-rain melt factor which occurs on December 21 ($\text{mm} \cdot ^\circ\text{C}^{-1} \cdot 6 \text{ hr}^{-1}$).
TIPM	Antecedent temperature index parameter ($0.0 < \text{TIPM} \leq 1.0$).
NMF	Maximum value of negative melt factor which occurs June 21 ($\text{mm}_e \cdot ^\circ\text{C}^{-1} \cdot 6 \text{ hr}^{-1}$). ¹
SI	Mean areal water-equivalent above which 100 percent areal snow cover always exists (mm).
PLWHC	Percent (decimal) liquid water holding capacity.
DAYGM	Daily melt at the soil-snow interface (mm).
ADC	Areal depletion curve.

¹ Note: 1 mm_e = the amount of energy per unit area required to freeze or melt 1 mm of water.

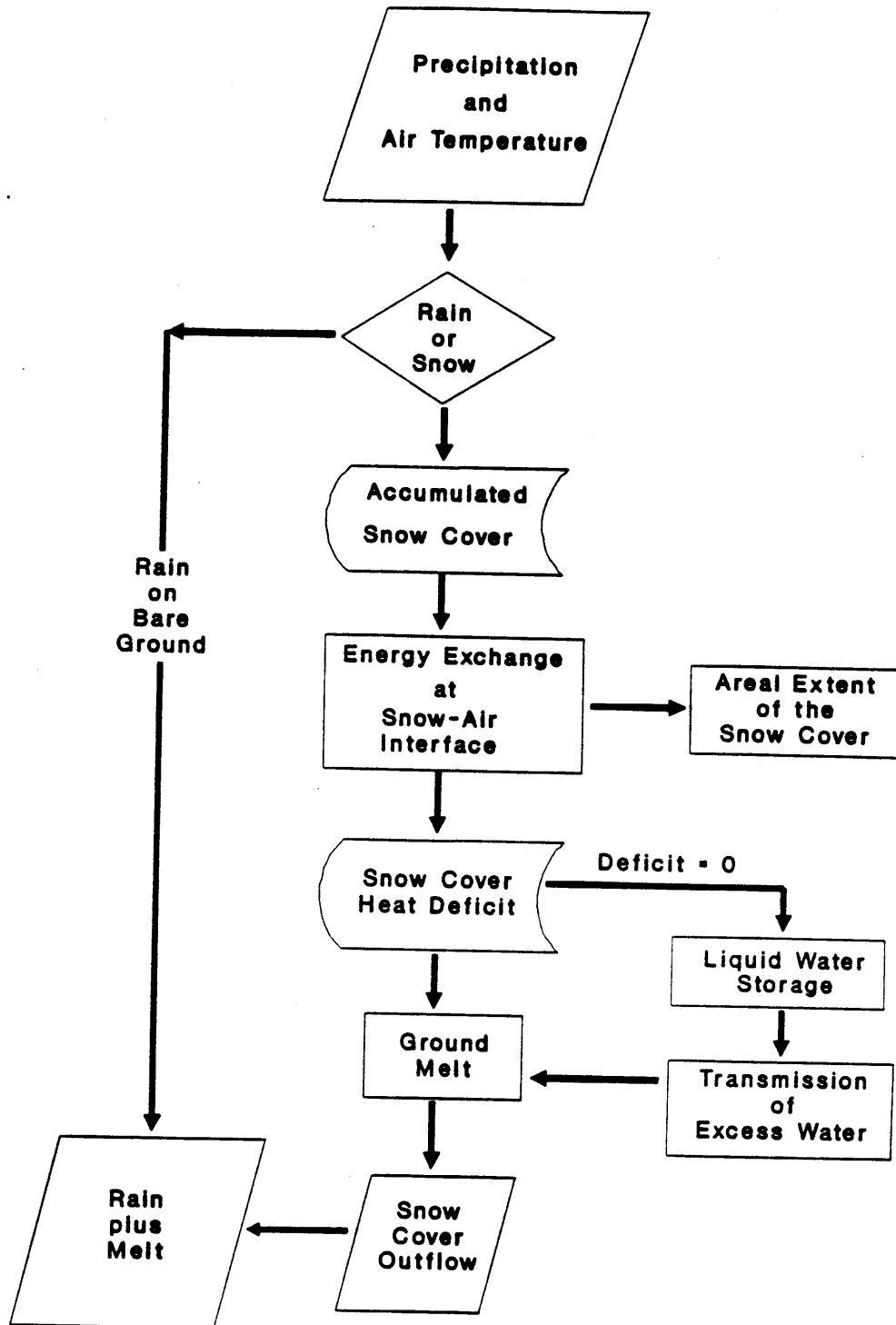


Figure 3.2 Flowchart for the Snow Accumulation and Ablation Model
 (From NWS River Forecast System User's Manual)

where, P_x = water-equivalent of precipitation (mm),
 $f(u_a)$ = function of the wind speed, u_a ($\text{mm} \cdot \text{mb}^{-1}$),
 e_s = air temperature saturation vapor pressure
 (mb), and
 P_a = atmospheric pressure (mb).

The atmospheric pressure is estimated in the model from an altitude-pressure relationship. The wind function is represented by the model parameter UADJ. Under these assumptions, the melt is reduced to a function of air temperature.

Energy is also exchanged between the snow cover and the air during non-melt periods. It is assumed that the heat exchanged during non-melt periods is proportional to the temperature gradient in the upper portion of the snow cover. The temperature at the snow surface is assumed to be air temperature, and the temperature within the snow cover is defined by:

$$TI_2 = TI_1 + TIPM \cdot (T_a - TI_1) \quad (3.4)$$

where, TI_1 = snow cover temperature index at the end of time period i ($^{\circ}\text{C}$).

The heat exchange is calculated as:

$$H = NMF \cdot \left(\frac{M_f}{MFMAX} \right) \cdot (TI_1 - T_a) \quad (3.5)$$

where, H = change in the snow cover heat deficit ($\text{mm}_e/6\text{hr}$).

(Note: 1 mm_e = the amount of energy per unit area required to freeze or melt 1mm of water.)

The model keeps continuous account of any negative heat storage that accumulates in the snow cover. This heat deficit represents the amount of heat that must be added to return the snow cover to an isothermal state at 0°C . Melt can only occur when the negative heat storage of the snow cover is reduced to zero.

As snow does not accumulate or melt uniformly in a basin, some areas become bare before others. This is important in snowmelt simulation, since the amount of melt is directly proportional to the amount of snow covered area. The model accounts for changes in the areal extent of a snow cover through an areal depletion curve, which defines the areal extent of snow cover as a function of the ratio of the current areal water-equivalent to a maximum areal water-equivalent. The maximum areal water-equivalent, A_I , is the smaller of the model parameter SI and the maximum areal water-equivalent accumulated in the current season. A sample areal depletion curve is shown in Figure 3.3. For values of water-equivalent greater than A_I , the basin is assumed to be completely covered with snow. As the water-equivalent

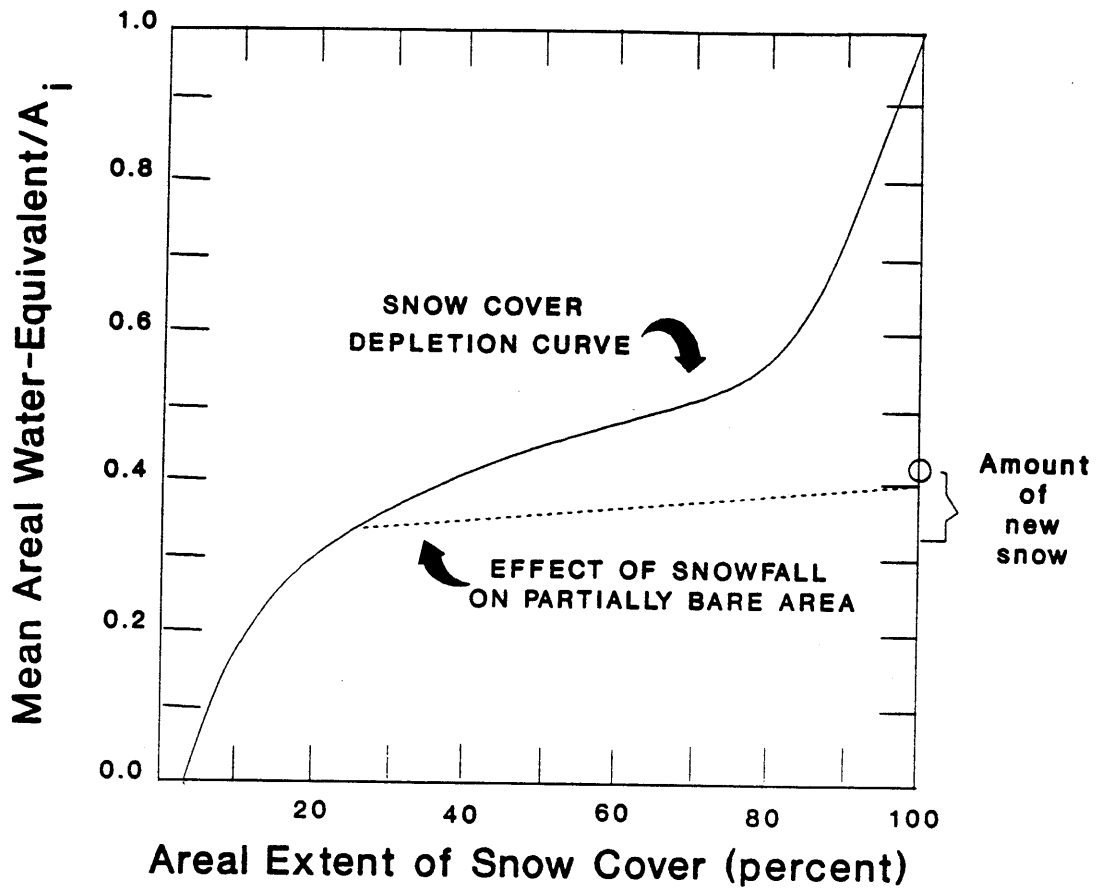


Figure 3.3 Sample Snow Cover Areal Depletion Curve
(From NWS River Forecast System User's Manual)

drops below A_I , the areal extent of snow cover is determined from the areal depletion curve. If a significant snowfall occurs when the areal extent of snow cover is less than 100 percent, the model assumes that the areal extent of snow cover is 100 percent until 25 percent of the new snow melts, and that it then returns to its original position on the areal depletion curve along the dashed line in Figure 3.3.

A snow cover can hold some liquid-water against gravity drainage. The model assumes that the maximum amount of liquid-water which can be held against drainage is a fraction of the frozen-water in the snow cover, and represents this fraction with the parameter PLWHC. Using empirical relationships, excess liquid-water is lagged and attenuated through the snow cover to simulate snow cover outflow.

It was necessary to convert the snow cover outflow to streamflow for calibration and verification of the methodology. The Sacramento soil-moisture accounting model (Burnash et al., 1973) was used to convert the snow cover outflow to runoff. The Sacramento model is one of a family of lumped, deterministic, conceptual watershed models, a schematic for which is shown in Figure 3.4. The model keeps continuous account of the contents of several soil moisture zones. The schematic shows how water moves between zones and eventually becomes runoff. The model has been used extensively by the NWS in conjunction with the Anderson snow model. It was compared against other models in a WMO rainfall-runoff model intercomparison study (WMO, 1975). The unit hydrograph procedure (Linsley et al., 1975) was used to time distribute the runoff to the basin outlet.

Kalman Filter Formulation

An optimal estimator processes measurements to produce a minimum error estimate of the state of a system by utilizing knowledge of system errors, measurement errors, and initial condition information (Gelb et al., 1974). The Kalman filter (Kalman, 1960, and Kalman and Bucy, 1961) is an optimal estimator which provides a linear unbiased minimum variance estimate of a model state. In order to apply the Kalman filter, the system and measurement dynamics must be expressed as linear functions of the model states. In discrete form, the system equation expresses the state vector at time $t+1$ as a function of the state vector at time t and any external driving forces. The measurement equation relates the state vector to the observations. Numerous sources describe the formulation and derivation of the filter equations (Gelb et al., 1974, and Jazwinski, 1970). The discrete form of the Kalman filter is:

System Equation

$$x_t = \phi_{t-1} x_{t-1} + G_{t-1} u_{t-1} + \Gamma_{t-1} w_{t-1} \quad (3.6)$$

Measurement Equation

$$z_t = H_t x_t + v_t \quad (3.7)$$

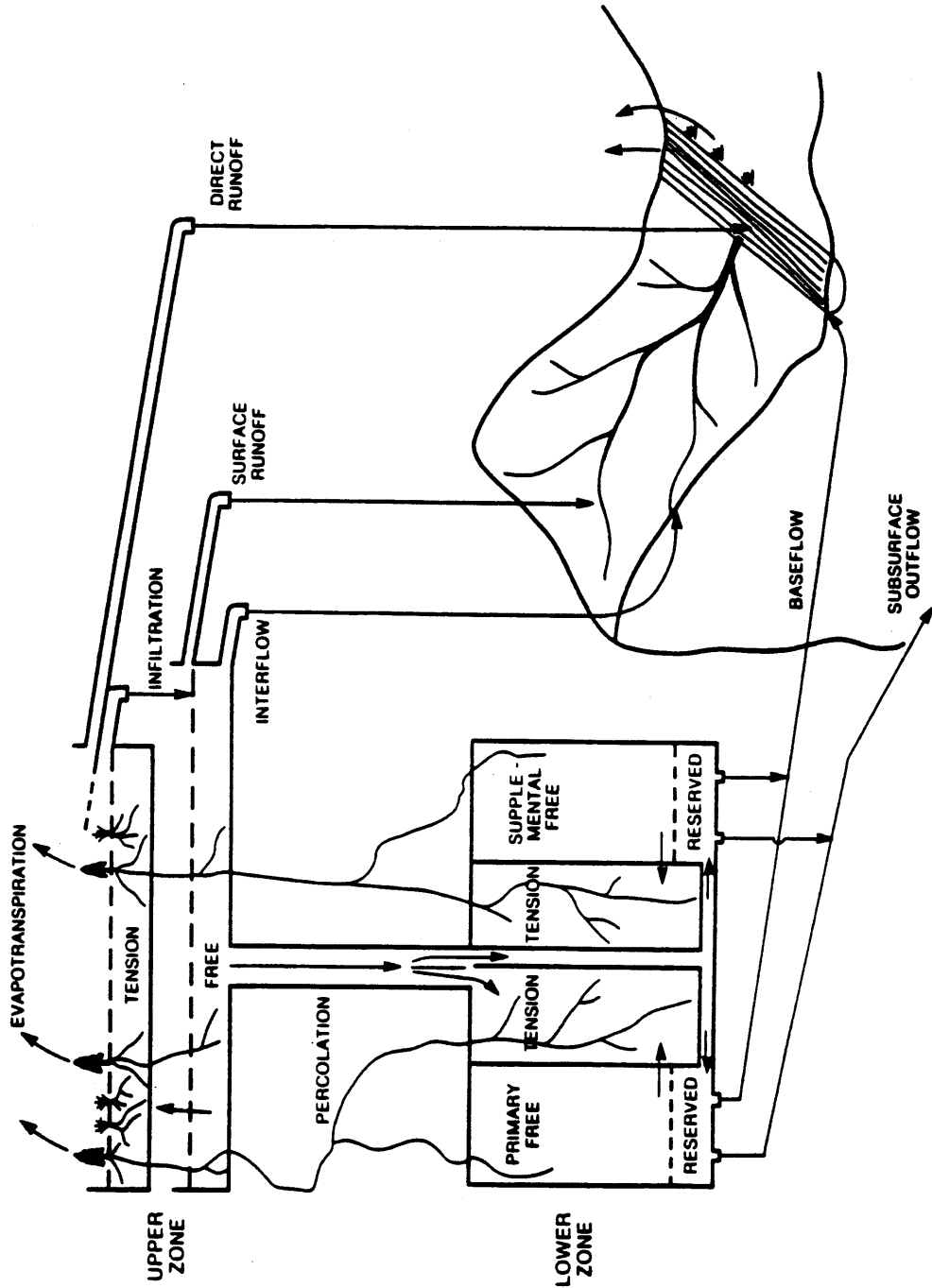


Figure 3.4 Schematic for the Sacramento Soil Moisture Accounting Model
(From Lawson and Shiau, 1977)

where, x_t = state vector at time t, (n x 1)
 z_t = measurement vector at time t, (m x 1)
 u_t = input vector at time t, (r x 1)
 w_t = system noise vector at time t, (p x 1)
 v_t = measurement noise vector at time t, (m x 1)
 ϕ_t = system transition matrix at time t, (n x n)
 G_t = input weighting matrix at time t, (n x r)
 Γ_t = system noise weighting matrix at time t, (n x p)
 H_t = state/observation weighting matrix at time t, (m x n).

System and measurement noise are assumed to be independently and identically distributed Gaussian random variables with the following properties:

$$E(w_t) = 0,$$

$$E(v_t) = 0,$$

$$E(w_t w_k^T) = Q \delta_{tk},$$

$$E(v_t v_k^T) = R \delta_{tk},$$

$$E(w_t v_k^T) = 0 \text{ for all } t, k,$$

where, Q = system error covariance matrix,

R = measurement error covariance matrix, and

δ_{tk} = Kronecker delta function, such that $\delta_{tk} = 1, t = k,$
 $\delta_{tk} = 0, t \neq k.$

The solution to the filter can be derived by assuming that the optimal estimator is a linear combination of the optimal state estimate before an observation and of the observation itself. The requirements that the estimator be unbiased and possess minimum variance lead directly to the solution:

$$\hat{x}_{t+1/t} = \phi_t \hat{x}_{t/t} + G_t u_t \quad (3.8)$$

$$P_{t+1/t} = \phi_t P_{t/t} \phi_t^T + \Gamma_t Q_t \Gamma_t^T + G_t U_t G_t^T \quad (3.9)$$

$$K_{t+1} = P_{t+1/t} H_{t+1}^T (R_{t+1} + H_{t+1} P_{t+1/t} H_{t+1}^T)^{-1} \quad (3.10)$$

$$\hat{x}_{t+1/t+1} = \hat{x}_{t+1/t} + K_{t+1} (z_{t+1} - H_{t+1} \hat{x}_{t+1/t}) \quad (3.11)$$

$$P_{t+1/t+1} = (I - K_{t+1} H_{t+1}) P_{t+1/t} \quad (3.12)$$

where, $\hat{x}_{t/s}$ = estimate of state vector at time t,
 given information at time s, (n x 1)
 $P_{t/s}$ = state estimate error covariance matrix at time t,
 given information at time s, (n x n)
 U_t = input noise covariance matrix, (r x r)
 K_t = Kalman gain matrix at time t, (n x m)
 I = identity matrix, (n x n).

A schematic diagram of the filtering procedure is shown in Figure 3.5. The filter is used to forecast the states and their error covariance matrix given observations up to time period t. Observations are made for time period t+1, the Kalman gain is calculated, and the states are updated for time period t+1 given observations up to time period t+1. The state error covariance matrix is updated, the time is incremented, and the procedure is repeated for the next time period.

As the Anderson snow model is extremely nonlinear, the Kalman filter can not be directly applied. The extended Kalman filter, however, allows a nonlinear system to be linearized about some nominal state vector, which is usually selected to be the current estimate of the conditional mean of the state vector. System state-space equations are usually written in the form:

$$\frac{dx}{dt} = f(x,u) \quad (3.13)$$

where x is the state vector and u is the vector of inputs. In this case, the equations were written in integral form:

$$f_i = \int_t^{t+1} \frac{dx}{dt} \quad (3.14)$$

where f_i is the integrated state-space equation for state i. First-order Taylor series approximations were then made for the integrated state-space equations to produce the following linear equation:

$$x_{t+1} - x_t = A_t x_t + B_t u_t + C_t \quad (3.15)$$

where A_t and B_t are (n x n) constant matrices at time t and C_t is a (n x 1) constant vector at time t. A_t , B_t , and C_t are recalculated at each time step. In practice, the complete nonlinear state-space

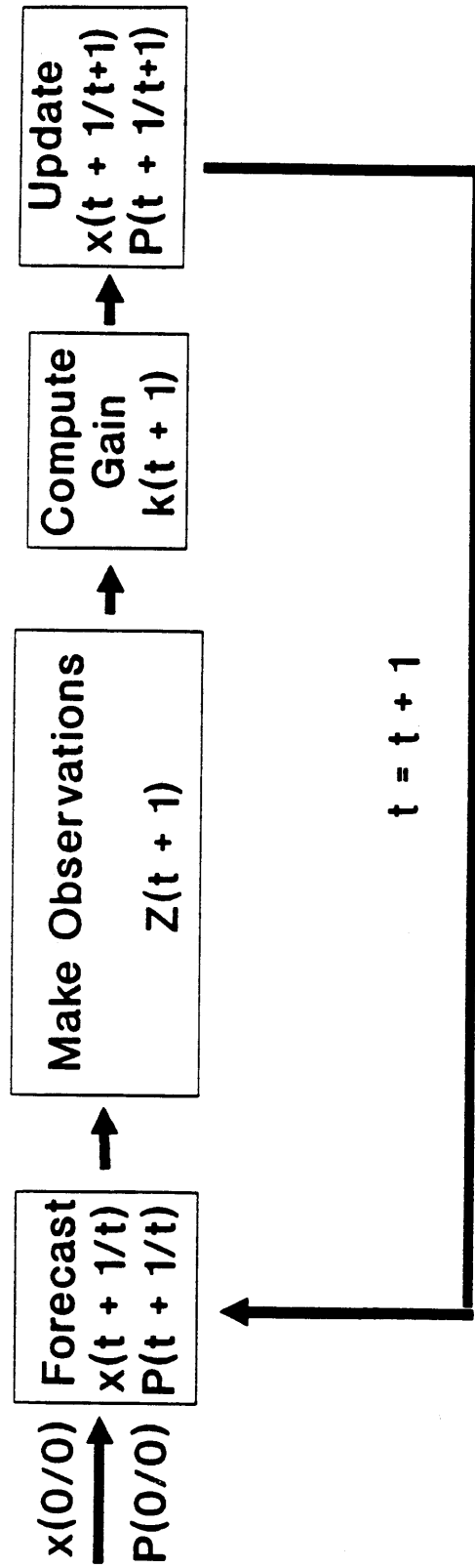


Figure 3.5 Schematic for the Filtering Procedure

equations are used to forecast the states, and the piecewise linearized equations are only used to propagate the state error covariance matrix.

The measurement equation (3.7) is also shown as a linear function of the states. The measurements in this case are snow course measurements of snow-water-equivalent. These measurements are combined external to the filter to form a single observation, z_t , of the model snow-water-equivalent states. H_t is simply a vector denoting the locations corresponding to the frozen and liquid-water-equivalent states.

Development of the Measurement Equation

The measurement equation requires forming an observation of the model snow-water-equivalent from the snow course measurements. The model states represent averages over a large area, but there is no guarantee that the model water-equivalent states would correspond to the true water-equivalent over the area, if the true areal water-equivalent could somehow be measured. Thus, how can a sparse network of snow course measurements be used to estimate the model snow-water-equivalent states?

An approach developed as part of this research takes advantage of the fact that streamflow observations provide information about precipitation and snow cover integrated over a basin. One of the most important forecasts generated in the West is the seasonal streamflow volume forecast for water supply. Errors in the seasonal volume forecasts result from errors in the model states, errors in the mean areal precipitation and temperature inputs, and inaccuracies in the models themselves. Once most of the snow has fallen, much of the volume error is due to inaccurate estimates of model snow-water-equivalent. Historical optimal estimates of model snow-water-equivalent can be made by adjusting the snow-water-equivalent states until the model simulates the proper seasonal volume. These estimates are called pseudo-observed states, and they represent our best estimates of the true model states conditioned on our knowledge of the historical seasonal streamflow volumes.

Given an historical record of pseudo-observed states for some date, e.g., April 1, and an historical record of snow course measurements for the same date, it is possible to develop a regression equation that estimates the pseudo-observation as a function of the snow course measurements. A linear relationship was assumed between the pseudo-observed state and the snow course measurements:

$$P.O. = \sum_{i=1}^n c_i x_i + c_0 \quad (3.16)$$

where, P.O. = pseudo-observation for April 1,
 c_1 = coefficient for snow course 1,
 c_0 = constant,
 x_1 = April 1 measurement for snow course 1, and
 n = number of snow course sites.

The coefficients are estimated from the historical data, so that the equation can be used in real-time to transform the snow course measurements into an observation, z_t . Different equations were developed for different times of year. The major disadvantage of the regression-based procedure is that an historical record of snow course measurements is required in order to estimate the coefficients. If a new station is added to the network, it can not be used in the procedure until many years of data are available.

A second procedure was developed that does not require a long historical record for estimation of the coefficients. The procedure is a spatial interpolation approach that was first applied to meteorological fields by Gandin (1965). It is assumed that a value in the field can be estimated as a linear combination of the observations:

$$\hat{Y}(x_0) = \sum_{j=1}^n \lambda_j y(x_j) \quad (3.17)$$

where, $\hat{Y}(x_0)$ = estimate of the process Y at location x_0 ,
 n = number of observation locations,
 λ_j = weight to be applied to observation j, and
 $y(x_j)$ = observation of process at location x_j .

The field is usually assumed to be statistically homogeneous and isotropic with a mean of zero, but the procedure can be adapted for more complicated fields. The procedure can also account for observation errors, but it is assumed here that the observation errors are zero. Mathematically, the problem can be expressed in terms of a state model, which defines the assumptions made about the process, and a data model, which defines the relationship between the process and the observations.

State Model

Y is a random process

$E[Y(x)] = 0$, where x represents location

$VAR[Y(x)] = VAR[Y]$ for all x

$COV(Y(x_i), Y(x_j)) = \rho(x_i, x_j) \cdot VAR(Y)$

where $\rho(x_i, x_j) = \rho(x_i - x_j)$ = correlation coefficient
 between two points $(x_i - x_j)$ apart.

Data Model

$$y(x_i) = Y(x_i)$$

The estimation error is given as:

$$e = Y(x_0) - \hat{Y}(x_0) = Y(x_0) - \sum_{j=1}^n \lambda_j y(x_j) \quad (3.18)$$

The technique is an optimal interpolation technique because the weights are derived by minimizing the error variance.

$$\begin{aligned} \text{VAR}(e) = \text{VAR}(Y) - 2 \sum_{j=1}^n \lambda_j \text{COV}[Y(x_0), y(x_j)] + \\ \sum_{i=1}^n \sum_{j=1}^n \lambda_i \lambda_j \text{COV}[y(x_i), y(x_j)] \end{aligned} \quad (3.19)$$

$$\begin{aligned} \frac{\partial \text{VAR}(e)}{\partial \lambda_i} = -2 \text{COV}[Y(x_0), y(x_i)] \\ + 2 \sum_{j=1}^n \lambda_j \text{COV}[y(x_i), y(x_j)] \quad i=1, n \end{aligned} \quad (3.20)$$

Setting $\frac{\partial \text{VAR}(e)}{\partial \lambda_i} = 0$, yields:

$$\text{COV}[Y(x_0), y(x_i)] = \sum_{j=1}^n \lambda_j \text{COV}[y(x_i), y(x_j)] \quad i=1, n \quad (3.21)$$

There are n linear equations and n unknowns. The vector of weights is computed using matrix algebra. By substituting equation (3.21) into equation (3.19) and simplifying, the error variance can be expressed as:

$$\text{VAR}(e) = \text{VAR}(Y) - \sum_{j=1}^n \lambda_j \text{COV}[Y(x_0), y(x_j)] \quad (3.22)$$

Three important characteristics of the technique (Gandin, 1965) are:

1. When the observation errors are assumed to be zero and one of the stations coincides with the point to be estimated, that station is assigned a weight of one and all of the other stations are assigned a weight of zero.
2. When all of the stations are located so far away from the point to be estimated that they are uncorrelated with it, all of the stations are assigned a weight of zero and the point is estimated as its mean.

3. When all of the stations are uncorrelated with one another, their weights reduce to their correlation coefficient with the point to be estimated.

The snow-water-equivalent field is extremely variable in both space and time. If, however, the mean and variance can be estimated, the field can be transformed into a field of standardized deviates.

$$z_{ij} = \frac{x_{ij} - \bar{x}_j}{S_j} \quad (3.23)$$

where, z_{ij} = standardized deviate for year i at location j ,
 x_{ij} = snow-water-equivalent for year i at location j ,
 \bar{x}_j = mean snow-water-equivalent at location j , and
 S_j = standard deviation of snow-water-equivalent at location j .

If the correlation structure of the field is known, the equations above can be used to interpolate the field of standardized deviates. The interpolation procedure can be outlined as:

1. Obtain snow-water-equivalent measurements.
2. Transform measurements into standardized deviates.
3. Interpolate standardized deviates at each grid point.
4. Transform grid point standardized deviates into snow-water-equivalent estimates.

Since the true areal water-equivalent may not correspond to the pseudo-observed state, some adjustment is needed for the interpolated water-equivalent values before they can be used to update the model states. Linear regression was used to develop a relationship between the pseudo-observed state and the estimated areal snow-water-equivalent from the interpolation procedure.

$$P.O. = C_1 \frac{\sum_{i=1}^m \hat{Y}(x_i)}{m} + C_0 \quad (3.24)$$

where, C_0, C_1 = constants,
 m = number of grid points in the subarea, and
 $\hat{Y}(x_i)$ = estimated snow-water-equivalent at grid point i .

The spatial interpolation procedure provides an approach that also estimates the pseudo-observed state as a linear combination of the observations, but it offers several advantages over the regression-based approach. It provides an estimate of the snow-water-equivalent at all of the grid points based only on snow measurements. In addition, long historical records are not required for all of the stations in the network, and changes to the network do not necessitate deriving new equations. As stations are removed from the network, the estimation

error will increase, but the same equations are valid. Conceptually, the interpolation approach is appealing because it provides a statistical framework for estimating station weights, that could be extremely useful in network design.

The interpolation procedure was used for different months throughout the snow accumulation and ablation season. The procedure required estimation of the mean and variance of the field, as well as the correlation structure of the standardized deviates for each month. The mean of the field was estimated in two ways. Precipitation maps for the period October through April are available for large portions of the West. Peck and Brown (1962) showed a relationship between the ratio of October through April precipitation to April 1 snow-water-equivalent and latitude and elevation for stations in Utah. This type of a relationship provided a basis for estimating the mean snow-water-equivalent field during the snow accumulation season given October through April precipitation.

After April 1, melt occurs in many areas, and the spatial variability of melt has a significant effect on the field of snow-water-equivalent. A procedure was developed to derive mean snow-water-equivalent fields throughout the snow accumulation and ablation season. This procedure uses the snow model to determine the spatial variability of melt. Each model subarea is divided into zones based on aspect, forest cover, and elevation, and the snow model is applied to each zone to determine the amount of melt that would occur provided there was snow. It is assumed that the major difference from zone to zone is the melt rate on clear days, and this difference in melt rates is accounted for by adjusting the model maximum and minimum melt factors. Zones were classified into three aspect categories: north, south, and horizontal. East and west aspects were included with horizontal, since all three receive equivalent amounts of solar radiation when the radiation is integrated over a day. Based on information published by the Corps of Engineers (1956), it was assumed that the ratio of a melt factor on a north-facing slope to that on a horizontal surface is 0.7 and the ratio of a melt factor on a south-facing slope to that on a horizontal surface is 1.2. These values are a function of season and latitude, but these assumptions are realistic for much of Colorado and Utah for the major part of the snowmelt season. Forested areas were distinguished from non-forested areas in the zone classification scheme. Kuusisto (1984) cited research by Kuzmin that showed how melt rates varied as a function of forest canopy density. These results indicate that a canopy density of 30 percent produces a ratio of the melt factor in a forested area to that in a non-forested area of 0.7. It was assumed that the melt factors used for the subareas in the lumped model would be reasonable first approximations for the melt rates for horizontal, non-forested zones in the subarea. Since all of the zone melt factors were related to the melt factors for horizontal, non-forested zones, the melt factors assigned to horizontal, non-forested zones could then be adjusted until the proper amount of melt was simulated over the subarea. The subarea temperature time series was lapsed to the appropriate zone elevation, and six hour melt calculations were performed for each zone for each year of record.

Monthly snow accounting was performed for each grid point taking into account the grid point precipitation and the melt from the appropriate zone. The monthly snow-water-equivalent was computed from:

$$SWE_{i+1} = SWE_i + SF_i - ZM_{ij} \quad (3.25)$$

where, SWE_i = grid point snow-water-equivalent at the beginning of month i ,
 SF_i = grid point snowfall during month i , and
 ZM_{ij} = snowmelt during month i for zone j , when grid point is contained in zone j .

The monthly snowfall at the grid point was estimated as:

$$SF_i = \frac{OAP_{gp}}{OAP_{sa}} \cdot ZSF_{ij} \quad (3.26)$$

where, OAP_{gp} = average October through April precipitation at the grid point,
 OAP_{sa} = average October through April precipitation for the subarea, and
 ZSF_{ij} = snowfall during month i for zone j , when grid point is contained in zone j .

These monthly calculations were performed for each historical year, and the mean snow-water-equivalent was computed at each grid point for each month. A relationship between the mean and standard deviation of the snow-water-equivalent at a point was developed based on the historical snow course observations. This relationship was used to estimate the standard deviation at each grid point given the mean at the grid point.

The correlation structure of the field is also needed before the standardized deviates can be interpolated. The correlation between the standardized deviates of each pair of stations was calculated and plotted as a function of distance. A simple correlation function of the form:

$$\rho = ae^{-bx} \quad (3.27)$$

where, ρ = correlation coefficient,
 a, b = constants, and
 x = distance between points.

was fit to these data. The interpolation procedure was tested by estimating the data at each of the snow course sites, and comparing the actual error to the predicted error. Peck and Schaake (1989) found that additional variability in the correlation between stations could be explained by including orographic precipitation as another variable in the correlation function. The Peck and Schaake correlation function was also tried on the Animas data.

Given the mean snow-water-equivalent at all of the grid points, a relationship between the mean and standard deviation of the snow-water-

equivalent, and a correlation function for the standardized deviates, the snow course measurements can be interpolated and grid point estimates of snow-water-equivalent can be made. The grid point snow-water-equivalent estimates can be averaged over the subareas to produce estimates of mean areal snow-water-equivalent. Equation (3.24) can be used to convert these values to observations of the model states.

Summary

A methodology has been presented for updating the states of a conceptual snow model. The methodology uses an extended Kalman filter to produce optimal model state estimates. Two techniques are presented for relating the snow course observations to the model state. One is based on regression and the other is an optimal interpolation technique that takes into account the correlation structure of the data.

Chapter 4

PROCEDURE DEVELOPMENT

Introduction

A methodology was presented in Chapter 3 for updating the states of a lumped conceptual snow model with point observations of snow-water-equivalent. This chapter details the development and testing of the state-space equations and the application of the Kalman filter equations. Data from the Animas Basin in Colorado is used in the development of the updating procedure and in assessing its value.

State-Space Model

The methodology presented in Chapter 3 requires the development of a system equation in order to apply the Kalman filter. The first step in the development of the system equation is to express the model in state-space form. This section describes the development of the state-space equations for the NWS snow accumulation and ablation model.

The NWS snow accumulation and ablation model is extremely nonlinear, and like many conceptual models, it makes frequent use of thresholds to indicate when the operating rules of the model change. Kitanidis and Bras (1980a) discuss two techniques for linearizing threshold functions and they use both techniques in linearizing state-space equations for the Sacramento soil-moisture accounting model. The first technique involves substituting a continuous nonlinear function for the threshold and linearizing the nonlinear function using a Taylor series approximation. The second technique is statistical linearization (Gelb et al., 1974), in which the coefficients are estimated by minimizing the error of the linear approximation to the nonlinear function. Gupta and Sorooshian (1985) observed that the thresholds used in conceptual models create a modality of behavior in the models. They treat the thresholds by writing separate state-space equations for the different operating modes of the model. The technique used here is similar to that of Gupta and Sorooshian. Zero-one integer variables were used to indicate when the model switches from one mode to another.

Nonlinear state-space equations were written for five snow model states: frozen water-equivalent, negative heat storage, liquid water-equivalent, snow cover temperature index, and areal extent of snow cover. In the original model, four states are used to describe the current areal depletion curve. The states are the maximum water-equivalent accumulated this season, the value of areal extent of snow cover where the new snow line leaves the areal depletion curve, the water-equivalent value where the new snow line leaves the areal depletion curve, and the water-equivalent value of the new snow line for 100 percent cover. In the state-space model formulation, these states are referred to as endogeneous states. They are treated as parameters that change in time. That is, they are carried along in time to describe the current areal depletion curve, but their variance is not

propagated. Any uncertainty introduced to the system through these endogeneous states is included as part of the system error term.

The areal depletion curve defines the areal extent of snow cover as a function of water-equivalent. In the state-space model, the curve is piecewise linearized at each time step. The model parameters are assigned symbols in Table 4.1 to simplify the notation. The model states, inputs, constants, and some computed variables are presented and defined in Table 4.2. The zero-one integer variables that are used to indicate the model modes are defined in Table 4.3. Snowmelt, free water, and heat exchange are defined separately in order to simplify the state-space equations.

As discussed in Chapter 3, the model calculates snowmelt differently for rain periods than it does for non-rain periods. The equations for computing melt during a 6-hour time period are given below for the two cases:

Snowmelt

During Non-rain Period --

$$M = (1 - L_{01}) [M_f (T_a - p_s) M_{01} + .0125 P_x (1 - F_s) \cdot T_a (1 - K_{10})] x_5 + L_{01} (x_1 + P_x F_s p_2 - G_m x_5) \quad (4.1)$$

During Rain Period --

$$M = (1 - L_{01}) x_5 [\sigma ([.01(T_a + 273)]^4 - 55.55) + p_4 (2.10291 \cdot 10^9 \cdot e^{-4278.63/(T_a + 242.792)} - 51.935) + .004845 P_a p_4 T_a + .0125 P_x (1 - F_s) T_a (1 - K_{01})] + L_{01} (x_1 + P_x F_s p_2 - G_m x_5) \quad (4.2)$$

Melt water and rainfall produce free water that must be absorbed or released by the snow cover. The free water that is produced during a time interval is defined as:

Free Water

$$W = M + P_x (1 - F_s) x_5 \quad (4.3)$$

The negative heat storage that accumulates in the snow cover during cold periods was also discussed in Chapter 3. The change in this negative heat storage during a 6-hour period is defined as:

Heat Exchange

$$H = (1 - N_{01}) \frac{M_f}{p_s} p_s [x_4 - H_{01} (x_4 - T_a K_{01}) - T_a K_{01}] x_5 - N_{01} x_2 - P_x F_s p_2 \quad (4.4)$$

Table 4.1
State-Space Model Parameters

<u>State-Space Notation</u>	<u>Model Parameter</u> ¹
P ₁	PXTEMP
P ₂	SCF
P ₃	MBASE
P ₄	UADJ
P ₅	MFMAX
P ₆	MFMIN
P ₇	TIPM
P ₈	NMF
P ₉	SI
P ₁₀	PLWHC
P ₁₁	DAYGM

¹ The parameters are defined in Table 3.1.

Table 4.2
State-Space Model Variable Definitions

Model States:

<u>Symbol</u>	<u>Name</u>	<u>Definition</u>
x_1	WE	Solid water-equivalent portion of the snow cover (mm)
x_2	NEGHS	Heat deficit (mm_e)
x_3	LIQW	Liquid water held against gravity drainage (mm)
x_4	TINDEX	Antecedent snow temperature index ($^{\circ}\text{C}$)
x_5	AESC	Areal extent of snow cover

Inputs:

<u>Symbol</u>	<u>Definition</u>
P_x	Precipitation
T_a	Temperature

Constants/Variables:

<u>Symbol</u>	<u>Definition</u>
σ	Stefan-Boltzman constant
S_n	Snowfall amount above which the temperature index of the snow cover is set to the air temperature.
F_s	Fraction of precipitation occurring as snow.
G_m	Groundmelt for the current time period.
T_w	Total water-equivalent.
A_I	The greater of the parameter S_I , or the maximum accumulated water-equivalent this season.
S_B	Water-equivalent value which defines the lower limit of the new snow line.
S_W	Water-equivalent value which defines the upper limit of the new snow line.

Table 4.3

State-Space Model Zero-One Integer Variables

<u>Variable</u>	<u>Definition</u>
F_{01}	= 0, If the heat deficit \leq the maximum amount of negative heat storage the snow cover can retain; = 1, otherwise.
G_{01}	= 0, If the temperature index $\leq 0^{\circ}\text{C}$, and physically realistic based on the values of the solid water-equivalent and the heat deficit; = 1, otherwise.
H_{01}	= 0, If the snowfall \leq the limit above which the temperature index of the snow cover is set to the air temperature; = 1, otherwise.
I_{01}	= 0, If the liquid water $>$ the maximum amount of liquid water that can be held in the snow cover; = 1, otherwise.
J_{01}	= 0, If (the heat deficit + the heat exchange) \geq free water; = 1, otherwise.
K_{01}	= 0, If the air temperature $\geq 0^{\circ}\text{C}$; = 1, otherwise.
L_{01}	= 0, If the snowmelt $<$ amount of frozen water available; = 1, otherwise.
M_{01}	= 0, If the air temperature \leq MBASE; = 1, otherwise.
N_{01}	= 0, If the change in heat storage is greater than the amount needed to bring the heat deficit to 0; = 1 otherwise.

The state-space equations were written in the integral form defined in equation (3.14). The equations represent the change in each state over a 6-hour period.

The change in the frozen-water-equivalent state for the time period is defined as:

Frozen Water-Equivalent

$$f_1 = P_x F_s p_2 - G_m x_5 - M + W + (x_2 + H - W) J_{o1} \quad (4.5)$$

The change in the negative heat storage state for the time period is defined as:

Negative Heat Storage

$$f_2 = [H - W - J_{o1}(x_2 + H - W)] (1 - F_{o1}) \quad (4.6)$$

$$+ F_{o1}[0.33(x_1 + f_1) - x_2]$$

The change in the liquid water-equivalent state for the time period is defined as:

Liquid Water-Equivalent

$$f_3 = -I_{o1} \frac{x_3}{x_1} G_m x_5 + J_{o1} I_{o1} (W - x_2 - H) \quad (4.7)$$

$$+ (1 - I_{o1}) [p_{1o} (x_1 + f_1) - x_3]$$

The change in the temperature index state for the time period is defined as:

Temperature Index

$$f_4 = [-H_{o1} (x_4 - T_a K_{o1}) + p_7 (x_4 - T_a) (H_{o1} - 1)] \quad (4.8)$$

$$\cdot (1 - G_{o1}) - G_{o1} x_4$$

The change in the areal extent of snow cover for the time period is defined for the four possible types of positions on the areal depletion curve. In the case where the snow cover is above the areal depletion curve, it is assumed that the areal extent of snow cover is 100 percent with complete certainty. In the other cases, it is assumed that the areal extent of snow cover state varies linearly with total water-equivalent for the time period. The change in the areal extent of snow cover state for the time period is defined as:

Areal Extent of Snow Cover

Case 1 ($T_w \geq A_I$) snow cover is above the areal depletion curve --

$$f_s = 1 - x_s \quad (4.9)$$

Case 2 ($T_w \leq S_B$) snow cover is following the areal depletion curve --

$$f_s = C_1 \Delta T_w \quad (4.10)$$

where, C_1 = average rate of change over the time period in areal extent of snow cover with respect to total water-equivalent, and

ΔT_w = change in total water-equivalent.

Case 3 ($T_w > S_B$) and ($T_w \geq S_w$) snow cover is 100% because of new snow --

$$f_s = C_1 \Delta T_w \quad (4.11)$$

Case 4 ($T_w > S_B$) and ($T_w < S_w$) snow cover is on the new snow line --

$$f_s = C_1 \Delta T_w \quad (4.12)$$

Results from the nonlinear state-space equations compared very closely with results from the original model. Values of the states and other model computed values were output at a six-hour time step for both the state-space model and the original model. Ten statistics, shown in Table 4.4, were computed from the output. The statistics resulting from a one-year simulation for one parameter set and one set of precipitation and temperature time series are given in Table 4.5. Different parameter sets and time series were tested to ensure that the comparison results were not limited to one basin. The results indicate that the state-space model very closely simulates the results of the original model. Several discrepancies were observed, however, when the state-space model simulations were compared to the original model simulations. Some of these observations led to changes in the original model to improve its simulation. The major reason for any remaining differences between the two models is that in the original model, the areal extent of snow cover is updated at the beginning of a time period for any snowfall that occurs during the period. In the state-space model, on the other hand, the areal extent of snow cover is updated at the end of the time period. This causes more groundmelt to be produced by the original model, since groundmelt occurs even during cold time periods which might have experienced snow. This has the effect of slightly delaying the snowmelt produced by the state-space model and causing a slight negative bias in the annual runoff. It was concluded that the differences were not significant and the state-space model formulation was accepted.

Table 4.4
Comparison Statistics

Average Error	$\frac{\Sigma(x - y)}{n}$
Absolute Maximum Error	$\text{MAX } x - y $
Average Absolute Error	$\frac{\Sigma x - y }{n}$
RMS Error	$\frac{\Sigma(x - y)^2}{n}^{1/2}$
Bias	$\frac{\Sigma(x - y)}{\Sigma y}$
Mean	$\frac{\Sigma x}{n}, \frac{\Sigma y}{n}$
Variance	$\frac{n \Sigma x^2 - (\Sigma x)^2}{n(n - 1)}, \frac{n \Sigma y^2 - (\Sigma y)^2}{n(n - 1)}$
Correlation Coefficient	$\frac{\Sigma xy - n \bar{x} \bar{y}}{n S_x S_y}$

where, x = state-space model discharge, and
 y = original model discharge.

Table 4.5
State-Space Model Verification Statistics

	<u>WE</u>	<u>NEGHS</u>	<u>LIQW</u>	<u>TINDEX</u>	<u>AESC</u>	<u>MELT¹</u>	<u>WATER²</u>	<u>HEAT³</u>	<u>GMRO⁴</u>	<u>RM⁵</u>
Average Error	0.7	0.00	0.02	0.01	0.004	0.00	0.00	0.00	-0.001	0.00
Absolute Max. Error	2.7	0.50	0.10	4.90	1.000	2.50	2.50	0.23	0.080	1.50
Average Abs. Error	0.7	0.01	0.02	0.01	0.005	0.01	0.01	0.00	0.001	0.01
RMS Error	0.8	0.03	0.04	0.22	0.059	0.08	0.08	0.01	0.007	0.06
Bias	0.0	0.00	0.01	-0.00	0.006	0.00	0.00	0.01	-0.009	0.00
Mean Y	347.2	7.87	3.61	-3.96	0.674	1.00	1.03	0.08	0.069	0.90
Mean X	347.8	7.86	3.62	-3.95	0.678	1.00	1.03	0.08	0.069	0.90
Variance Y	125450	152.2	30.68	21.39	0.194	5.60	6.07	0.12	0.000	4.26
Variance X	125610	152.2	30.70	21.41	0.192	5.60	6.08	0.12	0.001	4.26
Correlation Coef.	1.00	1.00	1.00	1.00	0.99	1.00	1.00	1.00	0.95	1.00

¹MELT = Melt(mm);

²WATER = Free Water(mm);

³HEAT = Heat Exchange(mm_e);

⁴GMRO = Ground melt runoff(mm);

⁵RM = Rain plus melt(mm)

Kalman Filter Formulation

As discussed in Chapter 3, application of the extended Kalman filter requires linear state-space equations. Linearizing these state-space equations produces an equation of the form given in equation (3.15). This equation can be rewritten as:

$$x_{t+1} = (I + A)x_t + B_t u_t + C_t \quad (4.13)$$

where, I = identity matrix.

This is the form needed for the filter and shown in equation (3.8). Using a Taylor series first order approximation, the elements of A_t and B_t are defined as:

$$A_{ij} = \frac{\partial f_i}{\partial x_j} \quad (4.14)$$

$$B_{ij} = \frac{\partial f_i}{\partial u_j} \quad (4.15)$$

The vector C_t is never defined, since the original nonlinear equations are used to propagate the states, and a constant term does not affect the propagation of the covariance matrix. The partial derivatives A_{ij} and B_{ij} are given in the Appendix. The analytical derivatives were verified by comparing them with derivatives calculated by finite differencing the state-space equations for 23 scenarios. These scenarios were designed to exercise different model components to ensure that the derivatives were correct for all of the model modes of operation.

Once the derivatives were verified, they were used in equations (3.8) through (3.12) with $\phi_t = (I + A_t)$ and $G_t = B_t$. Some tests were made with synthetic data to verify that the filter equations were working properly. The model was run and the states were output at the end of each day. The simulated states were corrupted with Gaussian noise and treated like observations. The first test used daily observations of each state to update the model states. Since the true model states and the uncertainty of the observations were known, the performance of the filter could be assessed. In one run, the model was given poor initial conditions and the updating quickly improved the estimates of the states. In another run, the model was given good initial conditions and the updating did not significantly change the state estimates, despite the noisy observations.

In reality, there will not be observations of all of the model states, but only an observation of total water-equivalent to use for updating. An updating test was made using daily observations of total water-equivalent that were corrupted with noise. During the accumulation season, most of the adjustment was made to the frozen-water-equivalent, and the liquid-water-equivalent was changed very little. During the melt season, the liquid-water content of the snow cover was at its maximum, and the adjustment was distributed proportionally between the frozen and liquid-water-equivalents, while the other three states did not change significantly.

The next set of tests used daily observations of total water-equivalent and added Gaussian noise to the precipitation and temperature inputs. This additional noise caused the water-equivalent to track more irregularly with the observed, but it remained reasonably close to the observed. This occurred even though a positive bias was created in the model simulation due to the precipitation. Gaussian noise was added to the precipitation, but the precipitation was set to zero whenever this resulted in a negative precipitation value. Since there are many periods of zero precipitation, this occurred frequently and produced a positive bias in the precipitation.

The last test with synthetic data used monthly observations of total water-equivalent and added noise to the precipitation and temperature time series. The water-equivalent states took longer to adjust because of the reduced number of observations, but the estimates of the water-equivalent states were significantly improved by the beginning of the melt season. All of the tests indicated that the filter was working properly. The next step was to test the filter with real data.

Test Basin

The Animas River at Durango, Colorado was selected as the test basin for the updating methodology. Located in Southwestern Colorado in the San Juan River Basin, the Animas, with a drainage area of 692 square miles, was considered a good candidate because of the limited irrigation and hydropower regulation that occur in the basin. Figure 4.1(a) shows the position of the Animas in the Upper Colorado Basin draining to Lake Powell, and Figure 4.1(b) shows the Animas drainage network and the locations of the snow courses used in this test. The basin ranges in elevation from approximately 6500 ft-MSL at Durango to over 13000 ft-MSL (see Figure 4.2), with a mean basin elevation of 10100 ft-MSL.

The basin was subdivided for modeling into an upper area and a lower area. One rationale for subdividing basins is to separate the part of the basin that contributes significant runoff only in extremely wet years from the part of the basin that always contributes significant runoff, since it is difficult for a lumped model to duplicate this effect otherwise. Based on the October through April precipitation map shown in Figure 4.3 and the snow cover depletion pattern observed from satellite photographs, the basin was subdivided at its mean elevation. Thirty-five years of mean areal precipitation and temperature time series were developed for the two subareas using data from twenty precipitation stations and nine temperature stations. All temperature and precipitation station data were checked to ensure consistency during the period of record.

Parameters were estimated for the snow, soil-moisture accounting, and unit hydrograph models by trial and error primarily, but some parameter fine-tuning was done using a hill climbing automatic optimization routine (Monro, 1971). The snow model parameter estimation was performed using the original snow model, and as an additional verification of the state-space model, the simulated versus observed streamflow statistics were computed for both the original model and the

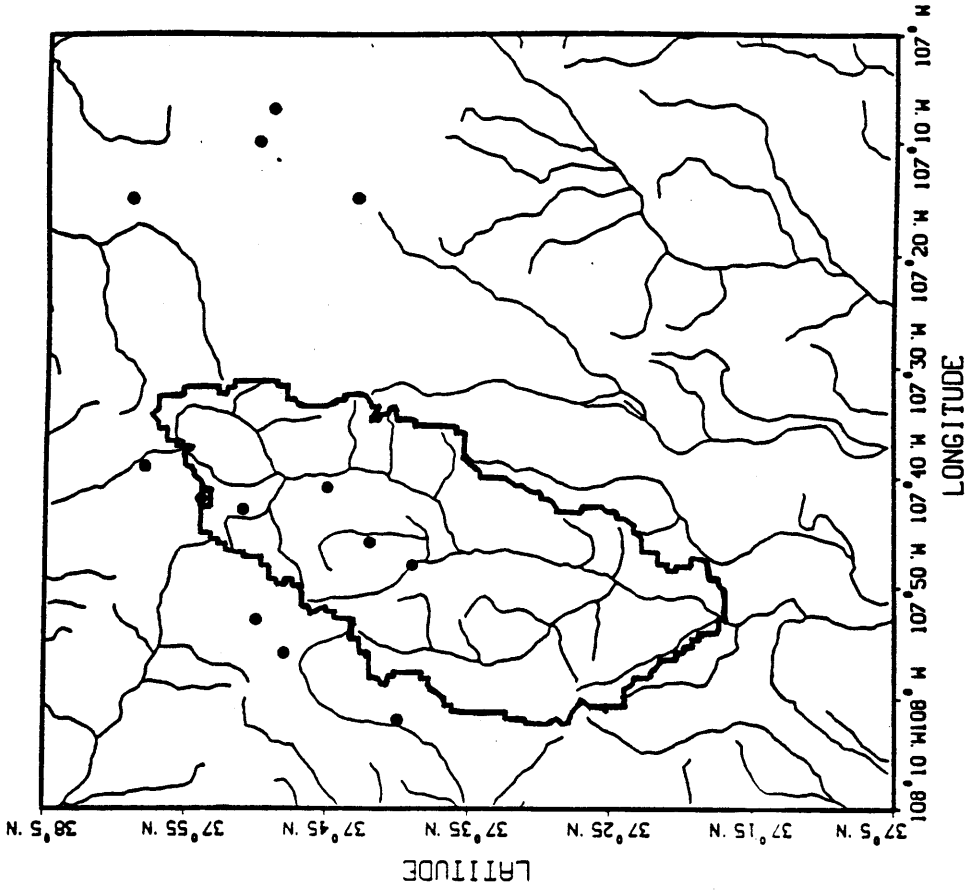


Figure 4.1(b) Animas Basin with Snow Courses

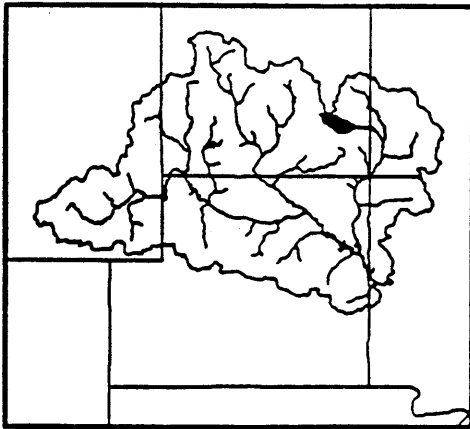


Figure 4.1(a)
Upper Colorado Basin Map

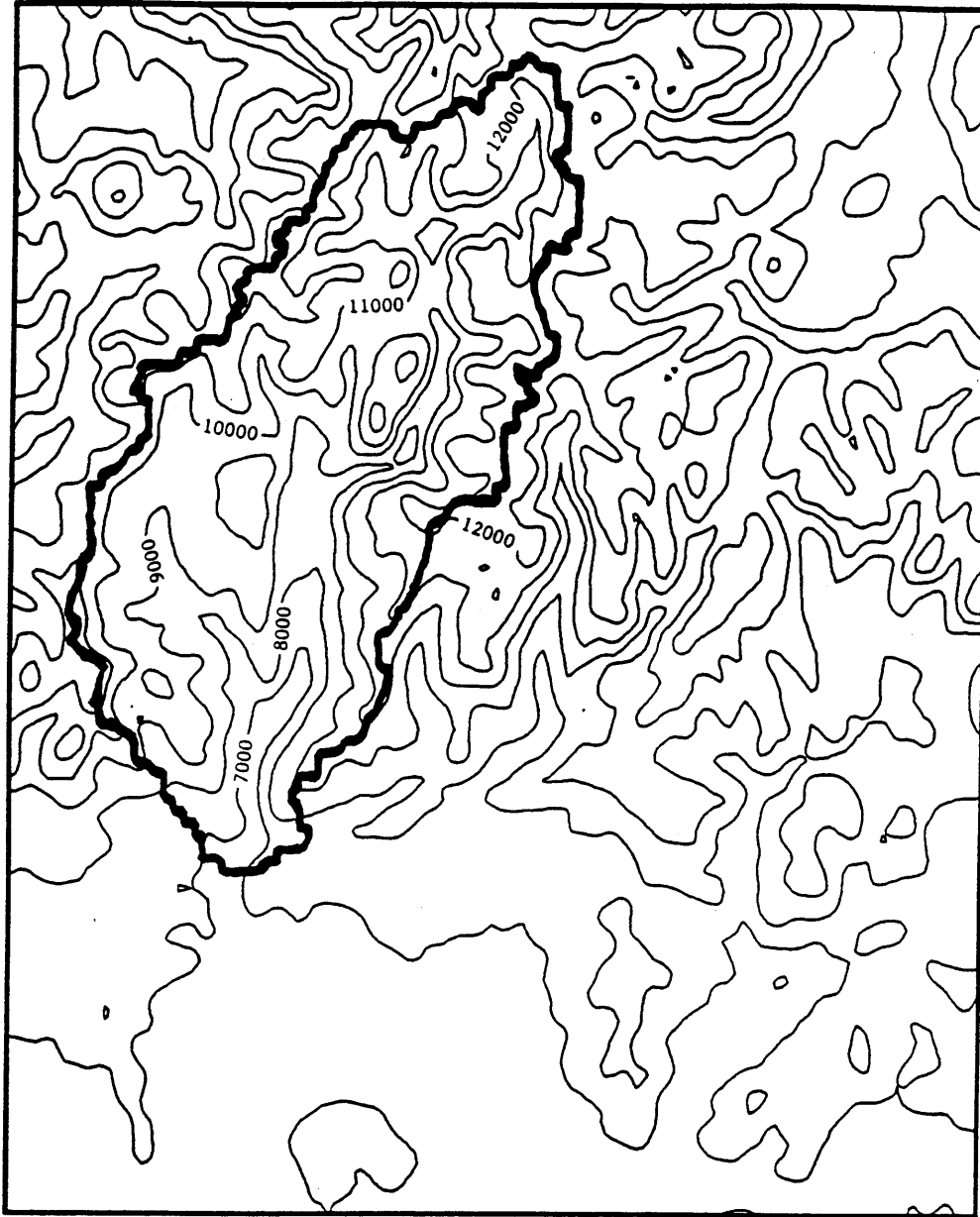


Figure 4.2 Animas Basin Elevation Contours (Ft-MSL) - 1000 Ft. Contours

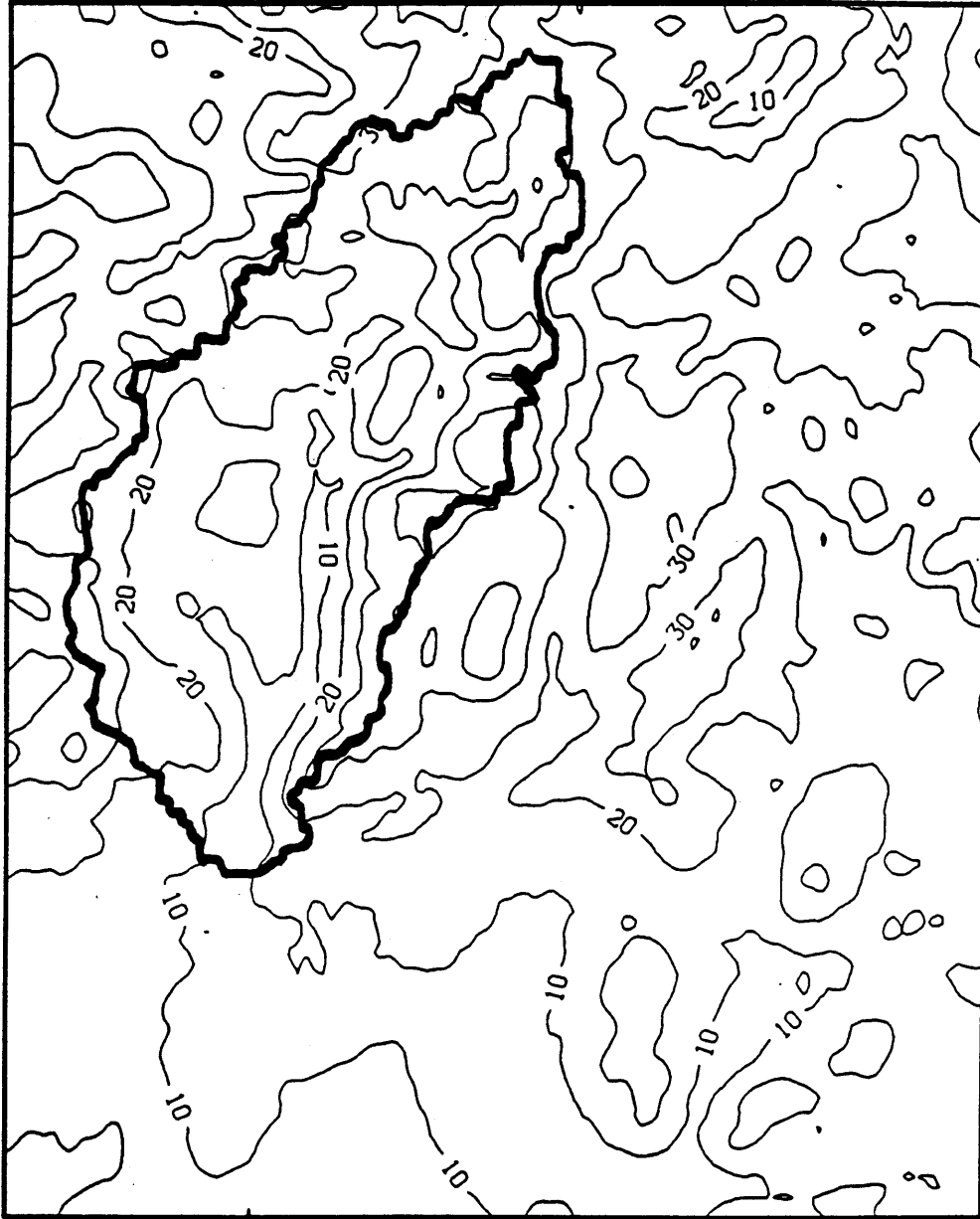


Figure 4.3 Animas Basin October-April Precipitation Map - 10 In. Isolines

state-space model (see Table 4.6). The original model produces a slightly larger volume on an annual basis than the state-space model because of the manner in which the areal extent of snow cover is updated at the beginning of a time step, but the other statistics from the two models are almost identical. Simulated and observed hydrographs for three years are plotted in Figures 4.4 through 4.6 to show how the model performs under different hydrologic conditions without updating. The years 1952, 1960, and 1981 produced high, medium, and low volumes of snowmelt runoff, respectively.

Thirteen snow courses in the vicinity of the basin were selected for this test, but only four of these were located inside the basin. Table 4.7 shows the characteristics of the thirteen sites. Preliminary measurement equations were created for both the upper and lower areas by developing a regression relationship between the pseudo-observed values and the four sites in the basin. These equations were used to test the filter with real data. A sensitivity analysis was performed to develop insight into the importance of various filter inputs. Base-run values were selected and the variance elements of the system error and input error covariance matrices were adjusted systematically. The system error variances were adjusted by a factor of ten and the input error variances were adjusted by a factor of two. The off-diagonal elements were set to zero to reduce the number of values that must be identified.

The base-run values were:

$$Q = \begin{matrix} & \begin{matrix} \text{WE} & \text{NEGHS} & \text{LIQW} & \text{TINDEX} & \text{AESC} \end{matrix} \\ \begin{pmatrix} 1.0 & 0.0 & 0.0 & 0.0 & 0.0 \\ 0.0 & 0.0025 & 0.0 & 0.0 & 0.0 \\ 0.0 & 0.0 & 0.01 & 0.0 & 0.0 \\ 0.0 & 0.0 & 0.0 & 0.0025 & 0.0 \\ 0.0 & 0.0 & 0.0 & 0.0 & 0.01 \end{pmatrix} \end{matrix}$$

$$U = \begin{matrix} & \begin{matrix} P_x & T_a \end{matrix} \\ \begin{pmatrix} 10. & 0. \\ 0. & 4. \end{pmatrix} \end{matrix}$$

The filter was run for the entire snow accumulation season and the model states were updated each April 1. The results from the sensitivity analysis are shown in Table 4.8. The error variance is shown for each state before and after the update for different variations from the base-run. The frozen-water-equivalent state error variance was sensitive to increases in the frozen-water-equivalent state

Table 4.6

Streamflow Error Statistics for the Animas (1949-1983)

	<u>Original Model</u>	<u>State-Space Model</u>
<u>Annual</u>		
Bias (%)	-0.34	0.00
<u>Monthly</u>		
Avg. Absolute Error (mm)	5.40	5.38
RMS Error (mm)	9.76	9.79
<u>Daily</u>		
Avg. Absolute Error (cmsd)	4.99	5.00
RMS Error (cmsd)	9.79	9.81
Correlation Coefficient	.946	.946

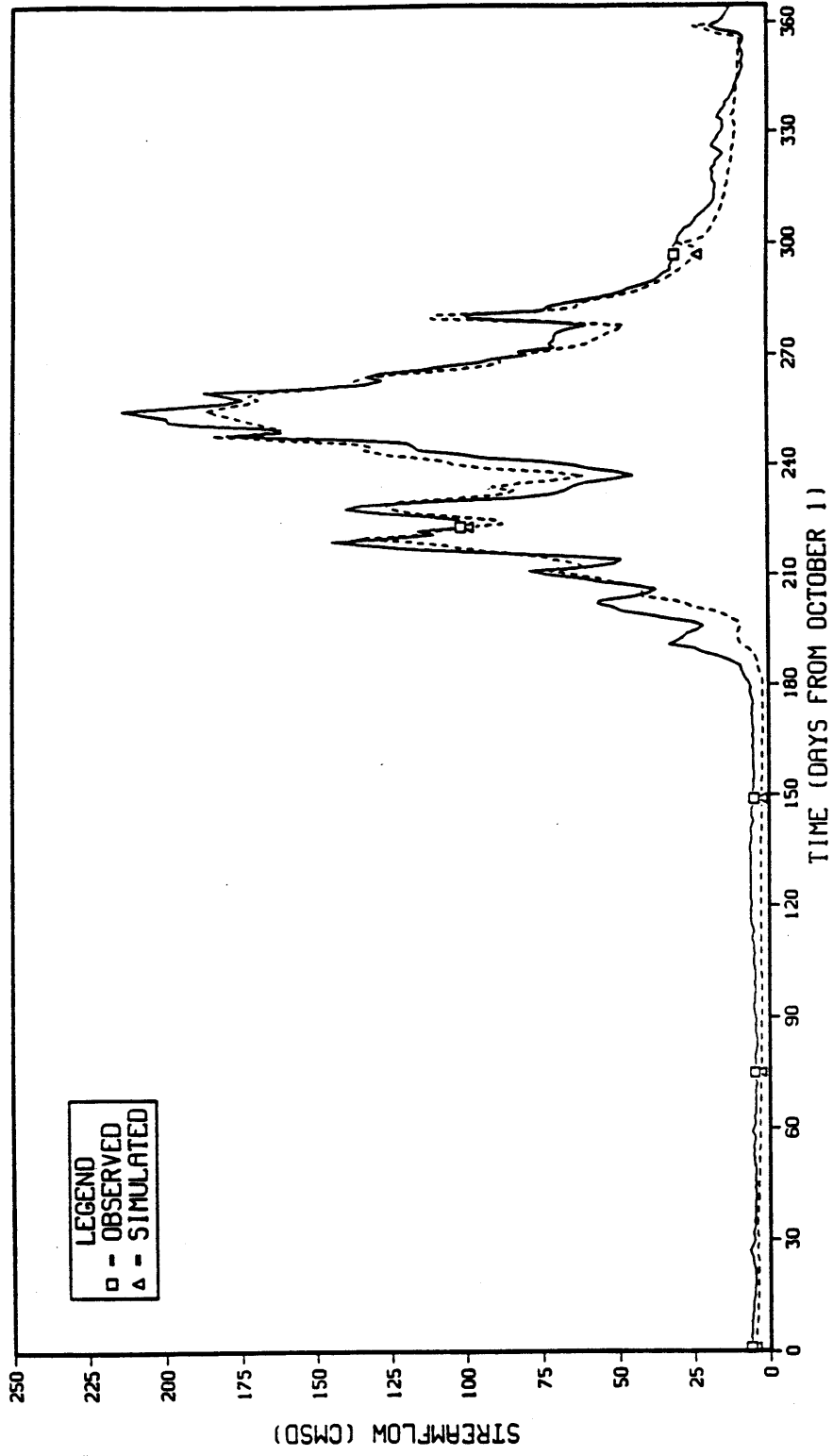


Figure 4.4 1952 Observed and Simulated Hydrographs

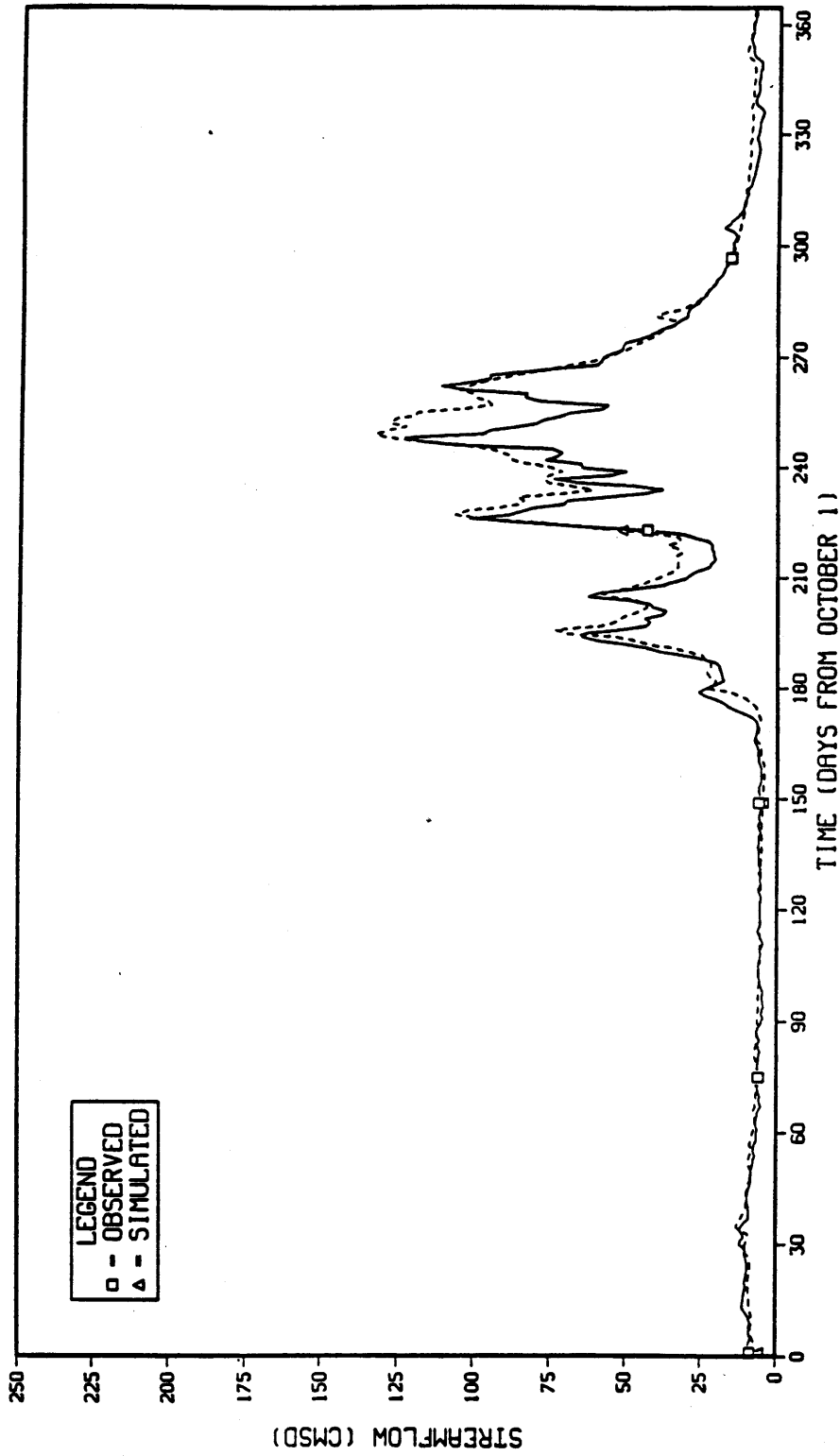


Figure 4.5 1960 Observed and Simulated Hydrographs

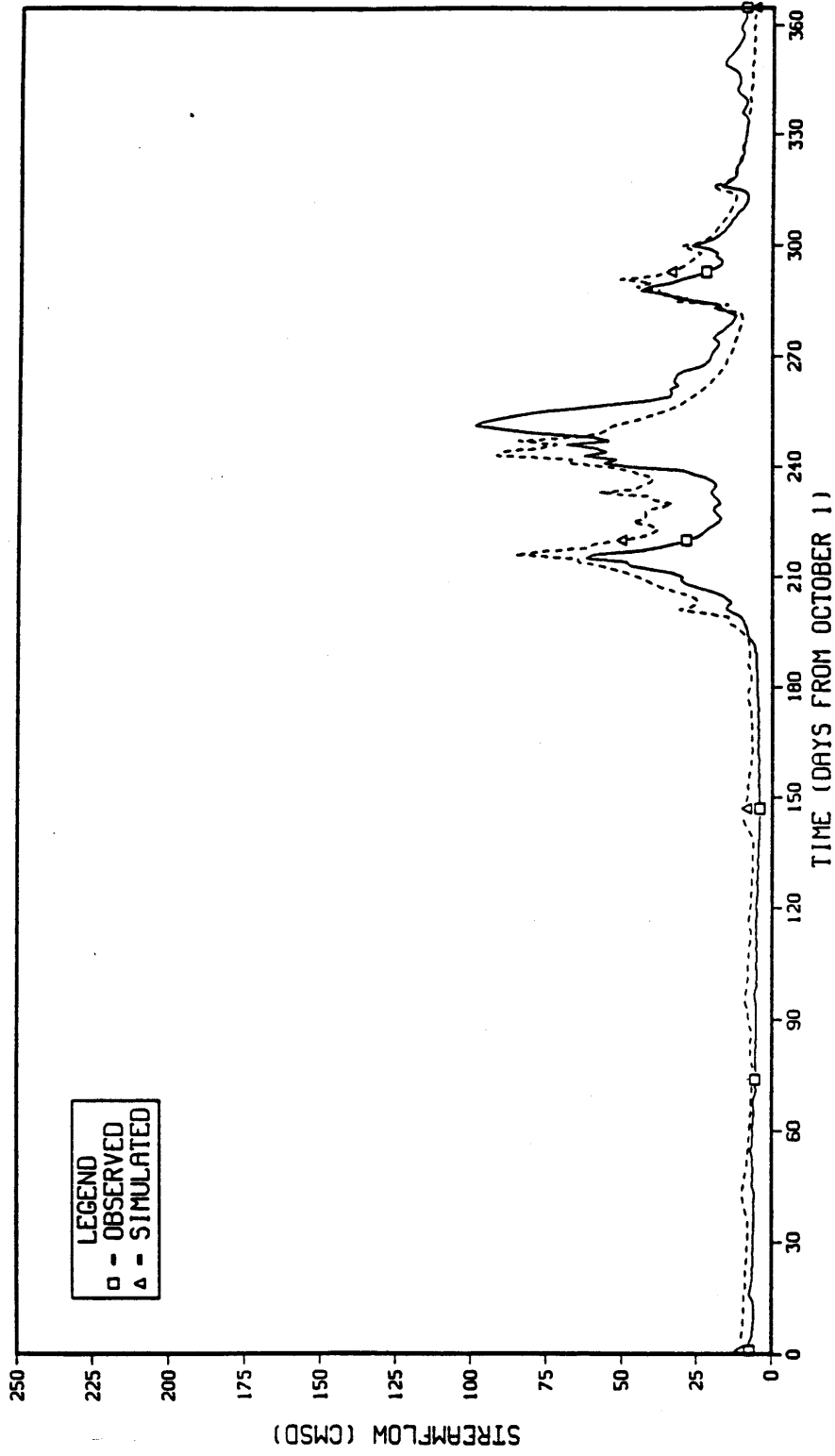


Figure 4.6 1981 Observed and Simulated Hydrographs

Table 4.7

Snow Courses Used for the Animas Basin Analysis

<u>Station Name</u>	<u>SCS ID</u>	<u>Latitude</u>	<u>Longitude</u>	<u>Elevation (ft-MSL)</u>	<u>Mean April 1 (in.)</u>
Lizard Head	07M03	37.80	107.93	10200	18.02
Cascade	07M05	37.65	107.80	8880	12.33
Ironton Park	07M06	37.97	107.65	9600	14.08
Lake City	07M08	37.98	107.25	10160	7.71
Trout Lake	07M09	37.83	107.88	9780	14.80
Spud Mountain	07M11	37.70	107.77	10660	25.08
Molas Lake	07M12	37.75	107.68	10500	13.66
Mineral Creek	07M14	37.85	107.72	10040	16.03
Red Mountain Pass	07M15	37.90	107.70	11020	32.18
Upper Rio Grande	07M16	37.72	107.25	9400	7.99
Santa Maria	07M17	37.82	107.12	9600	4.26
Porcupine	07M20	37.83	107.17	10200	10.47
Rico	08M05	37.67	108.03	8700	7.40

Table 4.8
Effects of Updating on the State Error Variance

<u>BEFORE</u> <u>AFTER</u>	<u>WE</u>	<u>NEGHS</u>	<u>LIQW</u>	<u>TINDEX</u>	<u>AESC</u>
BASE	8560	37.0	218	0.2	0.01
	1250	36.9	216	0.2	0.01
Q ₁₁ = 0.1	8000	37.0	218	0.2	0.01
	1250	36.9	216	0.2	0.01
Q ₁₁ = 10.	14100	37.0	218	0.2	0.01
	1290	37.0	217	0.2	0.01
Q ₂₂ = .00025	8560	36.9	216	0.2	0.01
	1250	36.8	215	0.2	0.01
Q ₂₂ = .025	8570	38.8	229	0.2	0.01
	1270	38.7	227	0.2	0.01
Q ₃₃ = .001	8560	37.0	213	0.2	0.01
	1250	36.9	211	0.2	0.01
Q ₃₃ = 0.1	8560	37.0	266	0.2	0.01
	1290	36.9	265	0.2	0.01
Q ₄₄ = .00025	8560	37.0	217	0.2	0.01
	1250	36.9	216	0.2	0.01
Q ₄₄ = .025	8560	37.8	220	0.4	0.01
	1260	37.7	218	0.4	0.01
Q ₅₅ = .001	8560	36.8	217	0.2	0.00
	1250	36.7	215	0.2	0.00
Q ₅₅ = 0.1	8570	39.6	227	0.2	0.10
	1260	39.5	225	0.2	0.10
U ₁₁ = 5.	4610	24.4	126	0.2	0.01
	1060	24.4	125	0.2	0.01
U ₁₁ = 20.	16465	62.3	401	0.2	0.01
	1500	62.1	397	0.2	0.01
U ₂₂ = 2.	8540	31.4	204	0.1	0.01
	1240	31.3	203	0.1	0.01
U ₂₂ = 8.	8590	48.3	244	0.5	0.01
	1280	48.1	242	0.5	0.01

system error variance, but it was not sensitive to decreases in this variance. The frozen-water-equivalent error variance was sensitive to both increases and decreases in the precipitation error variance. The negative heat storage error variance was not sensitive to changes in the negative heat storage system error variance, but it was sensitive to changes in both the precipitation and temperature error variances. The liquid-water-equivalent error variance reacted to changes in several of the system error variances, but it was only sensitive to changes in the precipitation and temperature error variances. The temperature index state error variance was sensitive to an increase in the temperature index system error variance and to changes in the precipitation and temperature error variances. On April 1, the area is still completely snow covered, so the areal extent of snow cover error variance is simply the system error variance for one time step.

Several things were learned from the trial runs with real data. Initially, it was assumed that the precipitation error had a constant variance. This assumption was causing the variance of the errors of several of the states to change abruptly even when no precipitation was occurring. A more reasonable assumption is that the precipitation error has a constant coefficient of variation. The variance of the precipitation error was calculated at each time step as:

$$\text{VAR}(p_e) = (CV_{pe} \cdot P_x)^2 \quad (4.16)$$

where, p_e = error in precipitation,
 CV_{pe} = coefficient of variation of precipitation error.

This modification resulted in smoother propagation of the state error variances. When the areal extent of snow cover decreased below 100 percent, there was a negative correlation between the frozen-water-equivalent and the areal extent of snow cover. This correlation added a significant amount of variance to the error in the frozen-water-equivalent state when the uncertainty of the areal extent of snow cover state was large, but in general, the uncertainty of the frozen-water-equivalent state was propagated smoothly.

The variance of the error in the negative heat storage state increased slowly, but it decreased to zero when the negative heat storage was zero. When the negative heat storage became zero, however, the uncertainty in the negative heat storage state produced an increase in the uncertainty of the frozen and liquid-water-equivalent states. This is expected since the model equations dictate that the negative heat storage is converted to water-equivalent when the negative heat storage is reduced. The uncertainty of the liquid-water-equivalent state increased slowly, except when the negative heat storage was equal to zero. When the negative heat storage is greater than zero, any free water is frozen, but when the negative heat storage is equal to zero, excess water is available to become liquid-water-equivalent.

Decreases were observed in the variance of the error in the liquid-water-equivalent state when the snow cover was at its maximum water content. When the snow cover contains its maximum water content, the

liquid-water-equivalent becomes a function of the frozen-water-equivalent:

$$x_3 = \text{PLWHC} \cdot x_1 \quad (4.17)$$

$$P_{33} = \text{PLWHC}^2 \cdot P_{11} \quad (4.18)$$

where, P_{ii} = state error variance for state i .

Typically, the parameter PLWHC is small, so the variance of the error in the liquid-water-equivalent state becomes a small fraction of the variance of the error in the frozen-water-equivalent state. This sometimes produced sudden changes in the variance of the error in the liquid-water-equivalent state when the snow cover reached its maximum water content. In reality, as this limit is approached, the uncertainty of the liquid-water-equivalent state may decrease, but it would probably happen gradually. The model does not detect that a threshold is approaching, so the estimates of the uncertainties of some of the states may not be accurate in the vicinity of these thresholds. This could affect the updating in some cases.

The variance of the error in the temperature index state assumed the value of the variance of the error in the temperature after a new snowfall and then receded. It does not appear to seriously affect the uncertainties of the other states.

The variance of the error in the areal extent of snow cover state assumed the value of the areal extent of snow cover system error variance as long as the snow cover was 100 percent. When the cover decreased below 100 percent, the variance increased. The state-space equation for areal extent of snow cover was written as a function of the change in total water-equivalent. Realistic values of the variance were propagated in most cases, but unrealistic values were observed when the slope of the areal depletion curve became extremely small. This sometimes occurred after a shallow snowfall that produced a large change in areal extent of snow cover. A small change in water-equivalent produced a large change in the areal extent of snow cover state. The uncertainty in the water-equivalent change was magnified in the uncertainty of the areal extent of snow cover state. One would expect a large uncertainty in the areal extent of snow cover state under these circumstances, but these values may not be reliable. A change was made in the original model to avoid the use of the new snow line for extremely small snowfalls. This smooths the propagation of the variance of the error of the areal extent of snow cover state and prevents it from driving the variance of the frozen-water-equivalent state to extremely large values. In general, the filter seems to be propagating reasonable estimates of the state error covariance matrix.

Regression Approach

One approach discussed in Chapter 3 for estimating observations of the model states is the development of a regression equation between the pseudo-observed values and the point snow-water-equivalent observations. The pseudo-observed values are model water-equivalent states that allow the model to simulate the correct seasonal runoff

volumes. Historical pseudo-observed values are determined by iteratively adjusting the model water-equivalent states until the model produces the correct seasonal volume. The adjustments are made to the liquid and frozen-water-equivalent states for the upper and lower areas by maintaining the ratio between the liquid and frozen-water-equivalent in each area and the ratio of total water-equivalent from one area to another. The pseudo-observed values for water years 1949 thru 1983 are plotted against the simulated total water-equivalent in Figure 4.7, for the upper area of the Animas, and in Figure 4.8 for the lower area of the Animas.

Forward stepwise regression with deletion (McCuen, 1986) was used to develop the regression equation to predict the pseudo-observed value from the snow-water-equivalent observations. In some cases, only two or three stations could explain significant variability in the pseudo-observed values with positive coefficients. The significance level for including stations was decreased, however, until at least four stations appeared in the equation with positive coefficients. All 35 years of data were used to determine which stations were selected. A special procedure was devised to verify the updating methodology with as much data as possible, while maintaining a valid verification. Observations of the model states were estimated by developing a separate regression equation between the pseudo-observed values and the point observations for each year, neglecting that year's data. This allowed the updating procedure to be verified on all 35 years of data. Spud Mountain, Red Mountain Pass, Upper Rio Grande, and Rico snow course data were used in the April 1 equation for the upper area, whereas Cascade, Spud Mountain, Upper Rio Grande, and Rico snow course data were used in the April 1 equation for the lower area. The results shown in Table 4.9 for the upper area indicate that eliminating one year does not produce much variability in the regression coefficients. Years 1949 and 1950 have the same coefficients, since both of these years contain missing data and the estimated coefficients are based on the data from 1951 through 1983. Figure 4.9 and Figure 4.10 show the pseudo-observed values plotted against the estimates of the pseudo-observed values from the regression equations for the upper and lower areas, respectively.

Before the filter equations can be used for updating, estimates of the Q, R, and U matrices are required. The square of the root-mean-square (RMS) error between the pseudo-observed values and their estimates from the regression equations was used as an estimate of the R value for each subarea. For the upper area on April 1, $R = 3000$, and for the lower area on April 1, $R = 1000$. Reasonable values were selected for the U matrix based on experience with hydrometeorological data. The coefficient of variation for the precipitation error was assumed to be 0.2 and the variance of the temperature error was assumed to be 1.0. The off-diagonal elements of the U and Q matrices were assumed to be zero. The diagonal element of Q for the frozen-water-equivalent state was determined by trial and error. It was adjusted until the average frozen-water-equivalent error on April 1 was approximately equal to the square of the RMS error between the pseudo-observed snow-water-equivalent and the simulated snow-water-equivalent. This error is much greater in the upper area than in the lower area, primarily because more snow occurs in the upper area. The

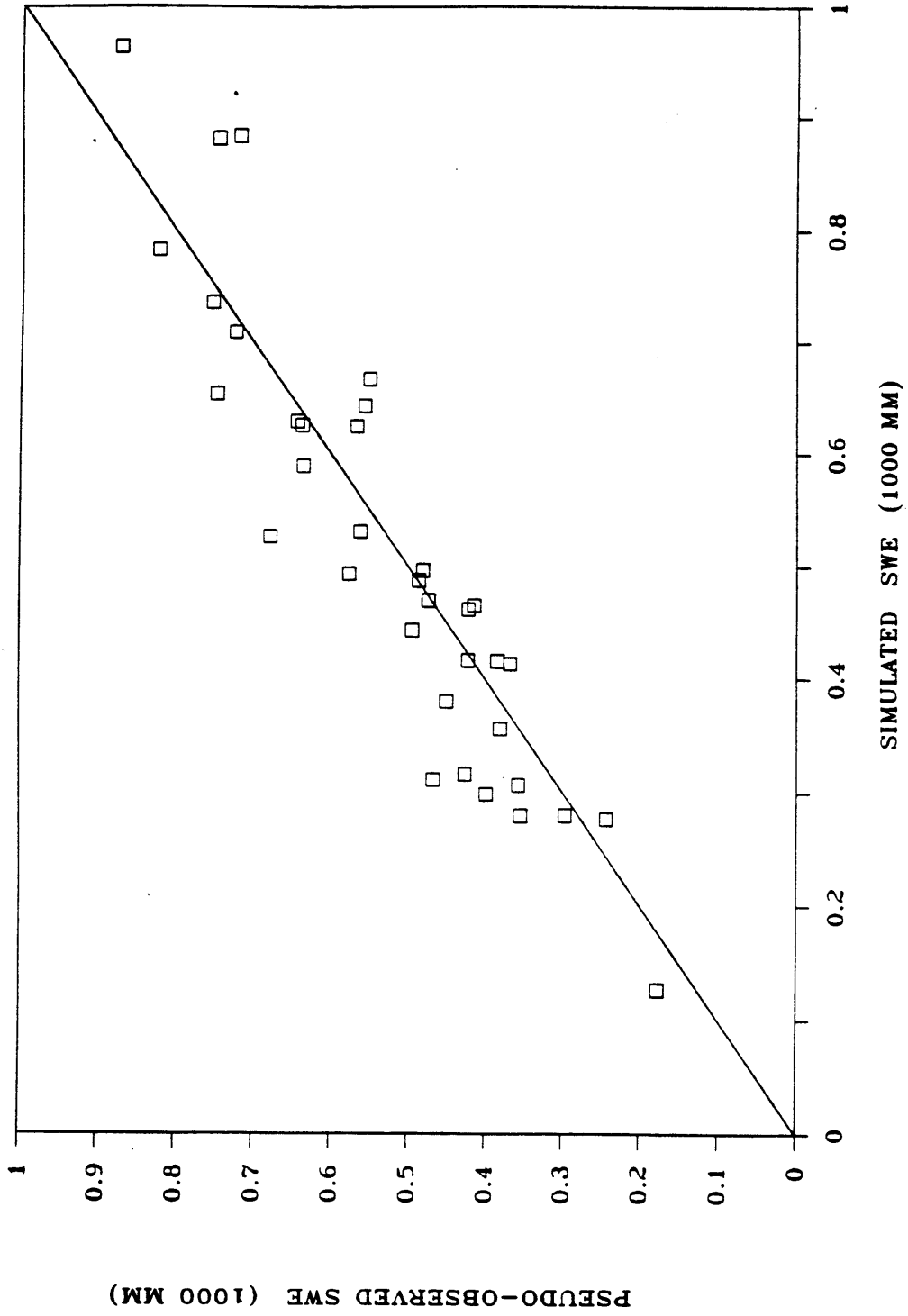


Figure 4.7 Pseudo-Observed vs. Simulated Snow-Water-Equivalent (Upper Area - April 1)

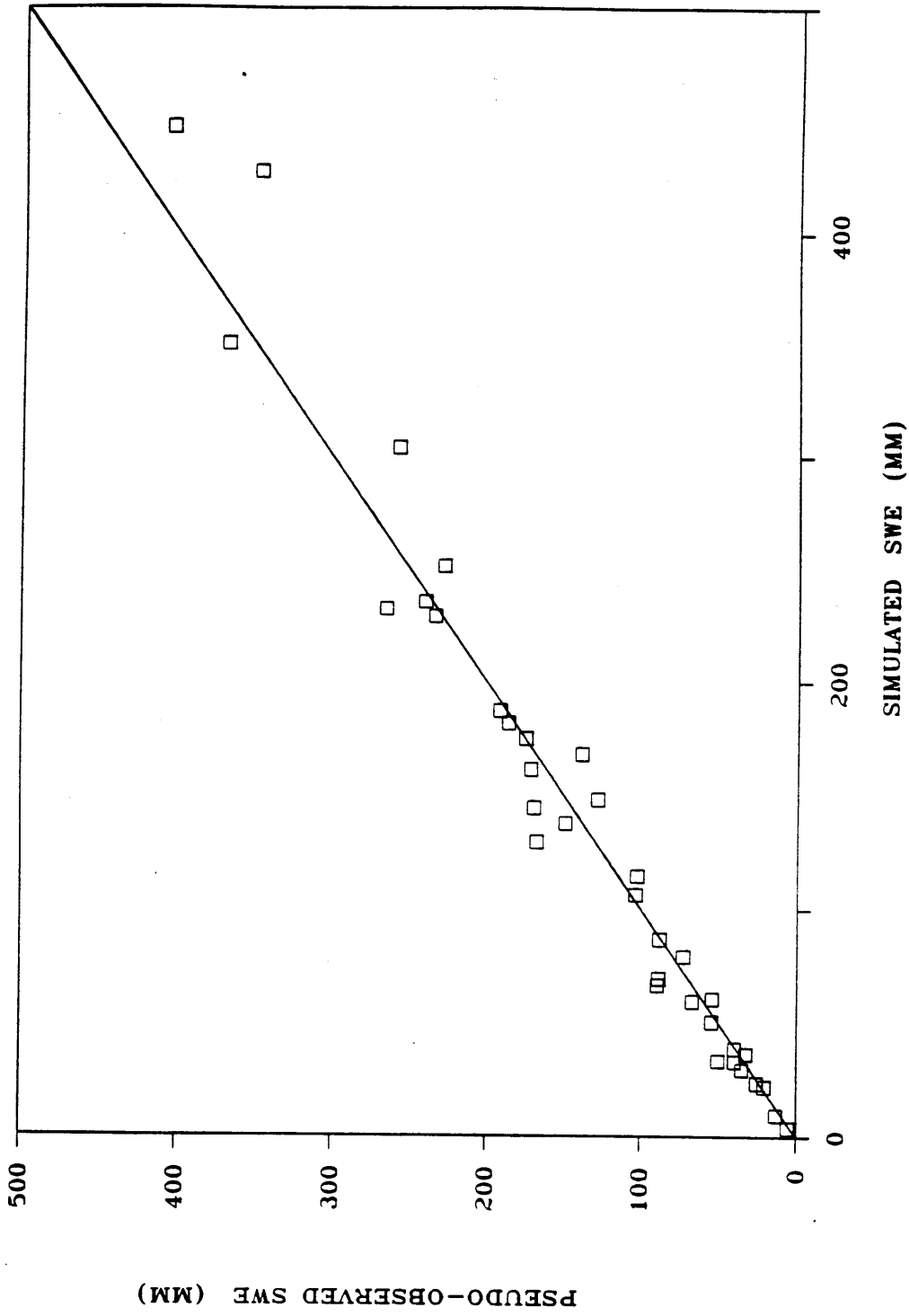


Figure 4.8 Pseudo-Observed vs. Simulated Snow-Water-Equivalent (Lower Area - April 1)

Table 4.9

Upper Subarea Regression Coefficients for April 1

	<u>SPUD MOUNTAIN</u>	<u>RED MT PASS</u>	<u>UPPER RIO GRANDE</u>	<u>RICO</u>	<u>CONSTANT</u>
1949	0.414	0.161	0.067	0.184	80.5
1950	0.414	0.161	0.067	0.184	80.5
1951	0.410	0.144	0.106	0.189	85.8
1952	0.419	0.158	0.070	0.161	82.0
1953	0.412	0.162	0.067	0.185	79.8
1954	0.416	0.159	0.065	0.183	81.5
1955	0.402	0.179	0.084	0.172	70.8
1956	0.438	0.163	0.026	0.166	76.0
1957	0.420	0.159	0.060	0.183	80.2
1958	0.377	0.174	0.094	0.199	83.0
1959	0.350	0.233	0.111	0.146	62.7
1960	0.412	0.163	0.066	0.184	79.8
1961	0.416	0.161	0.062	0.184	79.7
1962	0.433	0.139	0.044	0.188	88.3
1963	0.420	0.157	0.055	0.181	83.3
1964	0.393	0.157	0.093	0.201	90.2
1965	0.422	0.156	0.050	0.184	81.3
1966	0.415	0.158	0.068	0.182	81.8
1967	0.349	0.211	0.125	0.207	62.0
1968	0.417	0.160	0.060	0.184	80.5
1969	0.439	0.115	0.014	0.272	98.7
1970	0.437	0.132	0.086	0.167	86.7
1971	0.429	0.128	0.068	0.213	89.4
1972	0.410	0.166	0.071	0.178	79.2
1973	0.433	0.190	0.000	0.136	62.6
1974	0.413	0.159	0.067	0.185	82.1
1975	0.415	0.158	0.063	0.185	82.1
1976	0.423	0.161	0.071	0.161	79.0
1977	0.413	0.149	0.073	0.189	89.3
1978	0.404	0.210	0.006	0.194	59.1
1979	0.486	0.110	0.191	0.077	74.0
1980	0.422	0.147	0.058	0.202	84.9
1981	0.377	0.128	0.145	0.211	111.8
1982	0.409	0.181	0.033	0.199	72.7
1983	0.413	0.164	0.074	0.167	77.0
MEAN	0.413	0.160	0.070	0.182	80.5
STD. DEV.	0.024	0.024	0.036	0.028	9.9

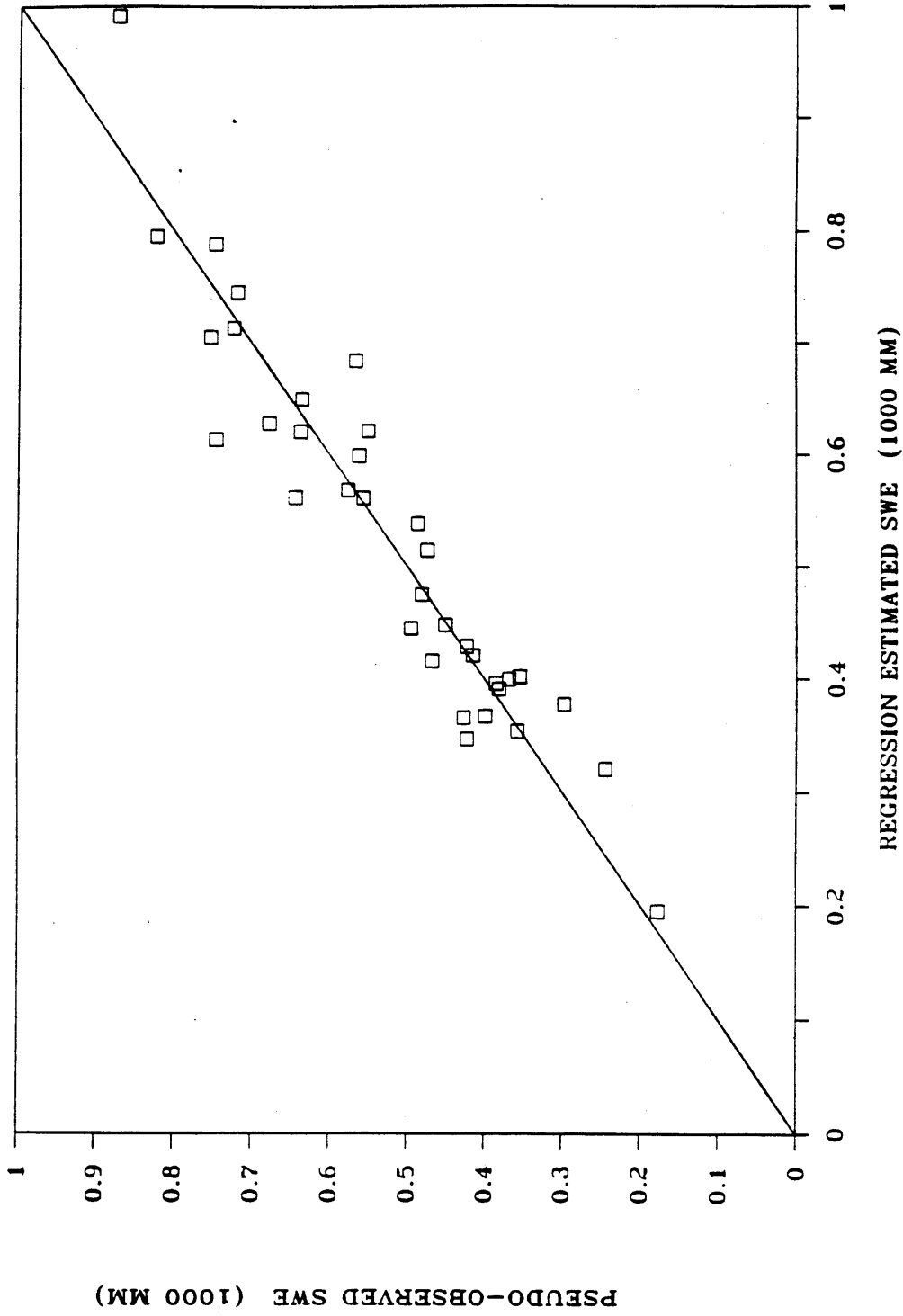


Figure 4.9 Pseudo-Observed vs. Regression Estimated Snow-Water-Equivalent (Upper Area - April 1)

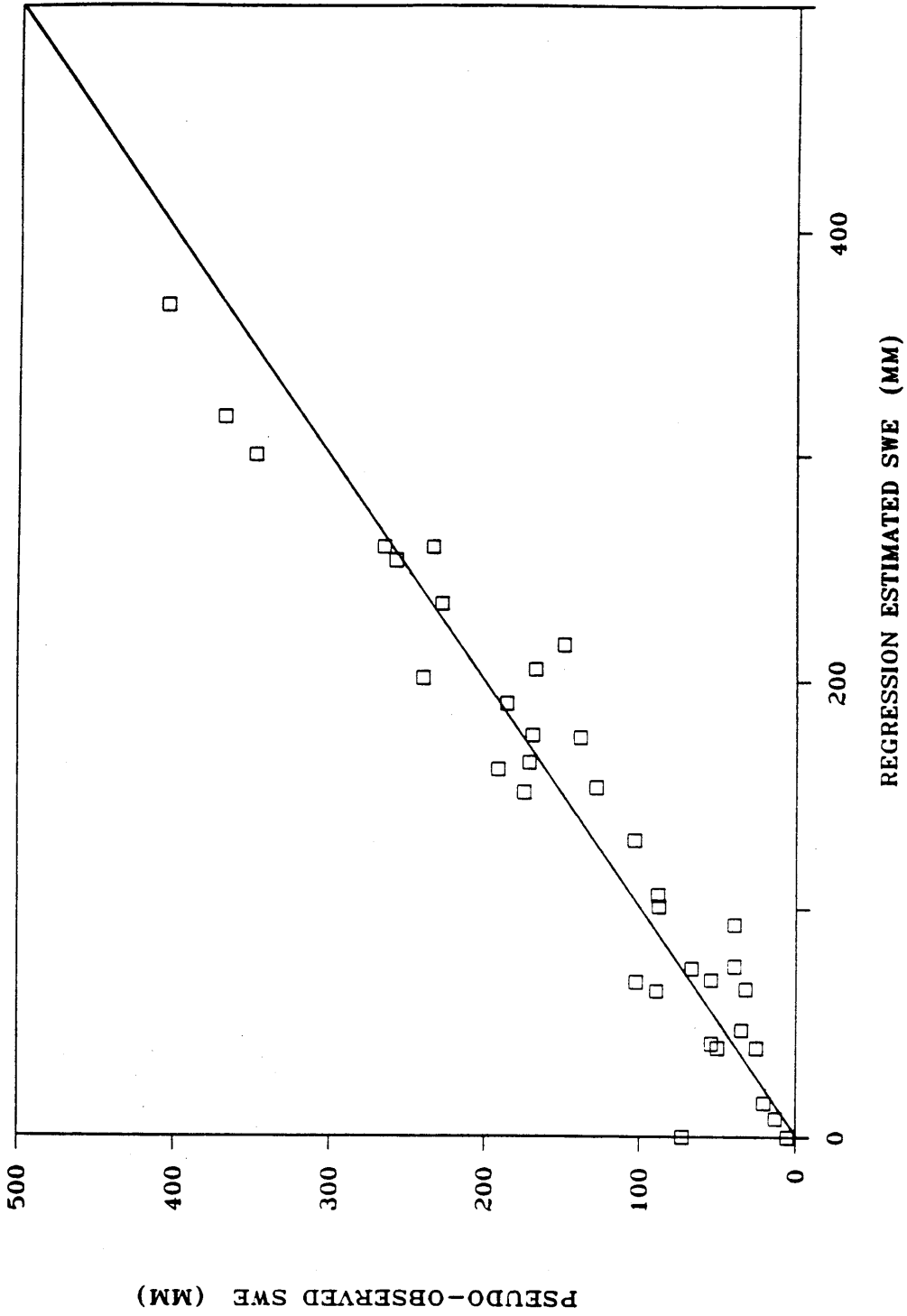


Figure 4.10 Pseudo-Observed vs. Regression Estimated Snow-Water-Equivalent (Lower Area - April 1)

other diagonal elements were assigned reasonable values based on the results of the updating sensitivity analysis. In the lower area:

$$Q = \begin{pmatrix} 0.5 & 0.0 & 0.0 & 0.0 & 0.0 \\ 0.0 & 0.01 & 0.0 & 0.0 & 0.0 \\ 0.0 & 0.0 & 0.01 & 0.0 & 0.0 \\ 0.0 & 0.0 & 0.0 & 0.01 & 0.0 \\ 0.0 & 0.0 & 0.0 & 0.0 & 0.0001 \end{pmatrix}$$

and in the upper area:

$$Q = \begin{pmatrix} 8.5 & 0.0 & 0.0 & 0.0 & 0.0 \\ 0.0 & 0.01 & 0.0 & 0.0 & 0.0 \\ 0.0 & 0.0 & 0.01 & 0.0 & 0.0 \\ 0.0 & 0.0 & 0.0 & 0.01 & 0.0 \\ 0.0 & 0.0 & 0.0 & 0.0 & 0.0001 \end{pmatrix}$$

Once the Q, R, and U matrices were estimated, the model states were updated with April 1 observations derived from the regression equations. Figure 4.11 shows the observed seasonal volumes plotted against the simulated seasonal volumes, and Figure 4.12 shows the observed seasonal volumes plotted against the updated seasonal volumes. The updating decreased the unexplained variance of the observed volumes from 10 to 5 percent. Daily, monthly, and seasonal streamflow statistics are shown for the simulation and the updating run in Table 4.10. The updating produced significant improvements in the streamflow simulation. Although the pseudo-observed values were developed based on the observed seasonal volumes, the updating improved the daily and monthly streamflow statistics, as well as the seasonal.

As a further test of the value of the filter, another updating run was made with R = 0.0 for the upper and lower areas. When R is set to zero, it implies that there is no error in the observations and the updated states are made consistent with the observations. The results from the run setting R equal to zero are also shown in Table 4.10. The seasonal volume statistics from the updating run with R = 0.0 are slightly inferior to the statistics from the updating run with realistic values for R. This indicates that the model simulation provides important information and that the filter is useful in combining the information from the model simulation with the information from the observations.

Regression Approach - Other Months

The results presented thus far are based on updating only on April 1, but the state error covariance matrix is propagated throughout the snow season. This leads to the following questions: Can updating improve earlier forecasts when the snow cover is still accumulating? Can earlier observations provide any additional information for April 1 forecasts? Can updates made during the melt season, e.g. after April 1, improve later forecasts? In order to address these questions, separate regression equations were developed for the first of each month from February to May. This required the iterative computation of pseudo-observed values for the first of each month. As before, a separate

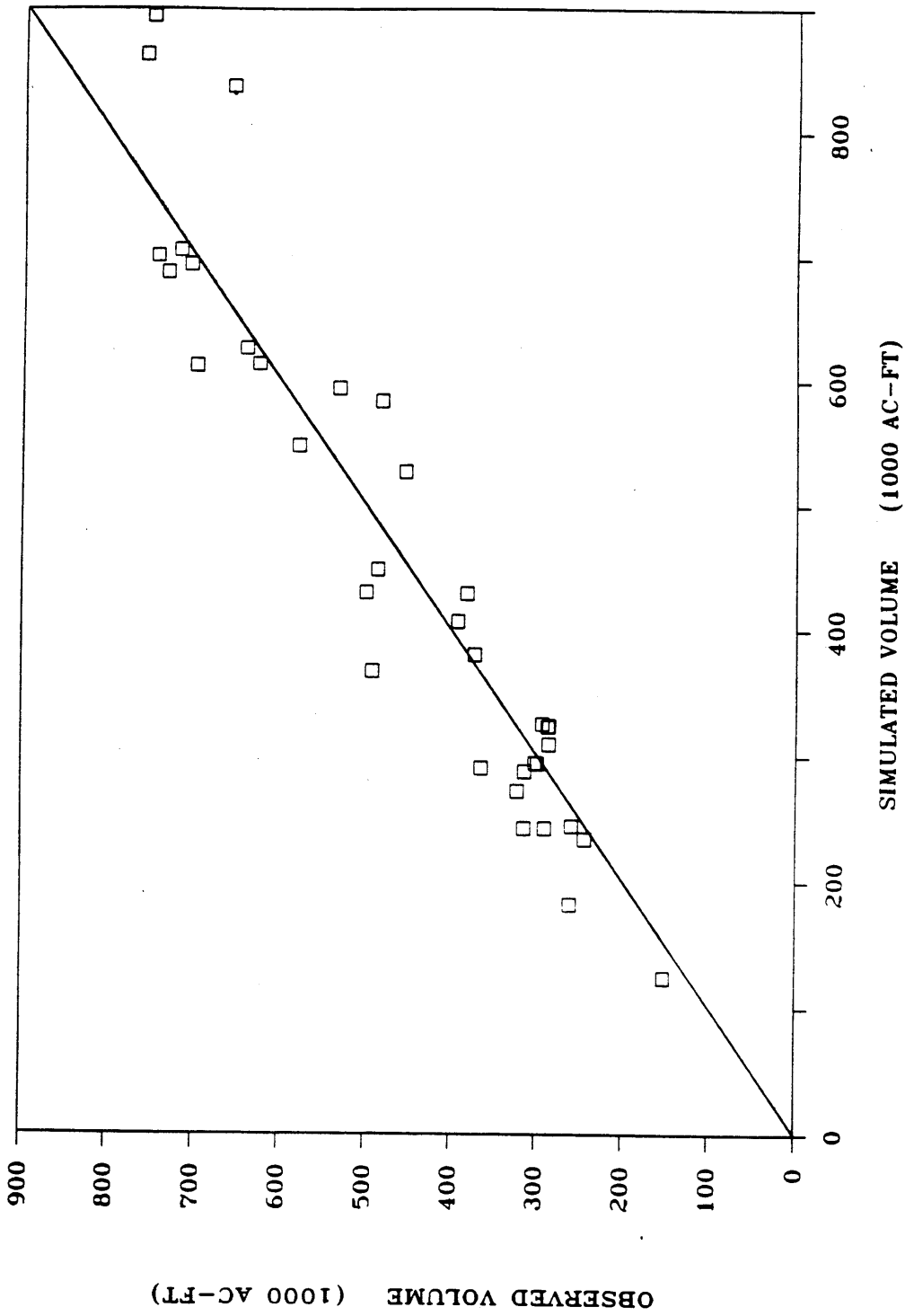


Figure 4.11 Observed vs. Simulated Seasonal Streamflow Volumes

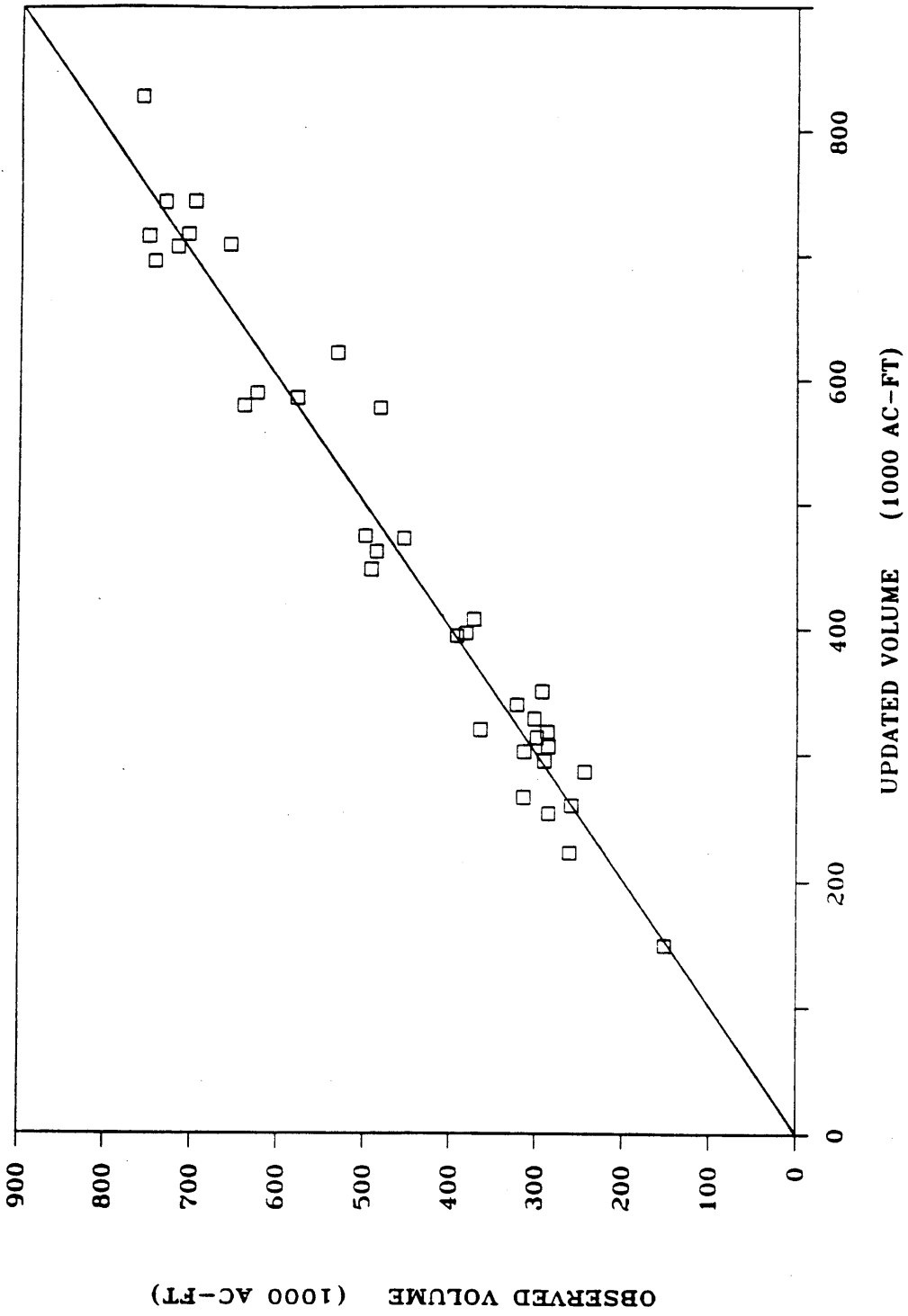


Figure 4.12 Observed vs. April 1 Updated (Regression) Seasonal Streamflow Volumes

Table 4.10
Streamflow Error Statistics - Updated with Regression

<u>Daily</u>	<u>Simulated</u>	<u>Updated (April 1)</u>	<u>Updated (April 1) R=0</u>
Avg. Absolute Error (cmsd)	5.00	4.52	4.52
RMS Error (cmsd)	9.81	8.52	8.51
Correlation Coefficient	.946	.958	.958
<u>Monthly</u>			
Avg. Absolute Error (mm)	5.38	4.57	4.56
RMS Error (mm)	9.79	7.56	7.71
<u>Seasonal (April - September)</u>			
Average Error (10^6m^3)	-2.3	2.8	7.0
Absolute Max. Error(10^6m^3)	220.4	116.3	126.1
Avg. Absolute Error (10^6m^3)	62.3	38.3	43.1
RMS Error (10^6m^3)	80.2	50.2	53.3
Bias (%)	-0.4	0.5	1.2
Correlation Coefficient	.951	.976	.972

regression equation was developed to predict each year by omitting that year from the analysis. R was again estimated by using the square of the RMS error between the pseudo-observed values and the estimated values from the regression equations between the pseudo-observed values and the point snow-water-equivalent observations. The statistics between the pseudo-observed values and their estimates from regression are summarized in Table 4.11 for both the upper and lower subareas.

In general, the relationship between the pseudo-observed values and the estimates from the regression equations improved as the season progressed. For the lower area, however, the correlation coefficient decreased for the May 1 equation. Although, the mean pseudo-observed value for the upper area increased slightly from a value of 523 mm to 539 mm from April 1 to May 1, the mean pseudo-observed value for the lower area decreased from 137 mm to 44 mm during this period. The elevations of the snow courses range from 8700 ft-MSL to 11020 ft-MSL, with six of the snow courses above the highest elevation in the lower area. Because of the significant amount of melt that occurs in the lower area, the snow courses may not be good indicators of what is happening to the snow-water-equivalent in the lower area after April 1. Despite this fact, the regression technique was able to explain 88 percent of the variability of the pseudo-observed values in the lower area on May 1.

The updating runs were made using the same Q and U matrices as before, and the streamflow error statistics are given in Table 4.12. Updates were made on the first of each month, beginning in February through the date shown. These results can be compared to the simulated streamflow error statistics given in Table 4.10. Updating only on February 1 reduced the unexplained variance in the seasonal streamflow volumes from 10 to 7 percent. Each month, the results were slightly improved over the previous month's results. The unexplained variances for the February, March, April, and May update runs were, respectively, 72, 52, 48, and 43 percent of the unexplained variance for the simulation without updating. The results from the updating run with updates on February 1, March 1, and April 1, however, were not significantly better than the results shown in Table 4.10, where updating was only done on April 1. Although the update was primarily designed to improve seasonal volume simulation, the daily and monthly streamflow error statistics also were improved. Figures 4.13 and 4.14 show the effect of updating on the frozen-water-equivalent state and its variance for the periods January to June, 1971 and January to June, 1980, respectively. Figures 4.15 and 4.16 show the effects of updating on hydrograph simulation for 1971 and 1980, respectively. Updating improved the hydrograph simulation in both years.

Regression Approach - Summary

Regression equations were used to relate the snow course measurements to the model states. The true model states for a particular date were estimated by iteratively adjusting the model water-equivalent states until the correct seasonal streamflow volume was simulated. These estimates of the model states, termed pseudo-observed,

Table 4.11
 Statistics for Regression Pseudo-Observed Estimates

<u>Upper Area</u>	<u>Feb 1</u>	<u>Mar 1</u>	<u>Apr 1</u>	<u>May 1</u>
Average Error (mm)	5.7	9.7	3.5	3.5
Absolute Max. Error (mm)	179.7	202.7	134.1	114.6
Avg. Absolute Error (mm)	52.5	44.3	41.9	41.1
RMS Error (mm)	67.5	59.4	54.4	50.3
Bias (%)	1.6	2.3	0.7	0.7
Correlation Coefficient	.863	.916	.946	.966
<u>Lower Area</u>				
Average Error (mm)	-0.6	-0.6	1.7	0.7
Absolute Max. Error (mm)	56.8	57.3	72.8	60.9
Avg. Absolute Error (mm)	25.5	24.2	25.8	11.7
RMS Error (mm)	30.4	29.3	32.0	17.4
Bias (%)	-0.4	-0.4	1.2	1.6
Correlation Coefficient	.909	.938	.952	.939

Table 4.12

Streamflow Error Statistics - Updated with Regression
- Other Months

	Updating Through			
	<u>Feb 1</u>	<u>Mar 1</u>	<u>Apr 1</u>	<u>May 1</u>
<u>Daily</u>				
Avg. Absolute Error (cmsd)	4.76	4.59	4.50	4.46
RMS Error (cmsd)	9.00	8.59	8.40	8.30
Correlation Coefficient	.954	.958	.959	.960
 <u>Monthly</u>				
Avg. Absolute Error (mm)	4.95	4.67	4.47	4.32
RMS Error (mm)	8.39	7.60	7.32	7.09
 <u>Seasonal (April - September)</u>				
Average Error ($10^6 m^3$)	1.7	5.4	5.6	3.5
Absolute Max. Error ($10^6 m^3$)	176.8	142.9	116.1	99.6
Avg. Absolute Error ($10^6 m^3$)	49.4	42.2	39.4	35.6
RMS Error ($10^6 m^3$)	63.3	52.8	48.7	46.4
Bias (%)	0.3	1.0	1.0	0.6
Correlation Coefficient	.965	.975	.977	.979

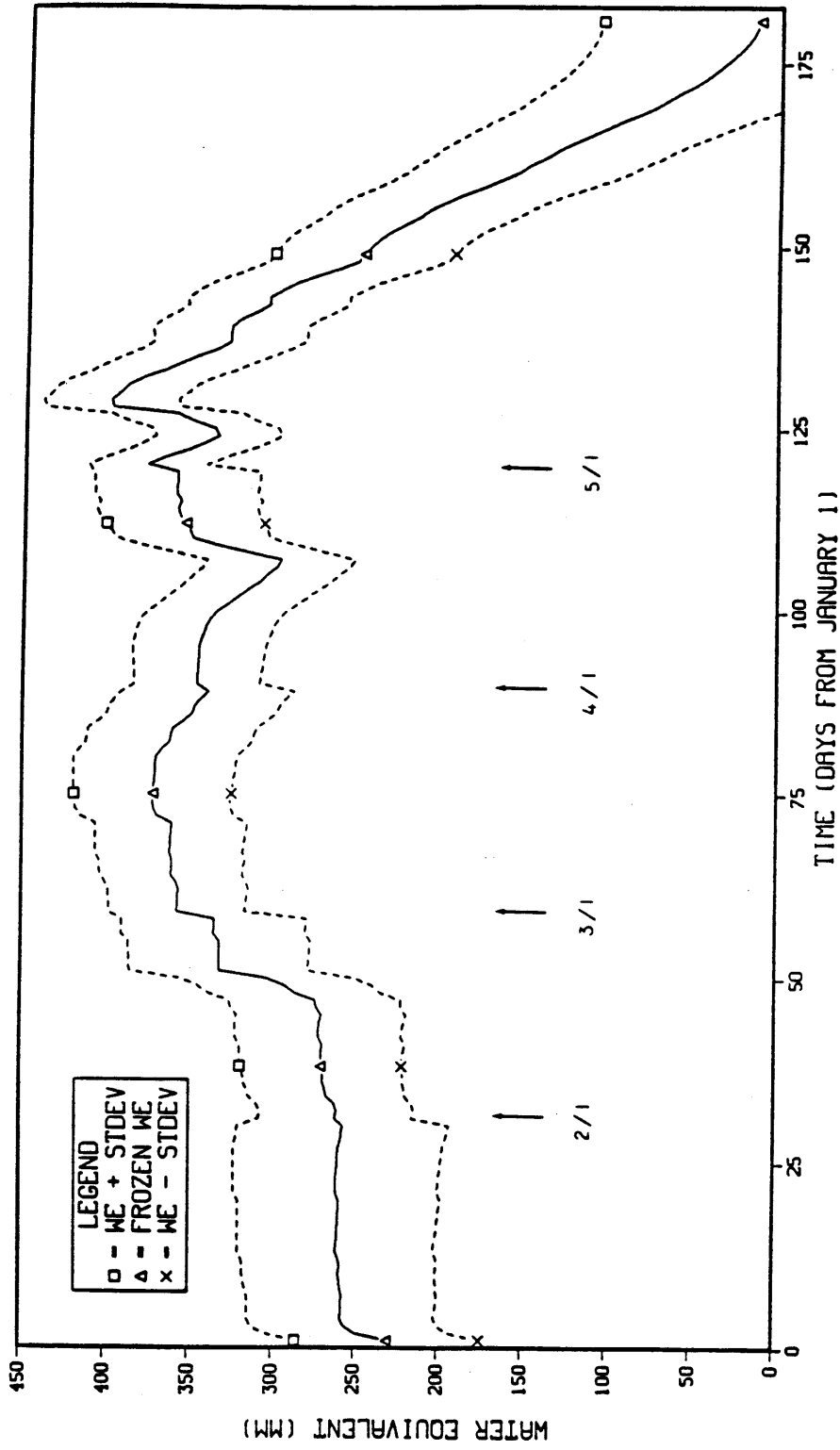


Figure 4.13 1971 Frozen-Water-Equivalent \pm Standard Deviation

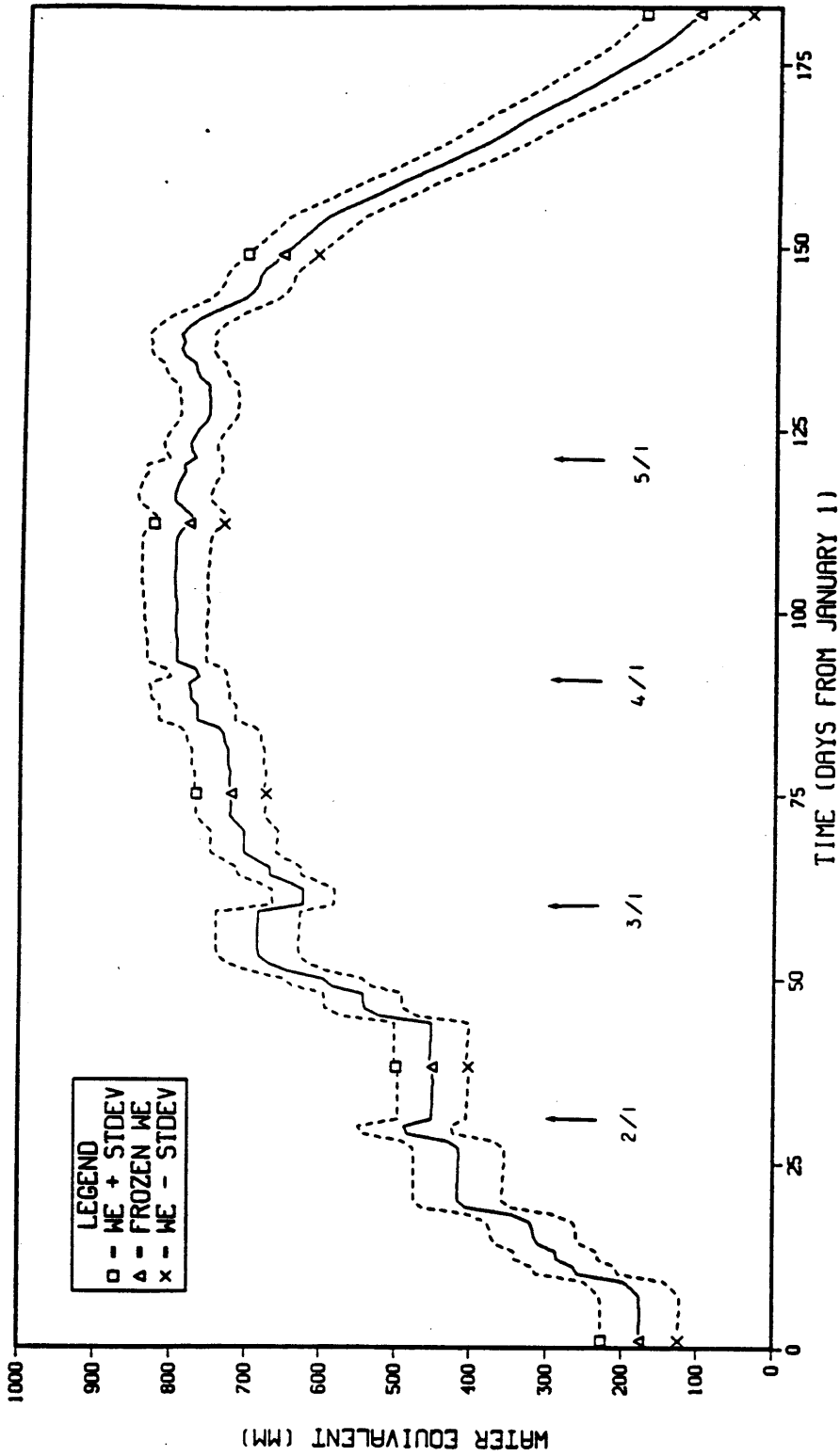


Figure 4.14 1980 Frozen-Water-Equivalent + Standard Deviation

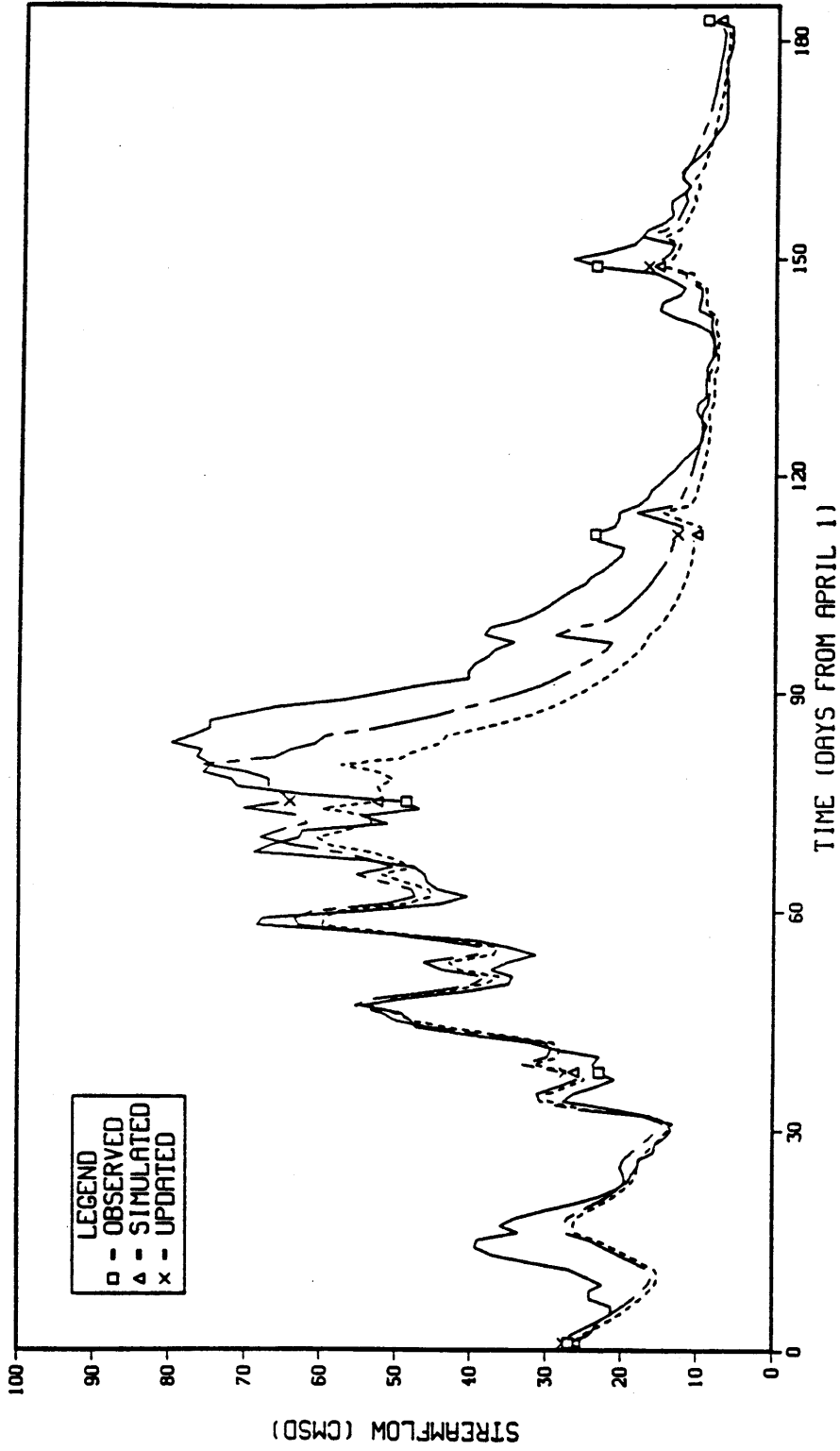


Figure 4.15 1971 Hydrographs (Regression Updated - all months)

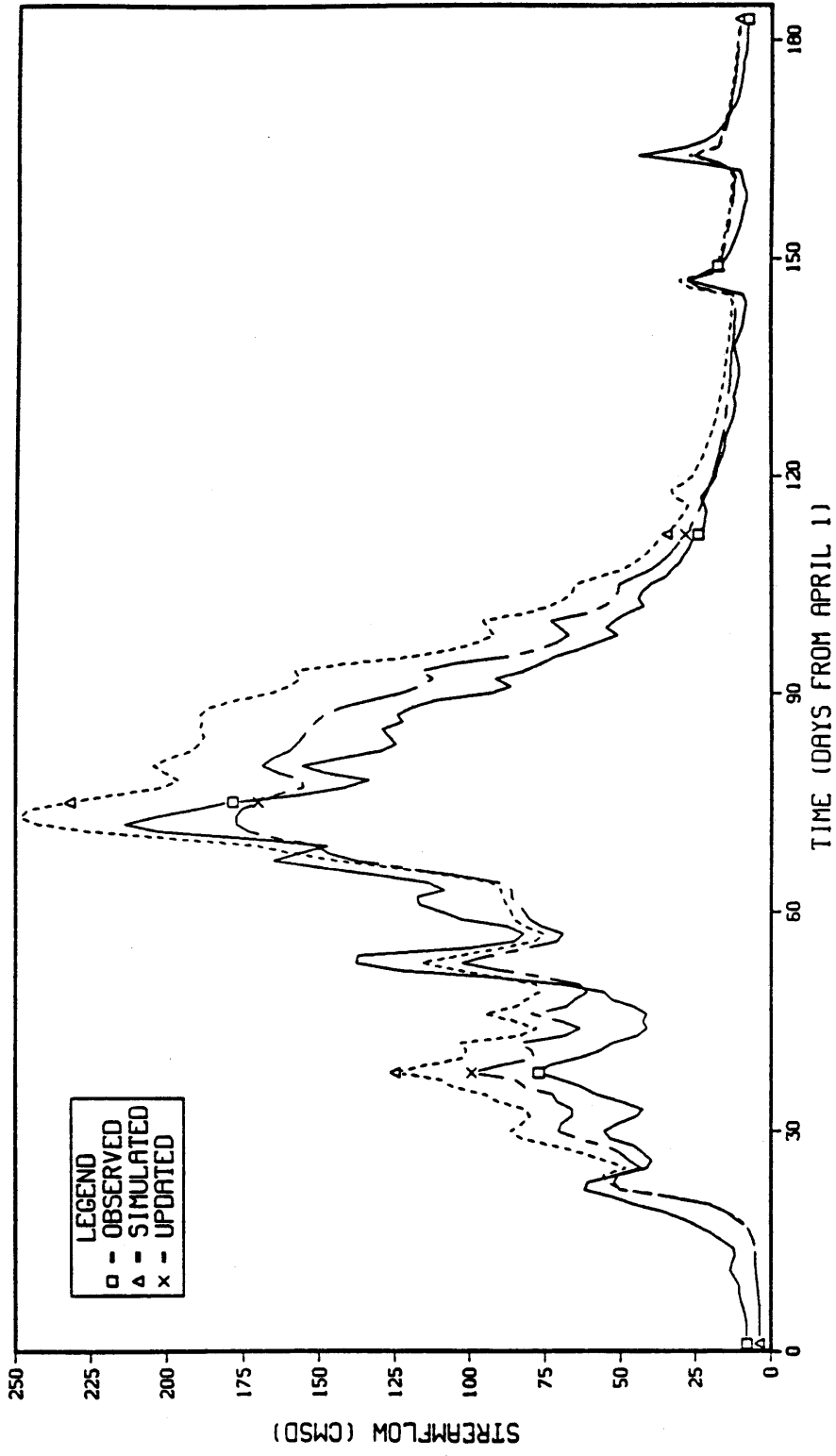


Figure 4.16 1980 Hydrographs (Regression Updated - all months)

were derived for the first of each month, February to May, for the 35 year period 1949-1983. These pseudo-observed values were used to develop the regression equations needed to estimate observations of the water-equivalent states for updating.

Updating with these derived observations of the water-equivalent states produced significant improvements in the streamflow simulation. The daily, monthly, and seasonal streamflow statistics all significantly improved as a result of the updating.

Spatial Interpolation Approach

As discussed in Chapter 3, a spatial interpolation approach offers several advantages over a regression approach. It provides an estimate of the entire snow-water-equivalent field, it does not require a long historical record of all of the observations, it is easily adaptable to a changing network, and it is conceptually appealing. In order to apply the interpolation approach as it was outlined in Chapter 3, the mean, standard deviation, and correlation structure of the field are required. In this approach, standardized deviates of snow-water-equivalent observations are interpolated. The mean and standard deviation of the observations are used to convert the observations into standardized deviates, and the mean and standard deviation at each grid point in the field are used to transform the field of interpolated standardized deviates into a field of estimated snow-water-equivalent. Areal estimates are computed by averaging the snow-water-equivalent values over the areas of interest. Regression can be used to relate the estimates of areal snow-water-equivalent from the spatial interpolation approach to the model states via the pseudo-observed values.

As with the regression approach, initial efforts were focused on updating using April 1 snow-water-equivalent observations. An April 1 mean snow-water-equivalent map was prepared for the Animas based on the October through April precipitation map for the area and an extension of the relationship between October through April precipitation and April 1 snow-water-equivalent shown in Peck and Brown (1962). Their relationship was extended to elevations below 8000 ft-MSL through extrapolation. Mean areal snow-water-equivalent values were calculated for the upper and lower areas from this relationship and compared to the pseudo-observed values. In the upper area, the mean computed from the map was 23.6 in. and the pseudo-observed value was 20.4 in., whereas in the lower area, the mean computed from the map was 10.1 in. and the pseudo-observed value was 5.2 in.

Several attempts were made to adjust the map values until they were consistent with the pseudo-observed values for the upper and lower subareas. The lower area required significantly more adjustment than the upper area, however, and it was difficult to balance the necessary adjustments without producing a discontinuity in the snow-water-equivalent at the border separating the subareas.

It was not clear why the adjustments were needed, but several factors that could contribute to an explanation were recognized. The October through April precipitation map was based on the period 1931-

1960 and the mean pseudo-observed value was for the period 1949-1983. Although the periods are not the same, the mean precipitation at the stations used in the study for the period 1949-1983 agreed reasonably well with values from the October through April precipitation map. In addition, the relationship between October through April precipitation and April 1 snow-water-equivalent is extremely sensitive at the lower latitudes and elevations, since significant snowmelt occurs in these areas by April 1. Additional data or other factors may be needed to better define the relationship in these areas. The relationship was developed primarily from snow course data, but locations selected for snow courses may not be representative of a large portion of a basin. Snow courses are located in protected areas that typically accumulate and retain more snow than much of the surrounding area. An underestimate of the snow that falls in these areas, along with unrepresentative snow retention, could lead to an overestimate of April 1 mean snow-water-equivalent using these snow course data.

To avoid this inconsistency between the snow-water-equivalent from a mean April 1 map and the pseudo-observed values, a new relationship was developed to express the April 1 snow-water-equivalent as a function of the October through April precipitation and elevation. The form of the function is:

$$\frac{\text{SWE}}{\text{OAP}} = 1 - e^{-C_1 \left(\frac{E}{1000} - C_3 \right) C_2} \quad (4.19)$$

where, SWE = April 1 snow-water-equivalent,
 OAP = October-April precipitation,
 E = Elevation (ft. MSL), and
 C_1, C_2, C_3 = Constants.

This function produced the shape that one would expect, and it provided three coefficients that could be fit to data from the basin. The constant, C_3 , is the highest elevation, in thousands of feet, below which there is never significant snow on the ground on April 1. This elevation was assumed to be 7000 ft-MSL for the Animas, producing a value of 7 for C_3 . The constants, C_1 and C_2 , were estimated by trial and error adjustments until the mean areal snow-water-equivalent values for the upper and lower areas, predicted using the function, were equal to the pseudo-observed values. A plot of the resulting function is shown in Figure 4.17. The mean April 1 snow-water-equivalent field computed using this function and the October through April precipitation map is shown in Figure 4.18.

Peck and Schaake (1989) report that the average coefficient of variation of winter precipitation is 0.33 in the Upper Colorado Basin. The snow courses around the Animas indicated a somewhat higher coefficient of variation in the April 1 snow-water-equivalent. Initial interpolation runs assumed a constant coefficient of variation of 0.4 in estimating the standard deviation of the field. Under this assumption, an interpolated standardized deviate of -2.5 implies no snow on April 1. If it is assumed that the standardized deviates are identically distributed, it follows that each point has the same probability of having no snow. In general, one would expect areas with

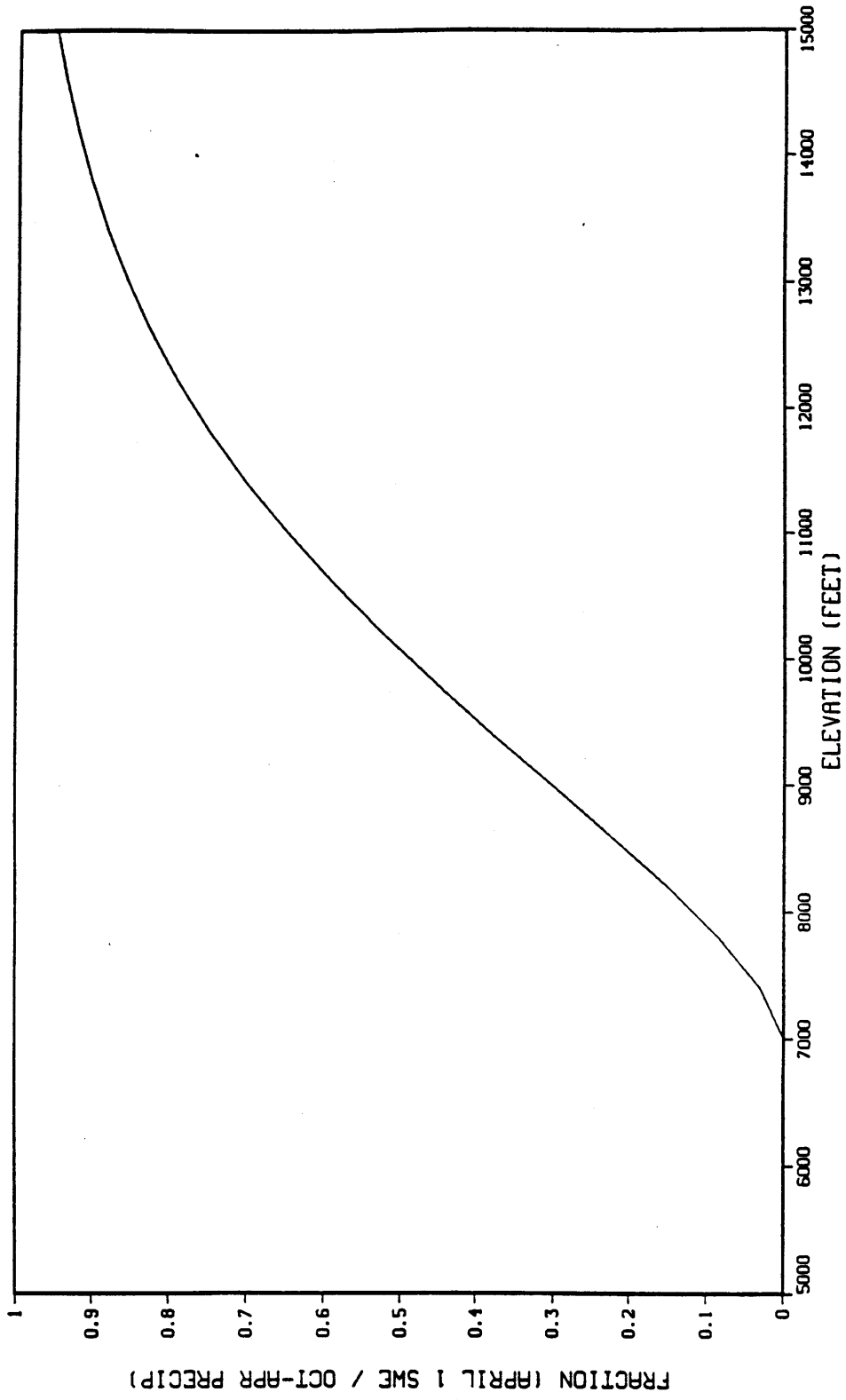


Figure 4.17 Function Used to Calculate Mean April 1 Snow-Water-Equivalent Map

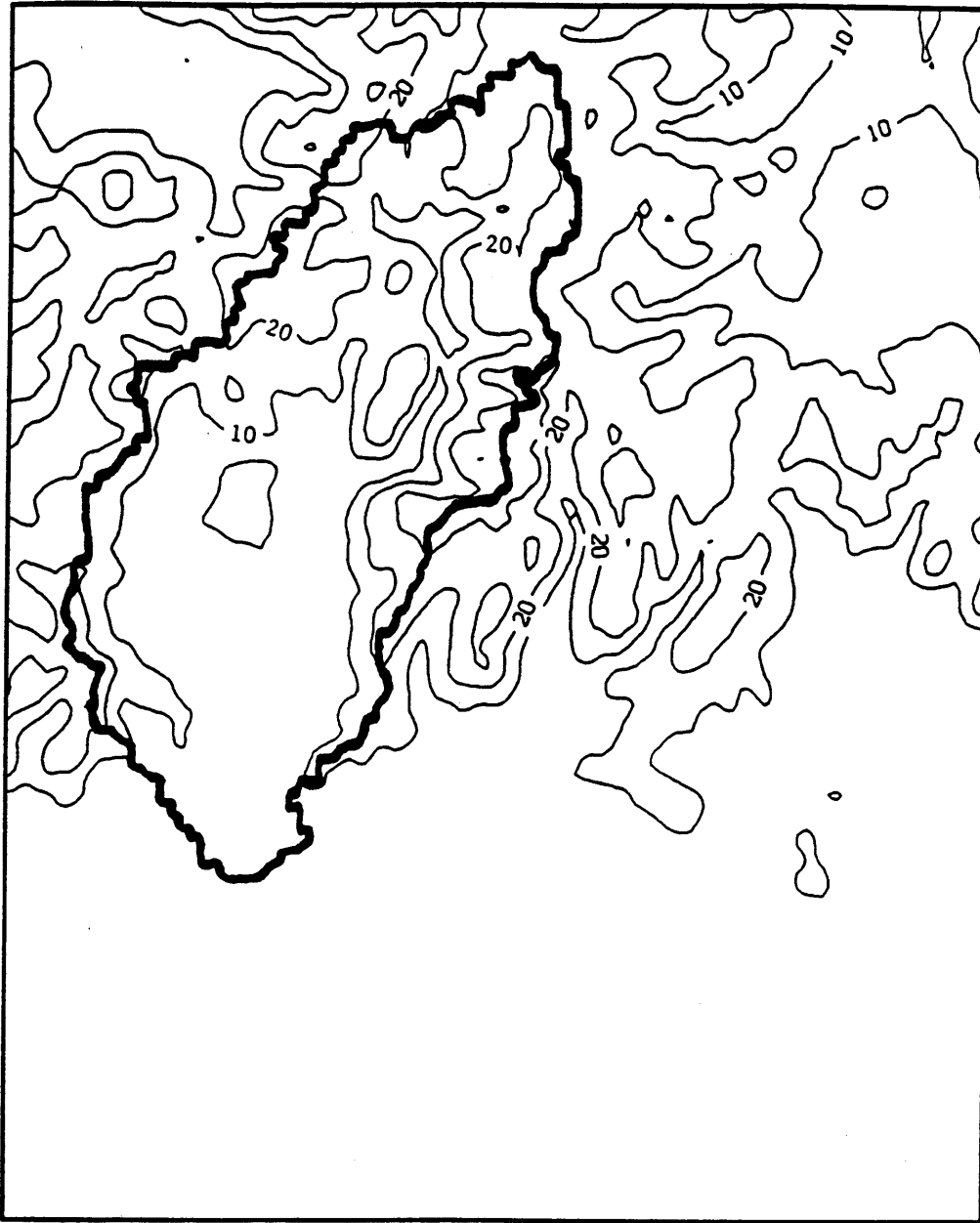


Figure 4.18 Mean April 1 Snow-Water-Equivalent Map (From Function) -
10 In. Isolines

little snow accumulation to have a much higher probability of having no snow on April 1 than areas with heavy snow accumulation. This apparent inconsistency occurs because areas with little snow accumulation have skewed distributions of snow-water-equivalent, but it also occurs because areas with little snow accumulation have coefficients of variation that are greater than those in areas with heavy snow accumulation. To account for this effect, it was assumed that the standard deviation could be expressed as:

$$S = C_1 \bar{x} C_2 \quad (4.20)$$

where, S = standard deviation of the snow-water-equivalent,
 \bar{x} = mean of the snow-water-equivalent, and
 C_1, C_2 = constants.

Several values of C_1 and C_2 were tested in the interpolation procedure. Adjustments to C_1 and C_2 produced slight improvements in the relationship between the pseudo-observed values and the interpolated snow-water-equivalent estimates for both areas, however, the year-to-year variability was still underestimated by the interpolation procedure in the lower area. Figure 4.19 is a plot of the function selected for April 1 with the snow course values also shown.

The correlation function was developed by fitting an exponential function of the form of equation (3.27) to the sample interstation correlation values. A more complicated form (Peck and Schaake, in press) that uses the geometric mean of the orographic component of precipitation between two points as an additional independent variable was also tested. When the more complicated correlation function was compared to the simple correlation function, however, by testing its performance in interpolating station values, its results were slightly inferior. The function used for April 1 is plotted with the sample values in Figure 4.20. It was noticed that several of the stations are responsible for much of the scatter in the plot. When these stations are removed, the correlation coefficient appears to decrease more slowly with distance. Despite this observation, the function was fit to the sample points from all of the stations, since this would probably be more representative of what could be expected throughout the basin. Three stations, however, (Ironton Park, Lake City, and Porcupine) were not used as estimator stations because the actual error was much larger than the predicted error at these stations, when they were estimated from the other stations. Table 4.13 shows the results from the tests of the interpolation procedure using all 13 stations as estimator stations and from using the 10 best stations as estimator stations.

Standardized deviates were calculated from the observations and interpolated for each historical year. Figures 4.21 and 4.22 show the fields of standardized deviates for 1971 and 1980, respectively. The resulting snow-water-equivalent fields are shown in Figures 4.23 and 4.24. The standardized deviates for 1971 were all negative, indicating that the basin had below normal snow accumulation, whereas the standardized deviates for 1980 were all positive, indicating that the basin had above normal snow accumulation. The snow-water-equivalent fields for each year were averaged over the upper and lower areas to

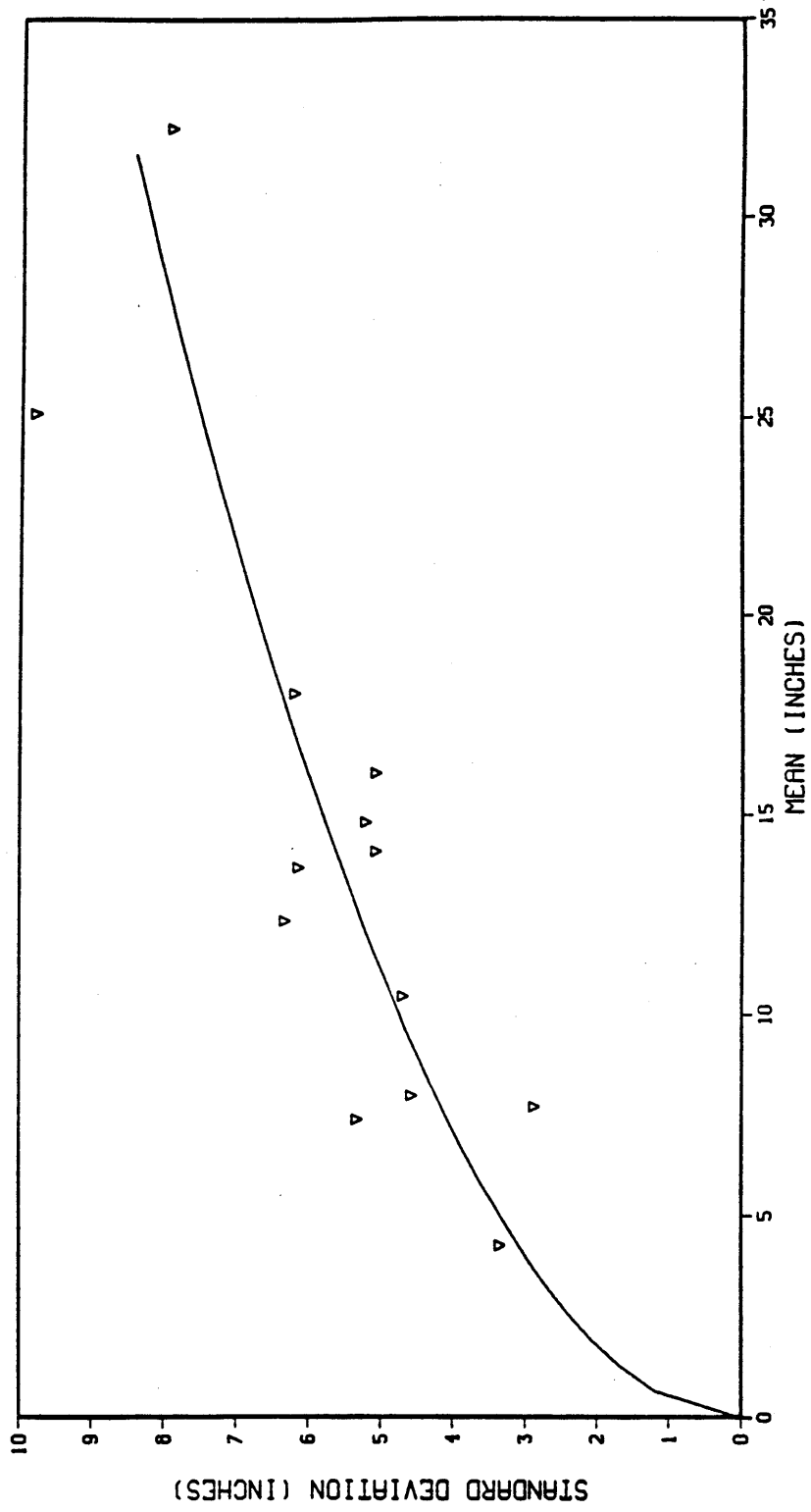


Figure 4.19 Standard Deviation Function - April 1

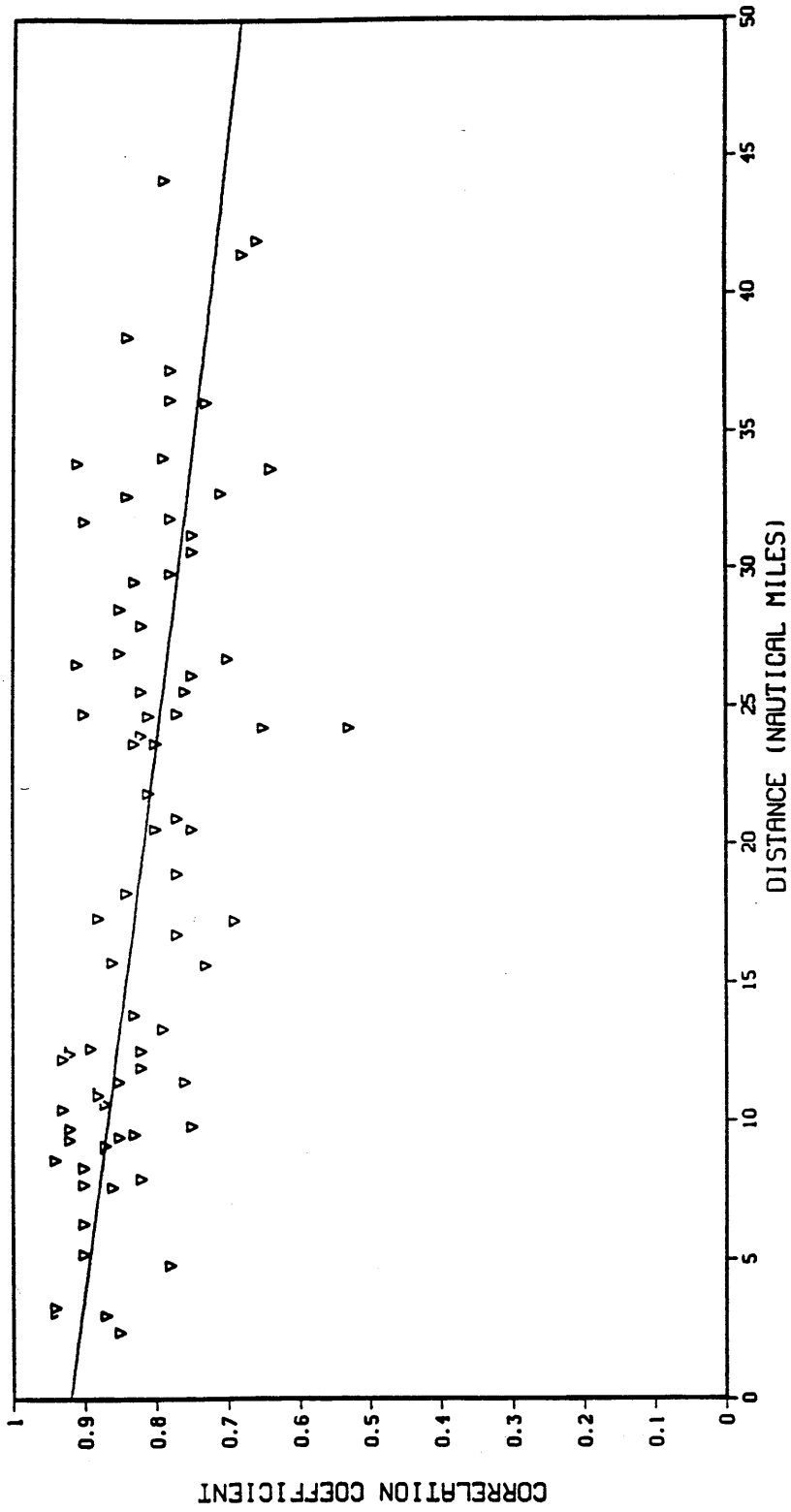


Figure 4.20 Correlation Function - April 1

Table 4.13

Station Interpolation Test Results (April 1)

Squared Errors in Interpolated Standardized Deviates

<u>Station</u>	No. of <u>Observations</u>	13 Stations		10 Stations	
		<u>Actual</u>	<u>Predicted</u>	<u>Actual</u>	<u>Predicted</u>
Lizard Head	35	.134	.134	.127	.134
Cascade	35	.095	.145	.097	.145
Ironton Park	34	.327	.158	-	-
Lake City	33	.302	.184	-	-
Trout Lake	35	.169	.130	.195	.132
Spud Mountain	33	.103	.124	.092	.124
Molas Lake	33	.140	.131	.148	.132
Mineral Creek	33	.070	.121	.070	.125
Red Mountain Pass	33	.119	.126	.099	.142
Upper Rio Grande	35	.125	.169	.114	.188
Santa Maria	35	.166	.148	.105	.218
Porcupine	33	.250	.133	-	-
Rico	35	<u>.195</u>	<u>.184</u>	<u>.195</u>	<u>.184</u>
		.167	.146	.126	.154

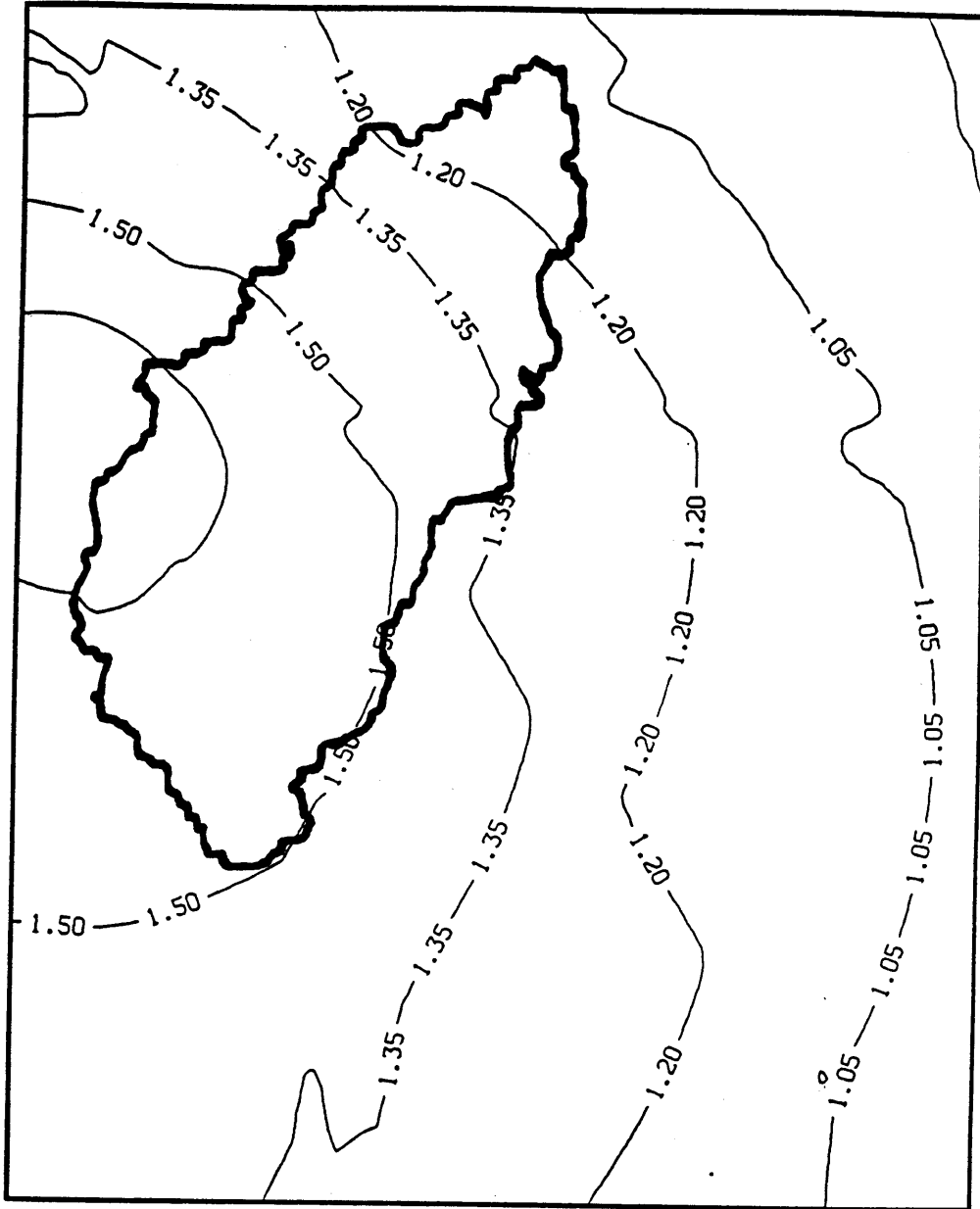


Figure 4.22 1980 Standardized Deviate Field

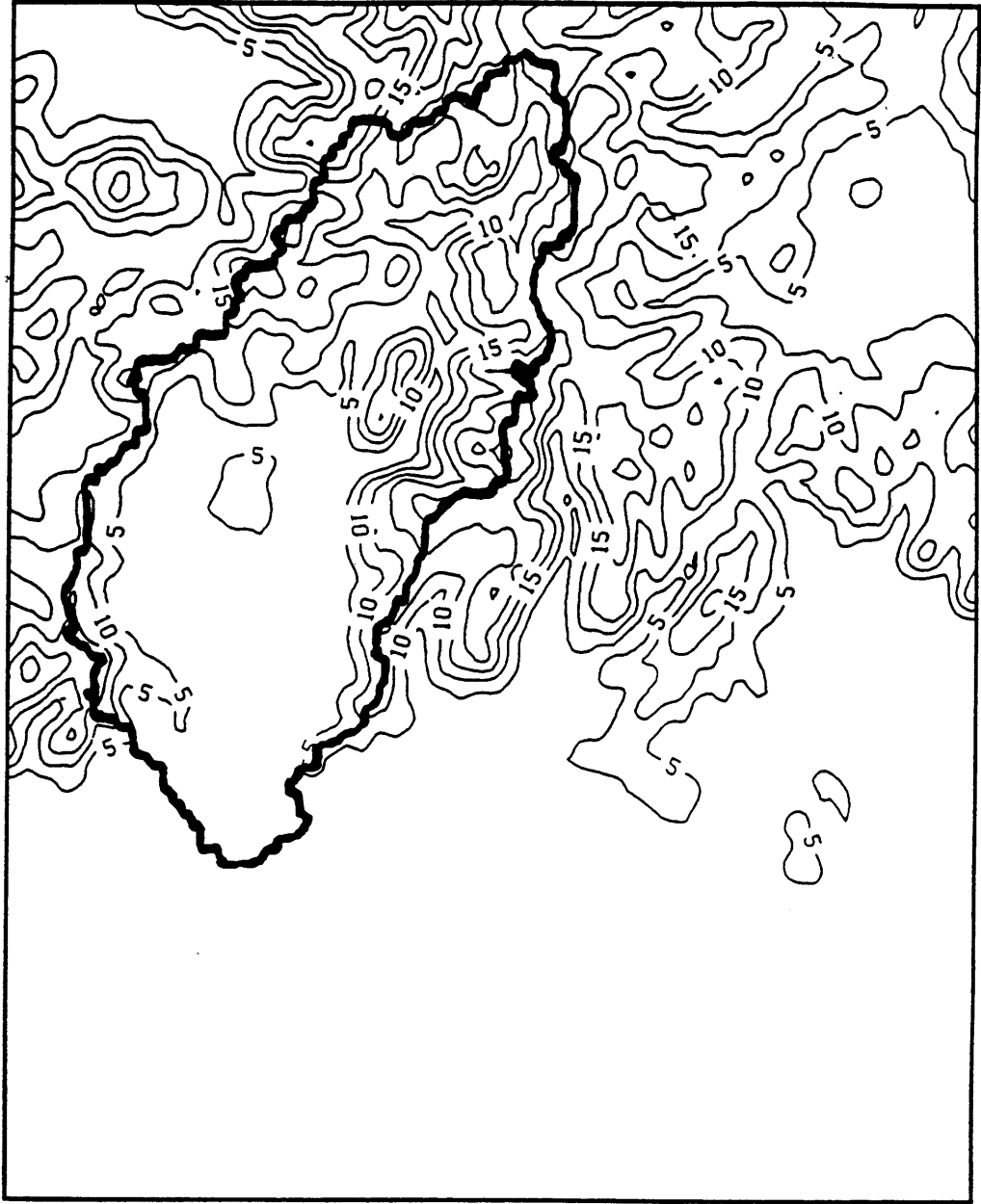


Figure 4.23 1971 Interpolated Snow-Water-Equivalent Map - 5 In. Isolines

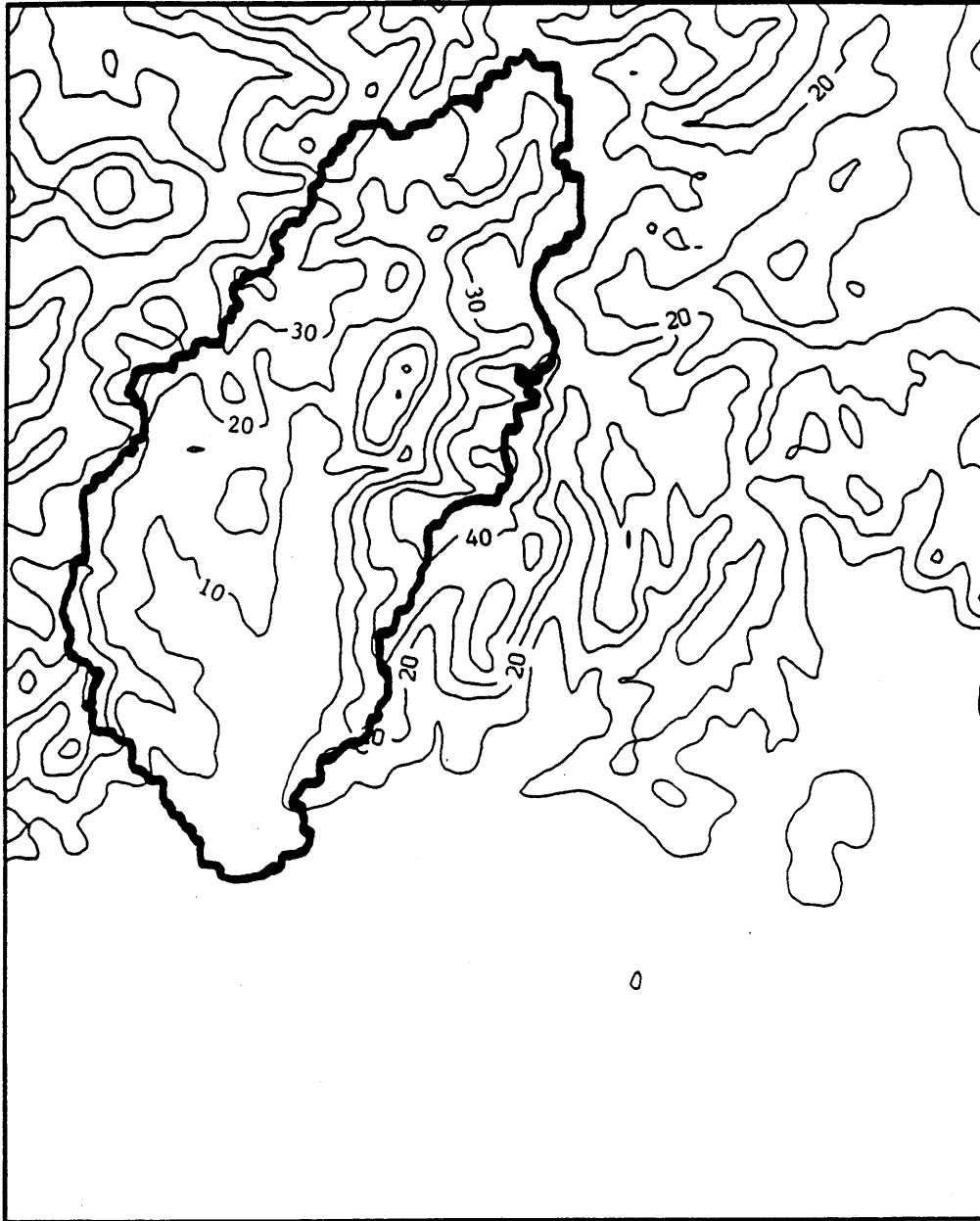


Figure 4.24 1980 Interpolated Snow-Water-Equivalent Map - 10 In. Isolines

produce areal estimates of snow-water-equivalent. The pseudo-observed values are plotted against the areal estimates from the interpolation procedure in Figure 4.25 for the upper area and Figure 4.26 for the lower area.

The final step in preparing estimates of observations of the model states using the interpolation approach is a regression step. This step adjusts for the fact that the model states may not correspond to the actual areal water-equivalent, and for the fact that there may be a bias in the interpolated estimates. A regression equation of the form given in equation (3.24) is developed between the pseudo-observed values and the areal snow-water-equivalent estimates from the interpolation procedure. For the purpose of verification, a separate regression equation was developed to predict each year, neglecting that year's data. Figures 4.27 and 4.28 show the pseudo-observed values plotted against these estimates for the upper and lower areas, respectively. The measurement error variance, R , was estimated as the square of the RMS error between the pseudo-observed values and the estimates from the interpolation regression equations. R was estimated to be 2700 for the upper area and 1000 for the lower area. The model states were updated each April 1 with the estimated observations of the model states using these values for R . Table 4.14 gives the streamflow statistics from the updating run. These statistics can be compared to the statistics given in Table 4.10 for the updating run with the observations derived using the regression approach. The results based on the interpolation approach are at least as good as, and in some cases slightly better than those based on the regression approach. Figure 4.29 is a plot of the observed seasonal volumes versus the updated seasonal volumes using the interpolation approach.

Spatial Interpolation Approach-Other Months

In order to apply the spatial interpolation approach to other months, mean snow-water-equivalent fields are needed for each of the months. In determining the mean snow-water-equivalent field for April 1, it was assumed that a simple elevation relationship could be used to adjust October through April precipitation. Assuming that the spatial pattern of precipitation is reasonably consistent throughout the winter, it may be possible to derive similar relationships for other months during the accumulation season. After April 1, however, significant snowmelt occurs at the lower elevations. As snowmelt is a function of many factors other than elevation, a simple function can not adequately describe the spatial variability of melt in the basin, even on an average basis. One way to define this spatial variability of melt is to actually model the melt at different points throughout the basin. This could provide a technically sound methodology for determining monthly mean snow-water-equivalent values throughout the accumulation and melt seasons.

An elevation data base was available for the area with data spaced at every 30 seconds of latitude and 30 seconds of longitude, a grid size that would provide an appropriate level of spatial detail for basins the size of the Animas. The elevation data base was used to compute aspect and slope at all of the grid points. A fire fuel data base, derived

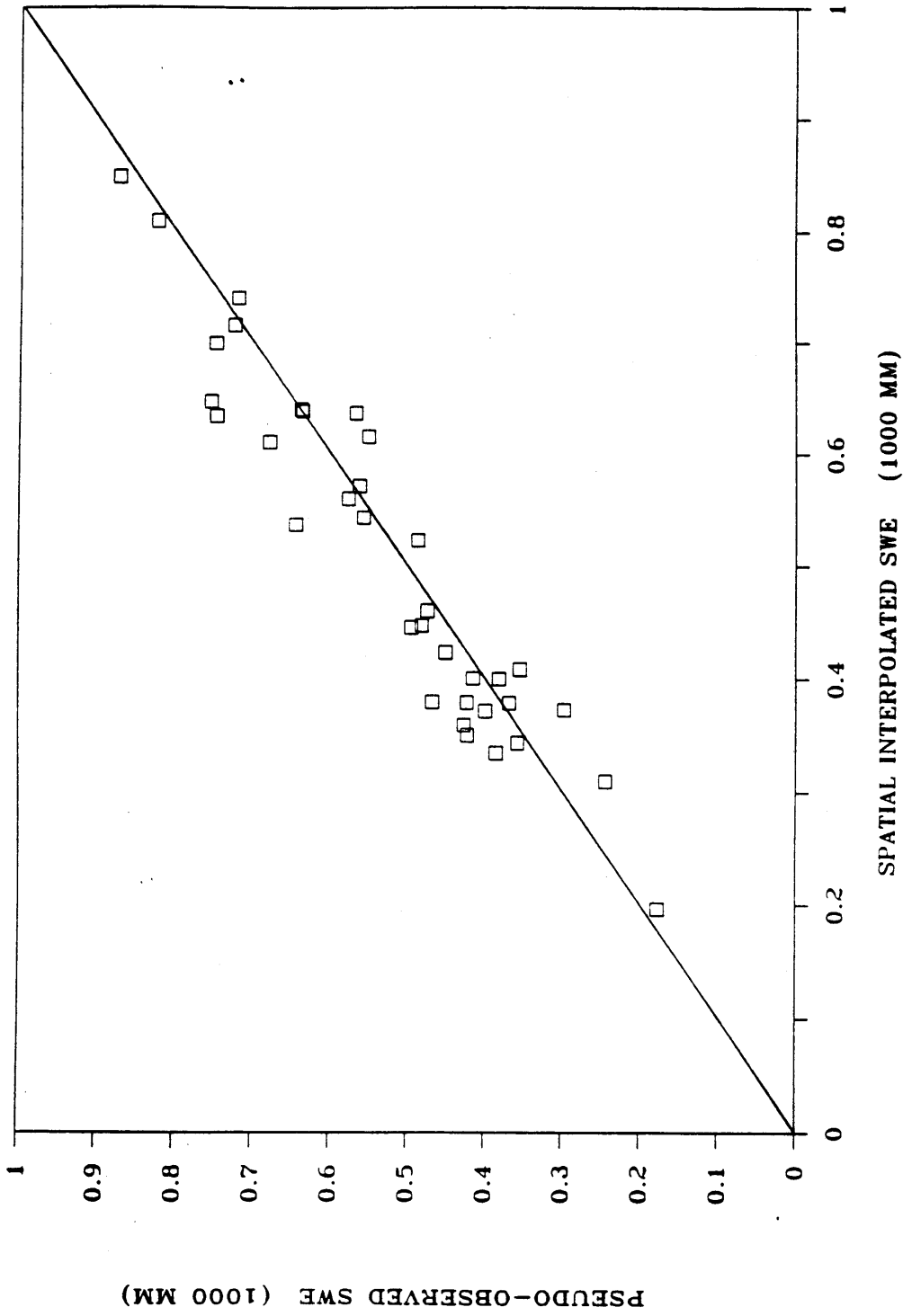


Figure 4.25 Pseudo-Observed vs. Interpolated Snow-Water-Equivalent (Upper Area - April - 1)

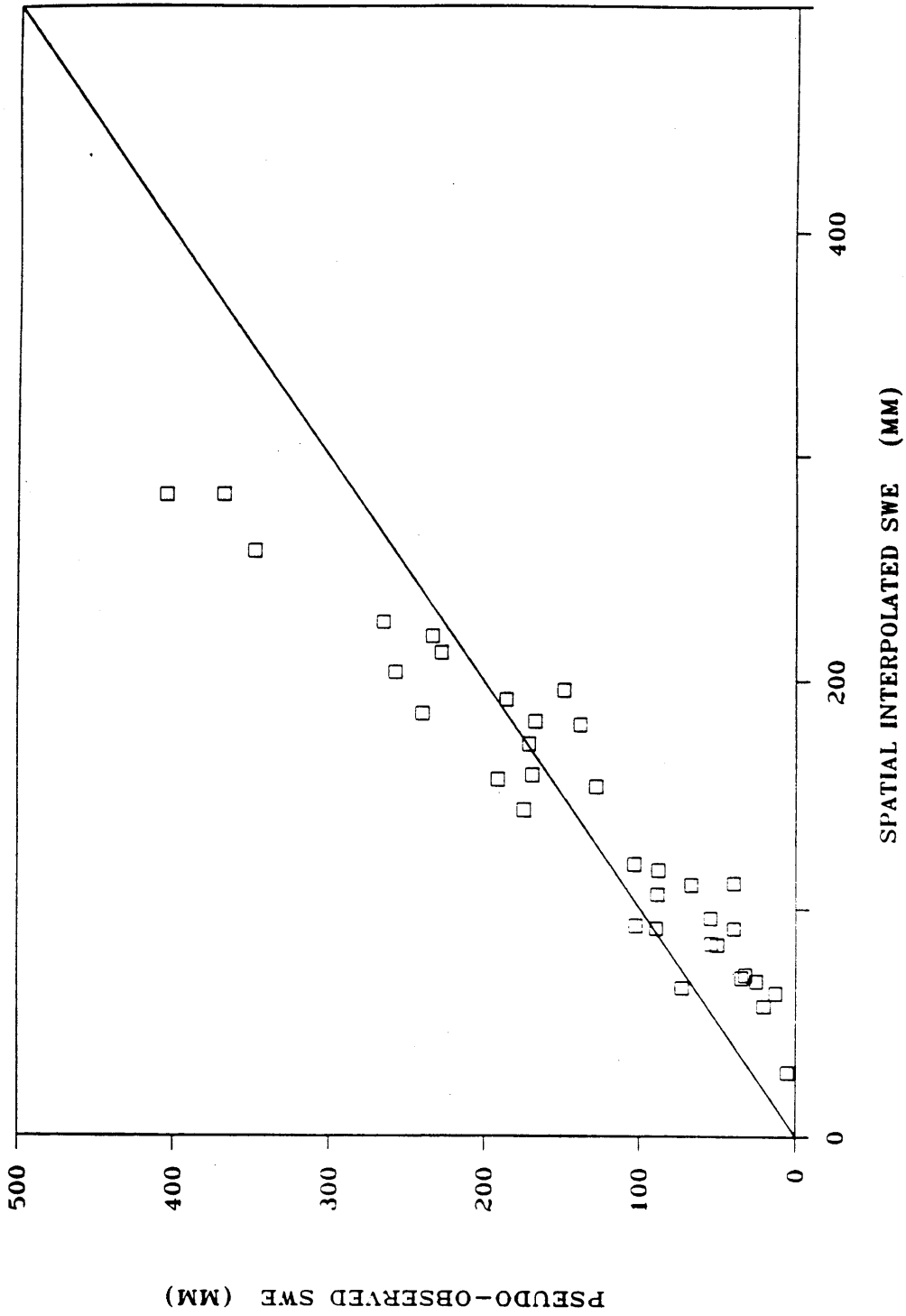


Figure 4.26 Pseudo-Observed vs. Interpolated Snow-Water-Equivalent (Lower Area - April 1)

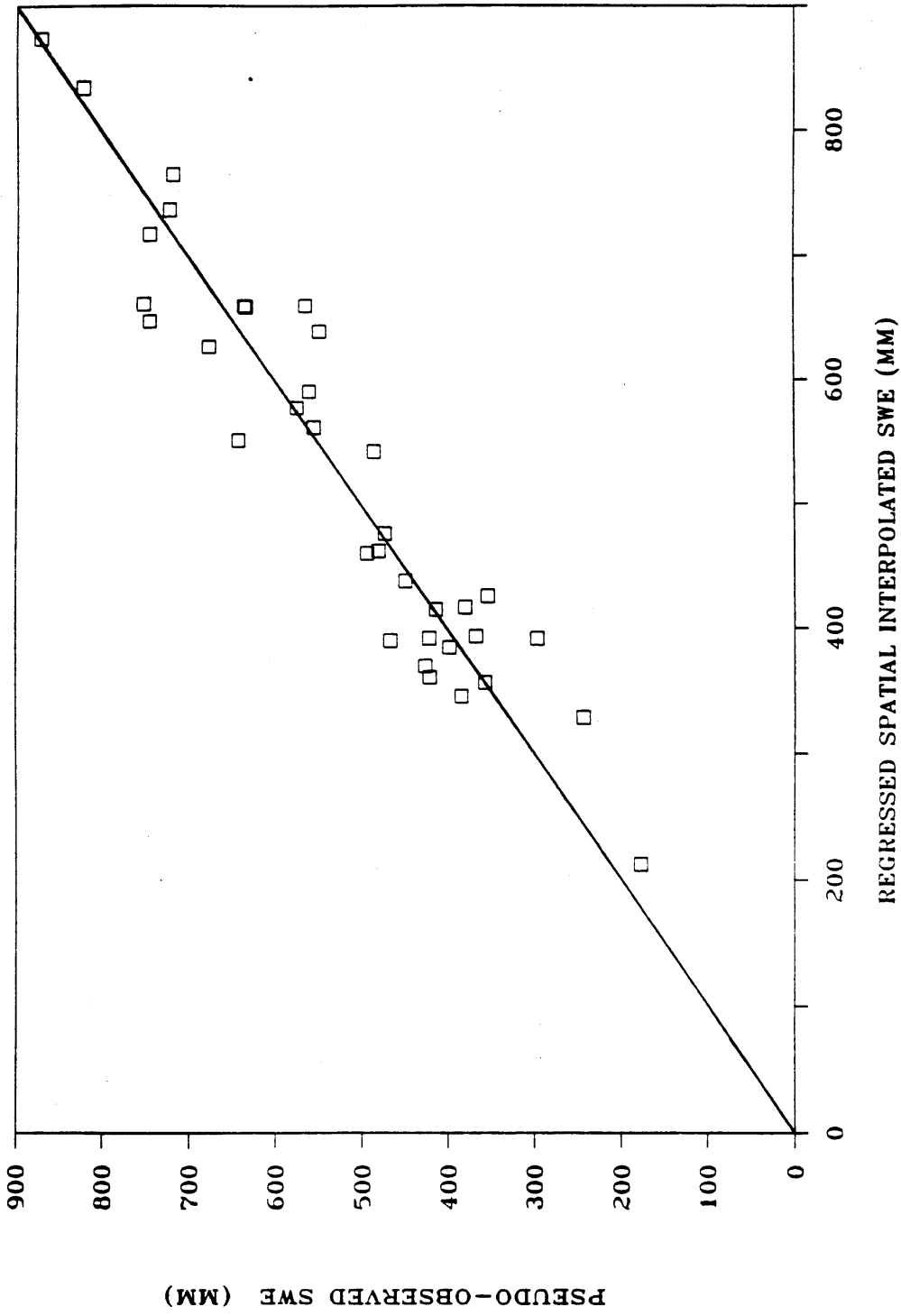


Figure 4.27 Pseudo-Observed vs. Regressed Spatial Interpolated Snow-Water-Equivalent (Upper Area - April 1)

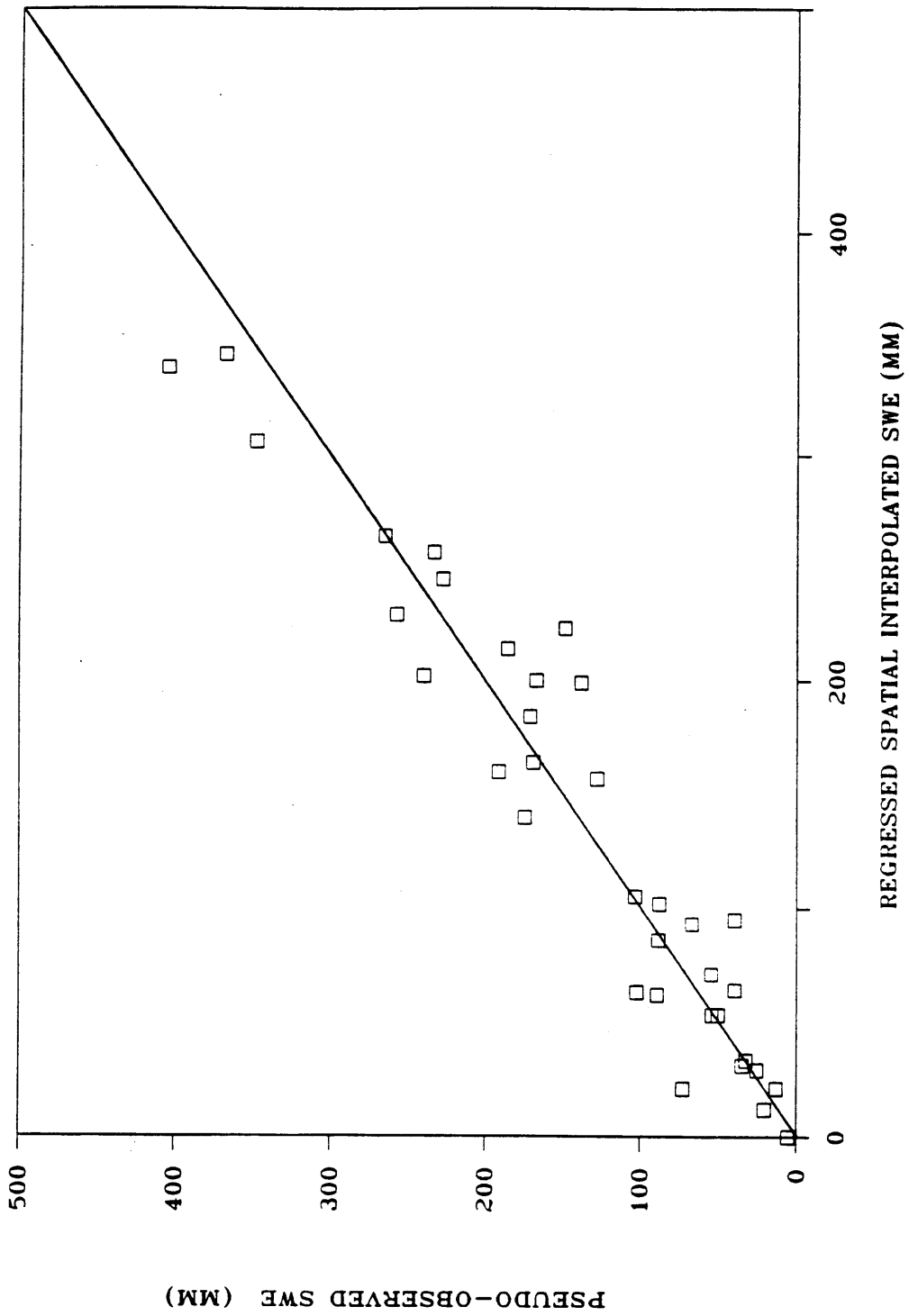


Figure 4.28 Pseudo-Observed vs. Regressed Spatial Interpolated Snow-Water-Equivalent (Lower Area - April 1)

Table 4.14

Streamflow Error Statistics - Updated with Interpolation

<u>Daily</u>	<u>Updated (April 1)</u>
Avg. Absolute Error (cmsd)	4.50
RMS Error (cmsd)	8.47
Correlation Coefficient	.958
 <u>Monthly</u>	
Avg. Absolute Error (mm)	4.51
RMS Error (mm)	7.39
 <u>Seasonal (April - September)</u>	
Average Error (10^6m^3)	1.0
Absolute Max. Error (10^6m^3)	116.7
Avg. Absolute Error (10^6m^3)	37.0
RMS Error (10^6m^3)	48.6
Bias (%)	0.2
Correlation Coefficient	.977

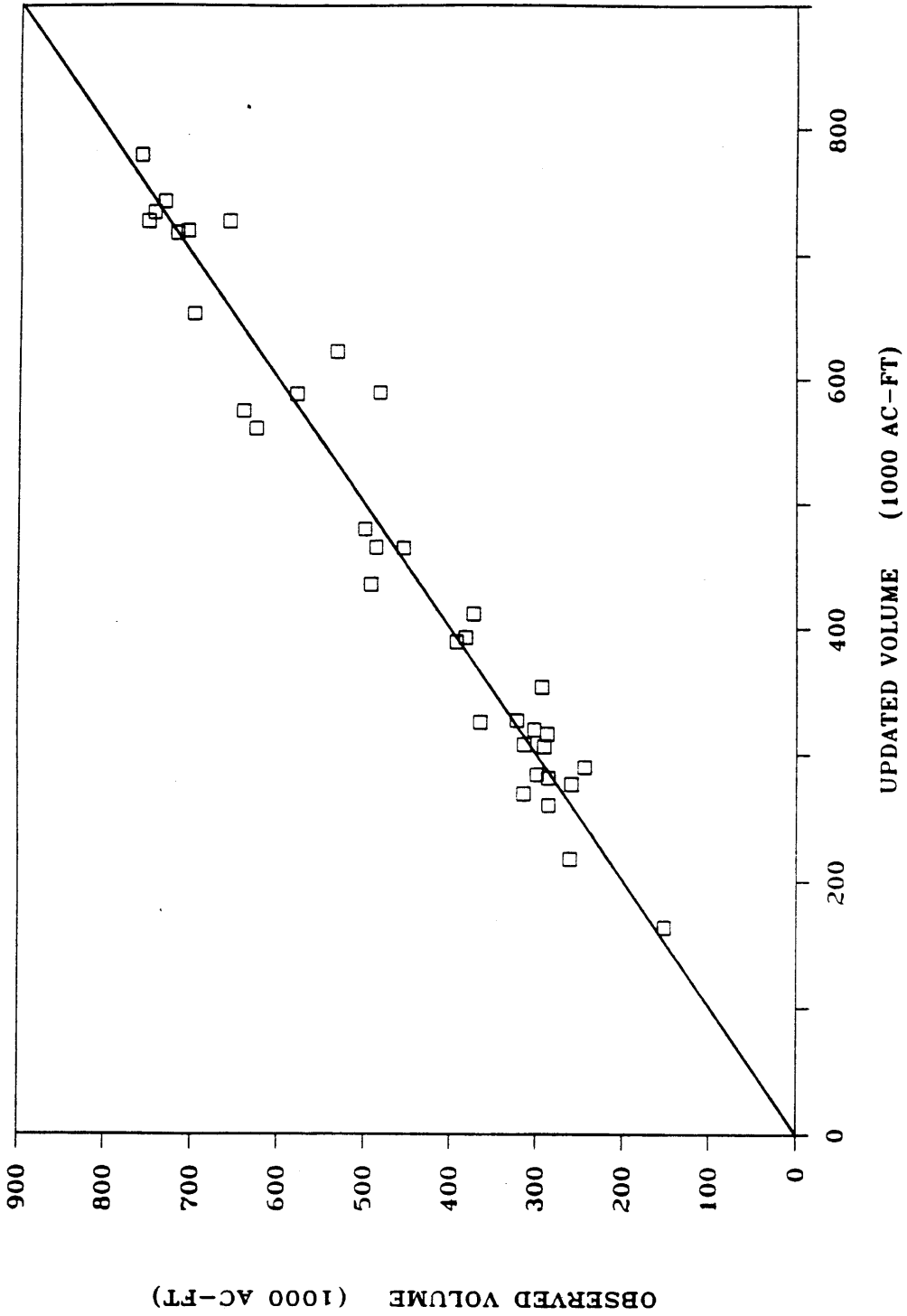


Figure 4.29 Observed vs. April 1 Updated (Interpolation) Seasonal Streamflow Volumes

from satellite images, was obtained from the Bureau of Land Management and used to determine which grid points were forest covered. Performing melt computations at each grid point would require a prohibitive amount of computer resources. To avoid this, grid points were assigned to zones based on melt characteristics. Table 4.15 shows how the various basin characteristics which affect melt are distributed in the Animas Basin. As discussed in Chapter 3, zones were classified by aspect as north-facing, south-facing, or horizontal. Grid points were assigned to horizontal zones if their aspect was east-facing, west-facing, or if their slope was less than 10 percent. It was assumed that the melt factor in a north-facing zone was 0.7 times the melt factor in a horizontal zone, and that the melt factor in a south-facing zone was 1.2 times the melt factor in a horizontal zone. It was also assumed that the melt factor in a forested zone was 0.7 times the melt factor in a non-forested zone. Using these relationships, it was possible to assign melt factors to each zone, once values were assumed for a horizontal, non-forested zone. The melt factors used in the lumped model were used as initial estimates of the melt factors for the horizontal, non-forested zone, and zone melt computations were performed for 36 zones. When the monthly snow accounting procedure described in Chapter 3 was applied to the Animas, no melt factor adjustments were required.

The resulting mean snow-water-equivalent maps for February 1, March 1, April 1, and May 1 are shown in Figures 4.30, 4.31, 4.32, and 4.33, respectively. Table 4.16 compares the mean area snow-water-equivalent values derived from the spatial model to the snow-water-equivalent values from the lumped model. The basin totals agree quite closely, but the spatial model estimates more snow in the lower area and less snow in the upper area than the lumped model on May 1.

As a qualitative check of these grid point snowmelt calculations, the average snow line predicted by the monthly mean maps was compared to a series of areal snow cover maps derived from satellite photographs for 1985 and 1986. There appeared to be reasonable agreement in the way snow cover retreated, except along the ridge on the southwest edge of the basin. The modeling results showed that the snow cover is not depleted in this area as quickly as the satellite photographs indicated. This could be due to an overestimate of the precipitation in this area or an underestimate of the melt rates.

Equation (4.20) was used to estimate the standard deviation of the snow-water-equivalent at each grid point. Figures 4.34, 4.35, and 4.36 show the functions plotted with the sample points for February 1, March 1, and May 1, respectively. Equation (3.27) was used to estimate the correlation function for each of the months. The functions used for February 1 and March 1 were very similar to the equation used for April 1, and are shown plotted with the sample points in Figures 4.37 and 4.38, respectively. The same 10 stations, which were used to estimate April 1 snow-water-equivalent, were also used to estimate February 1 and March 1 snow-water-equivalent. A different approach was taken for May 1, since many of the stations frequently reported zero snow-water-equivalent on May 1. These stations were eliminated from the May 1 analysis, leaving 7 stations to estimate the correlation function and to perform the interpolation. The correlation function and sample

Table 4.15

Animas Basin Characteristics

Fraction of the Basin in Each Category

Aspect	<u>North</u>	<u>East</u>	<u>South</u>	<u>West</u>
	.16	.33	.20	.31

Slope	<u><10%</u>	<u>>10%</u>
	.24	.76

Forest Cover	<u>Forested</u>	<u>Non-Forested</u>
	.50	.50

Elevation	<u><8000ft</u>	<u>8-9000ft</u>	<u>9-10000ft</u>	<u>10-11000ft</u>	<u>11-12000ft</u>	<u>>12000ft</u>
	.10	.15	.20	.23	.17	.15

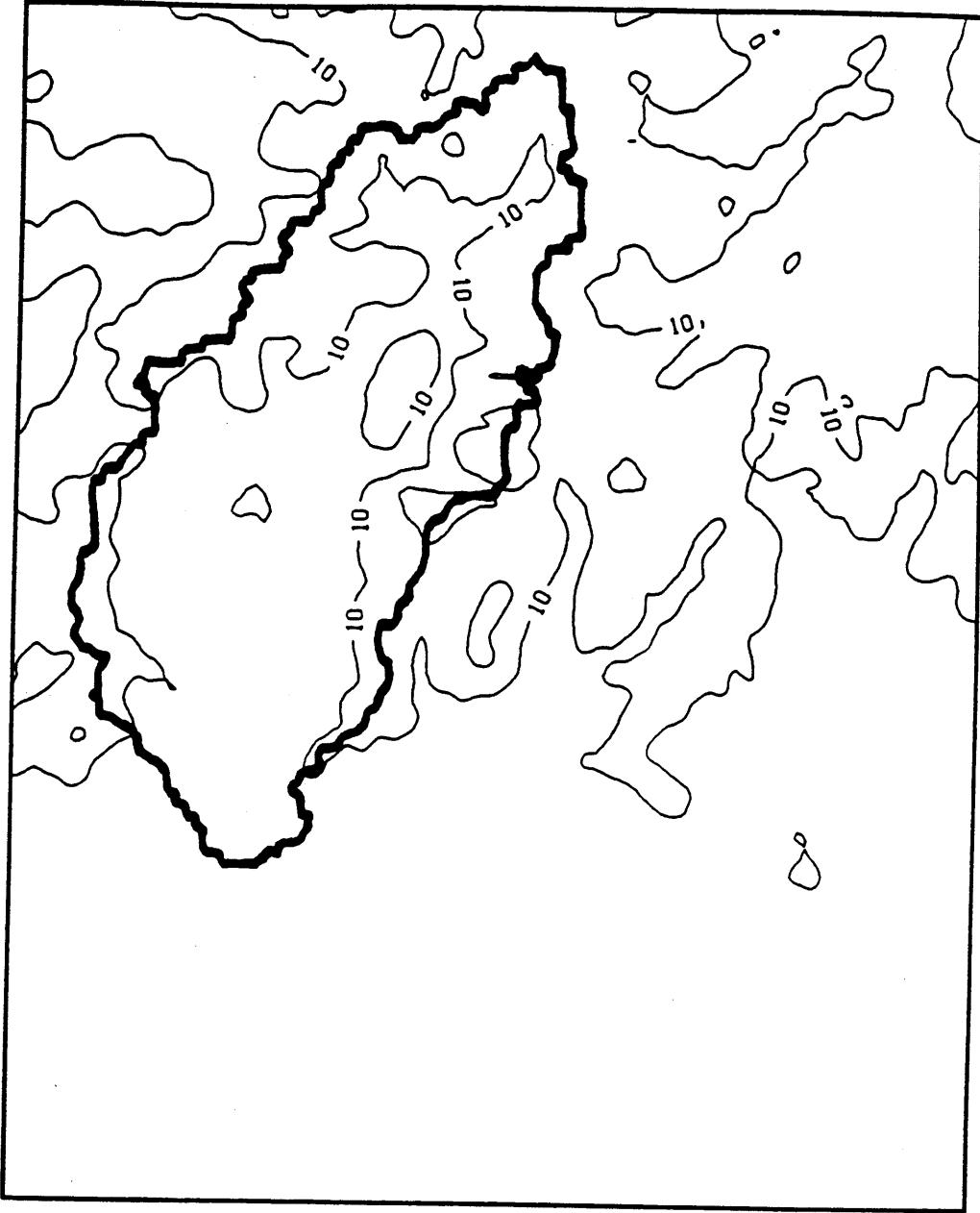


Figure 4.30 Mean February 1 Snow-Water-Equivalent Map (From Spatial Melt Analysis) - 10 In. Isolines

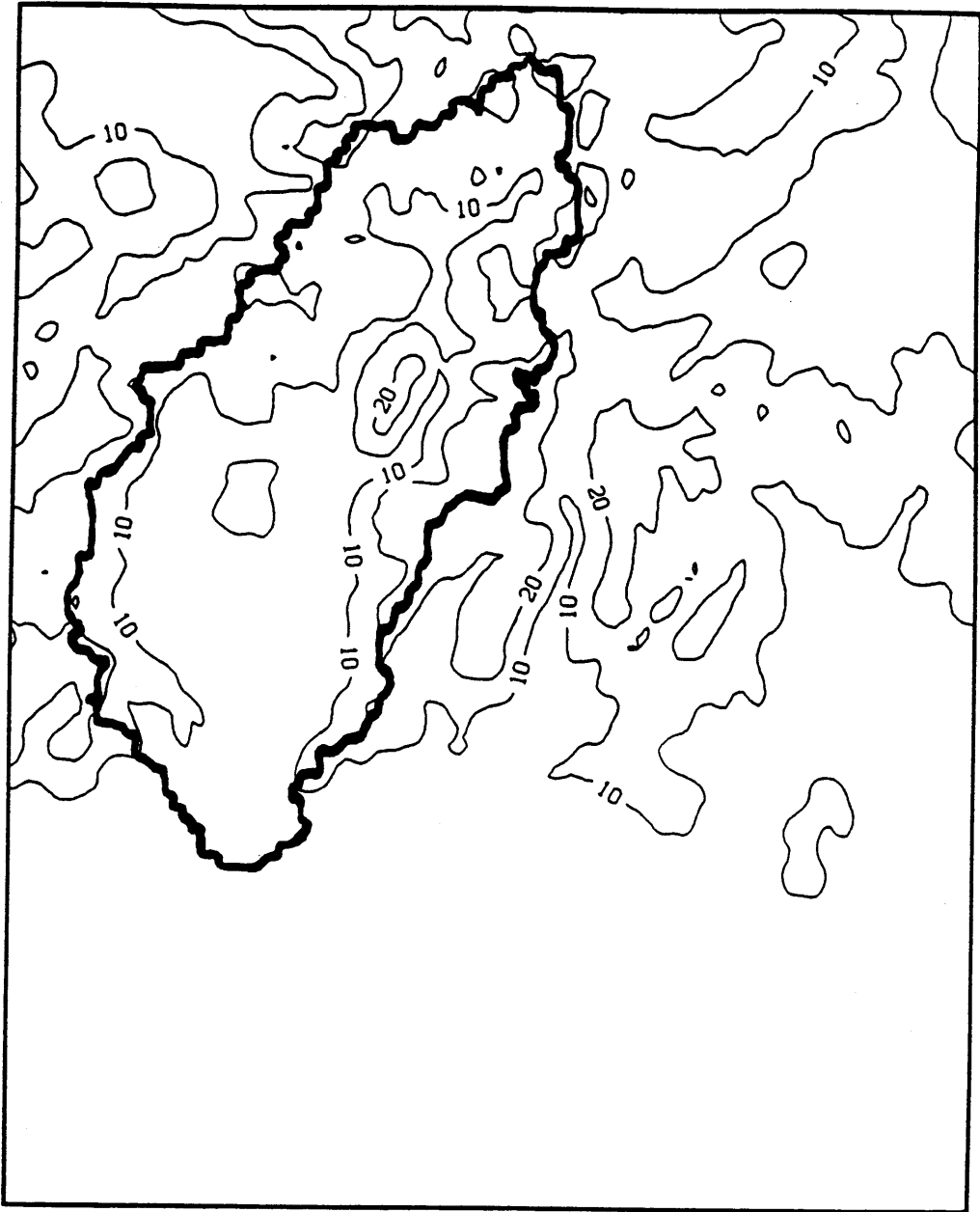


Figure 4.31 Mean March 1 Snow-Water-Equivalent Map (From Spatial Melt Analysis) - 10 In. Isolines

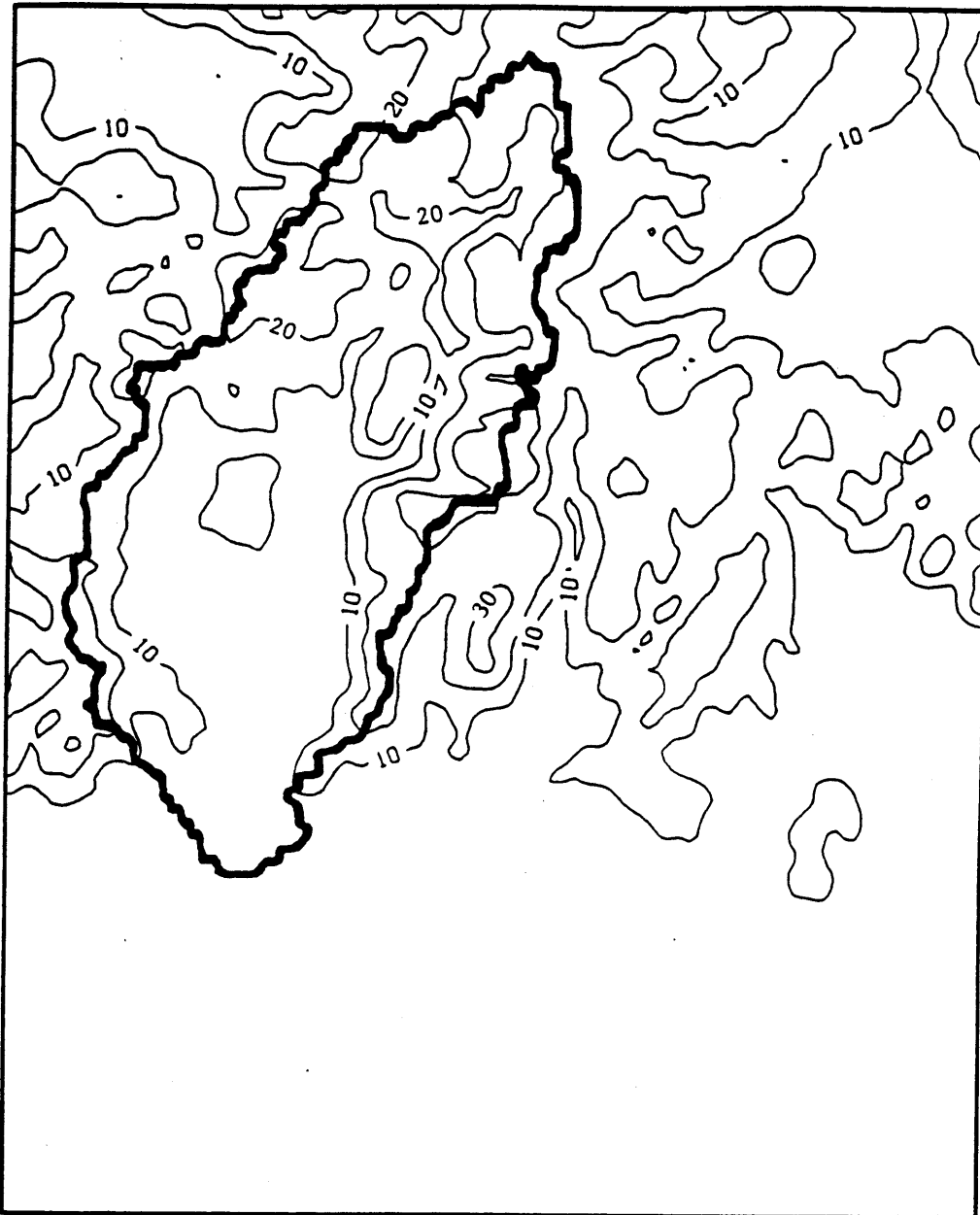


Figure 4.32 Mean April 1 Snow-Water-Equivalent Map (From Spatial Melt Analysis) - 10 In. Isolines

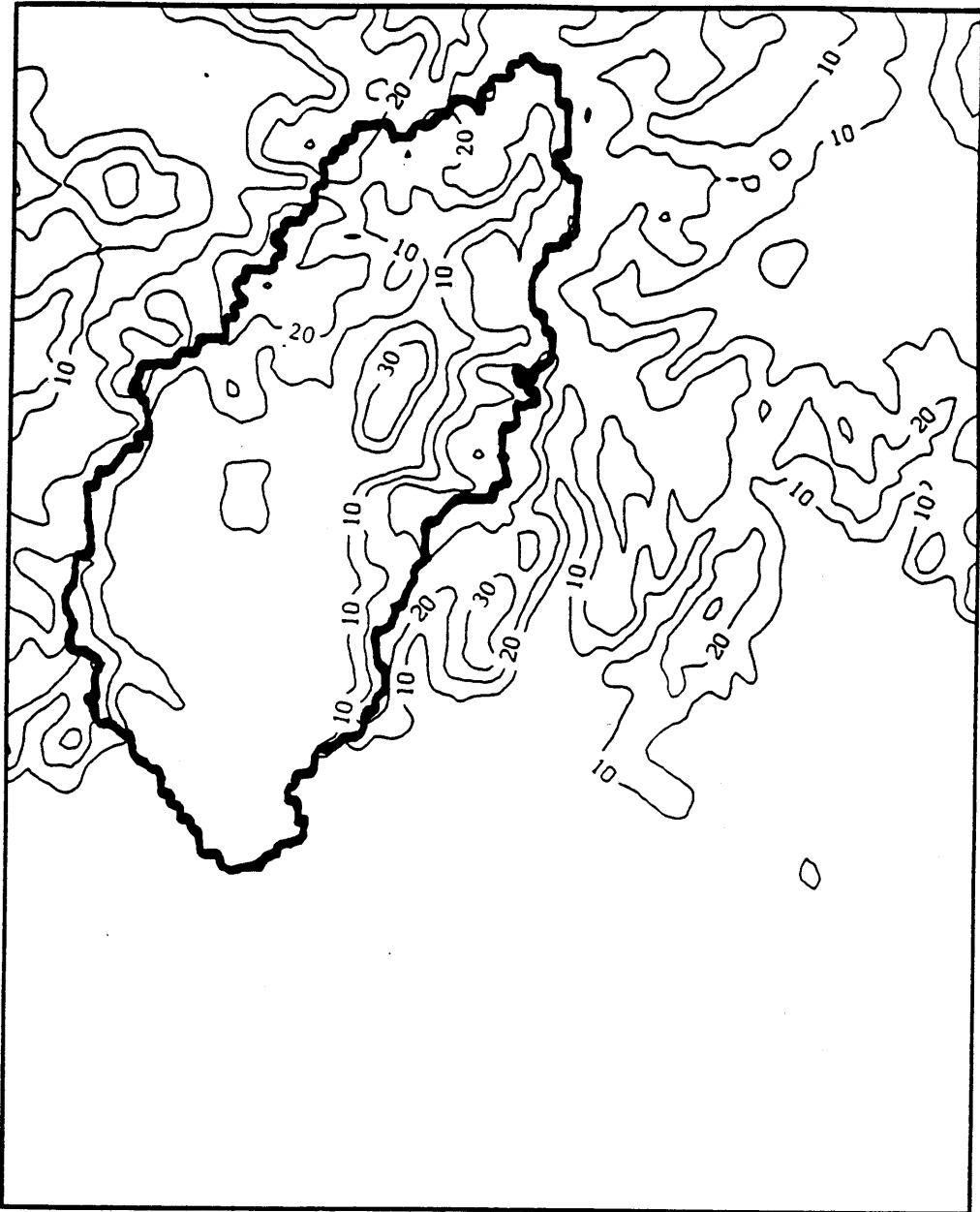


Figure 4.33 Mean May 1 Snow-Water-Equivalent Map (From Spatial Melt Analysis) - 10 In. Isolines

Table 4.16
Comparison of Spatial Model to Lumped Model

Mean Areal Snow-Water-Equivalent (mm)

Spatial Model

	<u>Feb 1</u>	<u>Mar 1</u>	<u>Apr 1</u>	<u>May 1</u>	<u>June 1</u>
Upper Area	341	419	508	514	299
Lower Area	<u>116</u>	<u>140</u>	<u>141</u>	<u>79</u>	<u>11</u>
	457	559	649	593	310

Lumped Model

	<u>Feb 1</u>	<u>Mar 1</u>	<u>Apr 1</u>	<u>May 1</u>	<u>June 1</u>
Upper Area	340	418	512	534	300
Lower Area	<u>127</u>	<u>152</u>	<u>137</u>	<u>45</u>	<u>0</u>
	467	570	649	579	300

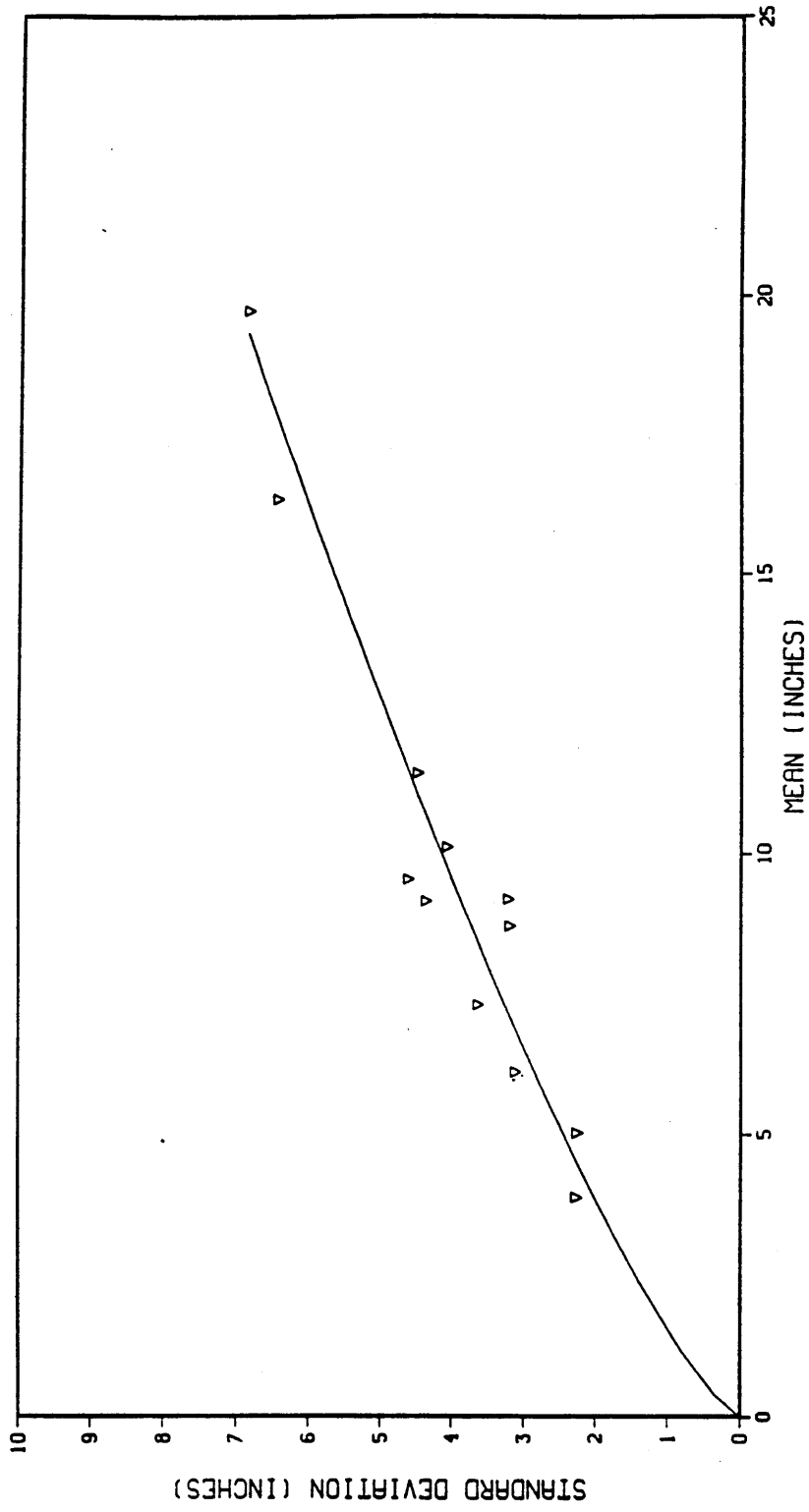


Figure 4.34 Standard Deviation Function - February 1

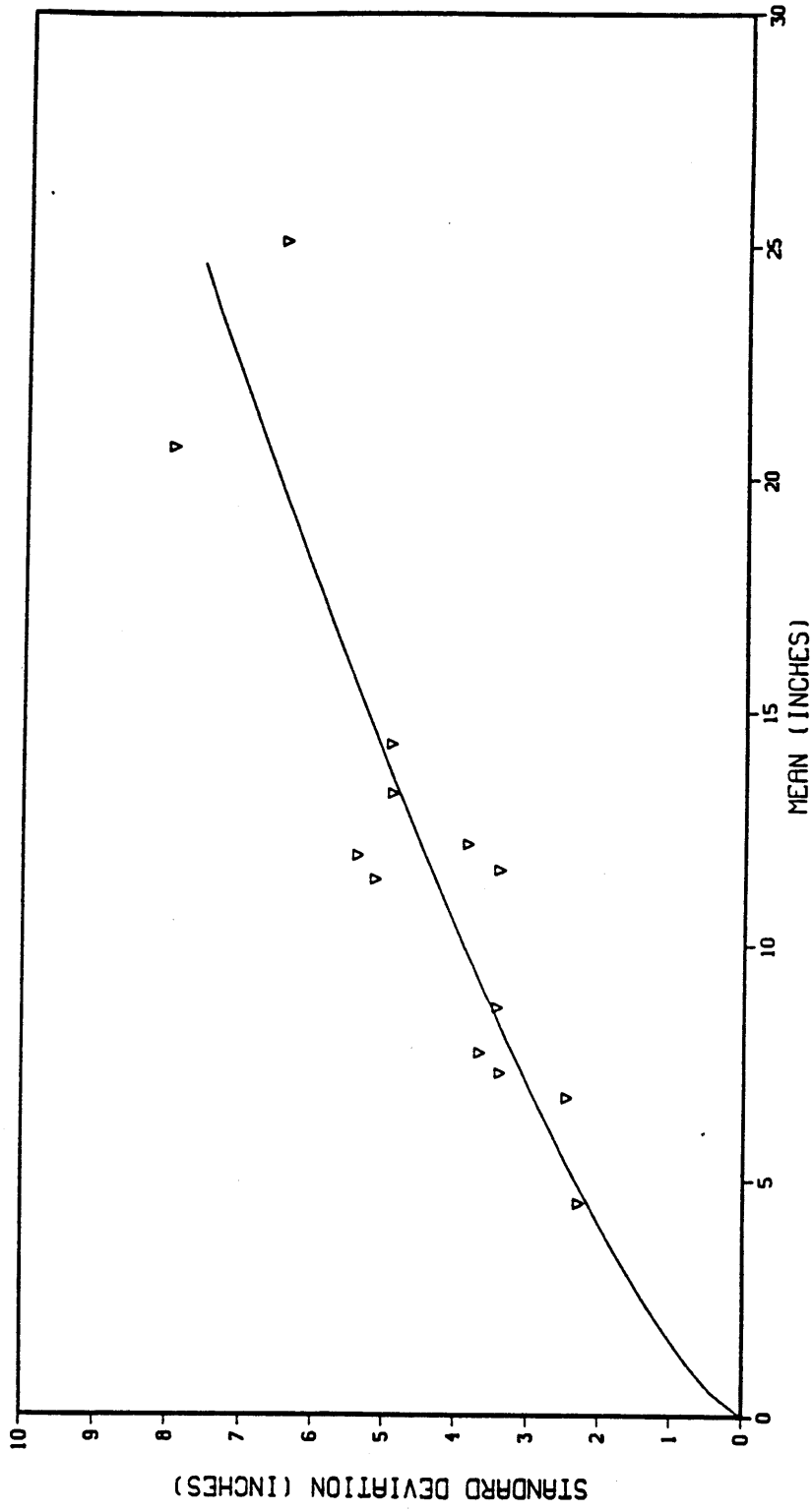


Figure 4.35 Standard Deviation Function - March 1

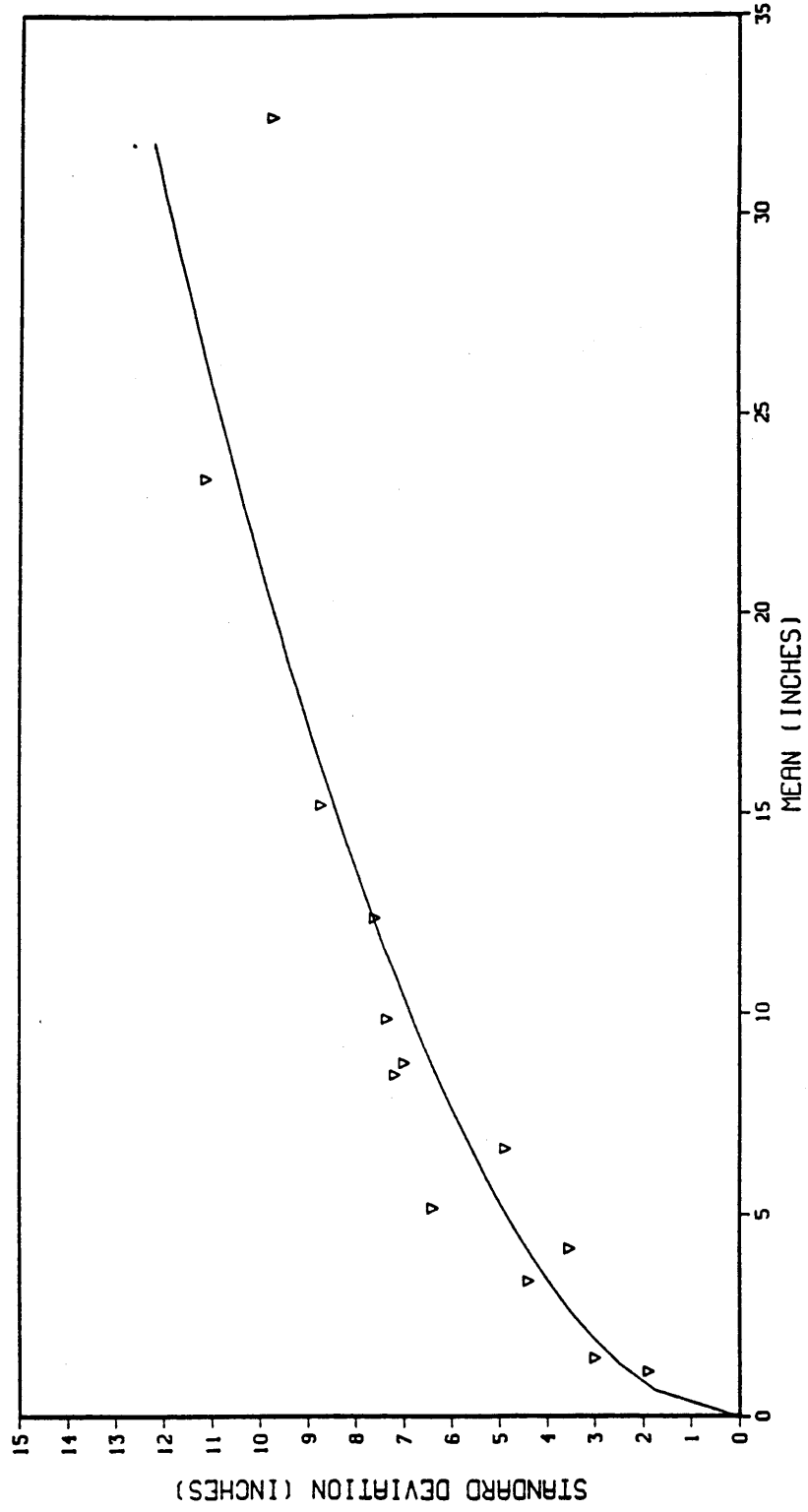


Figure 4.36 Standard Deviation Function - May 1

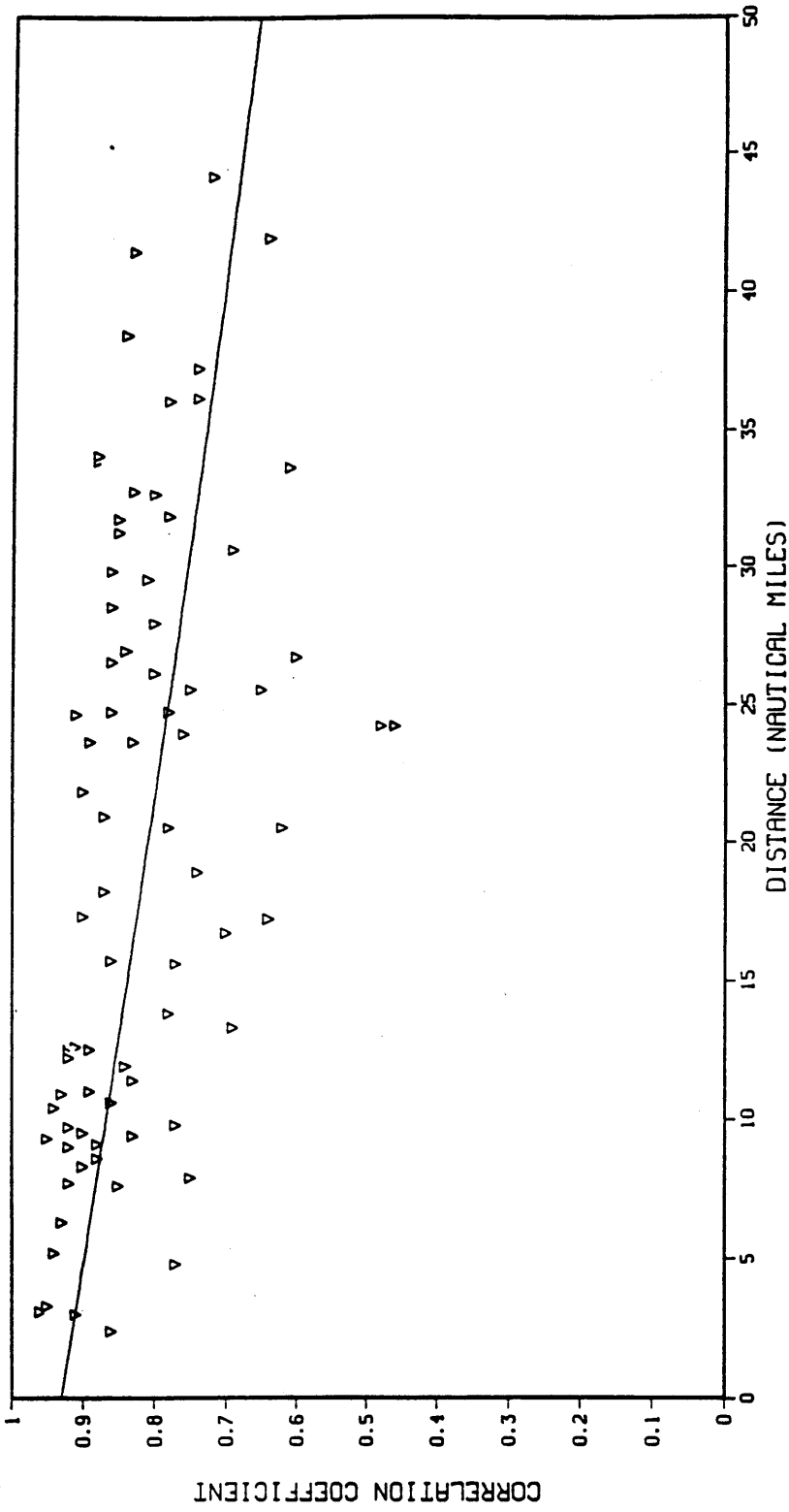


Figure 4.37 Correlation Function - February 1

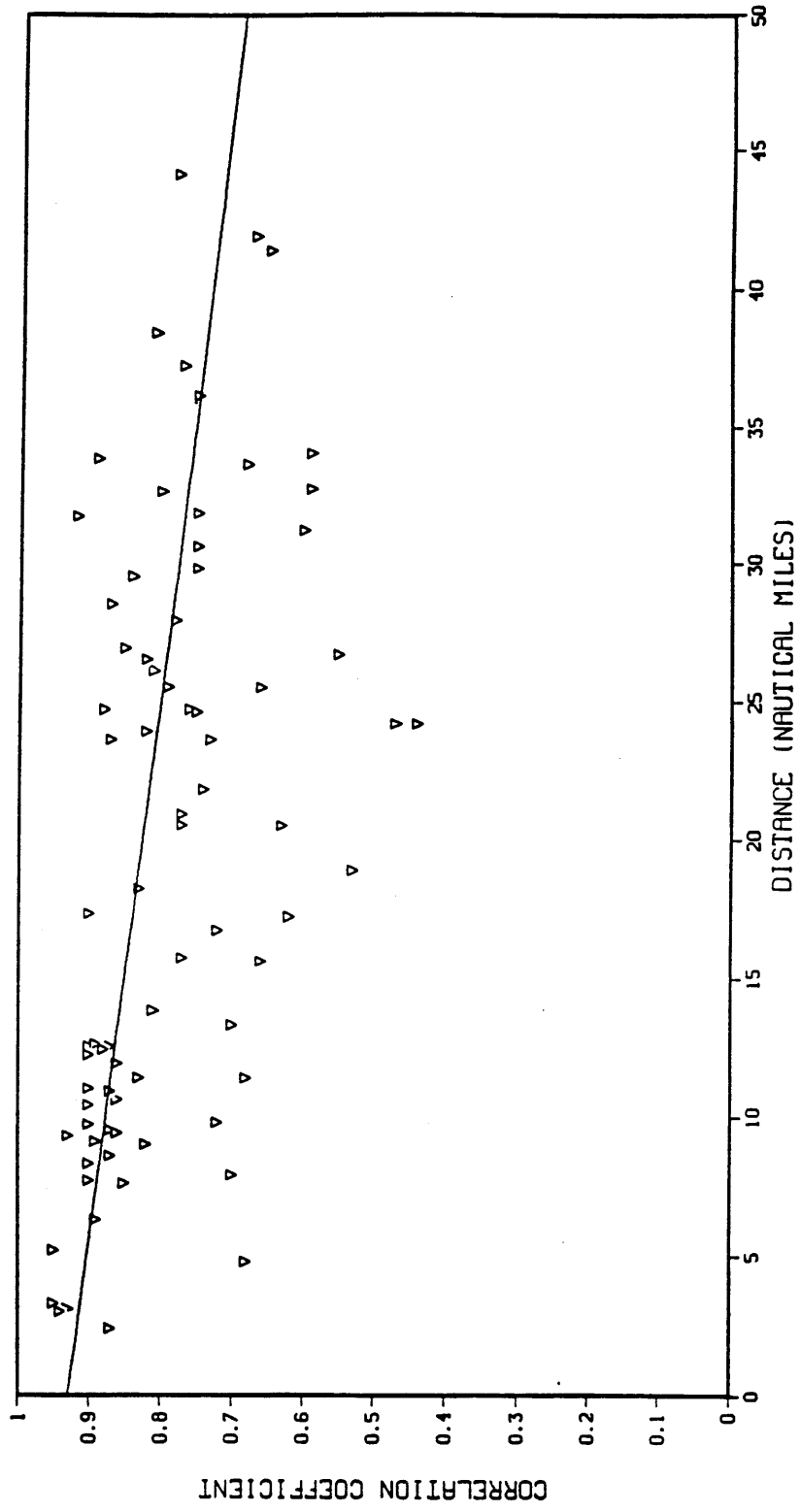


Figure 4.38 Correlation Function - March 1

points for May 1 are shown in Figure 4.39. The correlation coefficient decreases more slowly with distance for May 1 than it did for the other months. Despite the small amount of scatter in the sample points, this function may actually overestimate the correlation throughout the basin, since the function has been fitted to only points that receive and retain significant snow in most years.

The interpolation approach was used for each month, February to May, for all 35 years of data. Areal values were computed for the lower and upper areas from the interpolated snow-water-equivalent fields. As before, pseudo-observed values were estimated by developing a regression equation between the pseudo-observed values for the month and the areal estimates from the interpolation procedure. A separate equation was developed for each year, neglecting that year's data. This procedure was applied to each month, and the resulting statistics between the pseudo-observed values and their estimates from the interpolation regression equations are shown in Table 4.17. The relationship between the pseudo-observed values and their estimates improved from February to April, but degraded in May. The square of the RMS error was used to estimate the R values in the filter, and the estimates of the pseudo-observed states were used to update the simulated snow-water-equivalent states the first of each month from February to May. The streamflow error statistics are given in Table 4.18 and show that the updating produced significant improvements in the daily, monthly, and seasonal streamflow statistics. The results improved as additional observations were included from February to April, but updating with May observations did not seem to improve the simulation. When these results are compared to those in Table 4.14, the results of updating with April 1 observations are seen to be slightly better than those in which the states were updated with February, March, and April observations. When the results from updating with interpolated observations are compared to the results in Table 4.12 (obtained from updating with regression-derived observations), the results are seen to be slightly better using the observations from the regression approach. Figures 4.40 and 4.41 show the resulting snowmelt hydrographs for 1971 and 1980, respectively. These updated hydrographs are not significantly different than the updated hydrographs that were produced using the regression approach.

Spatial Interpolation Approach-Summary

Optimal interpolation was used to estimate the entire snow-water-equivalent field. Standardized deviates of the snow course observations were computed and interpolated at grid points. Estimates of the mean and standard deviation of the snow-water-equivalent field were then used to compute an estimate of the snow-water-equivalent field from the field of standardized deviates. The snow-water-equivalent field was averaged over the subareas to produce estimates of areal snow-water-equivalent,

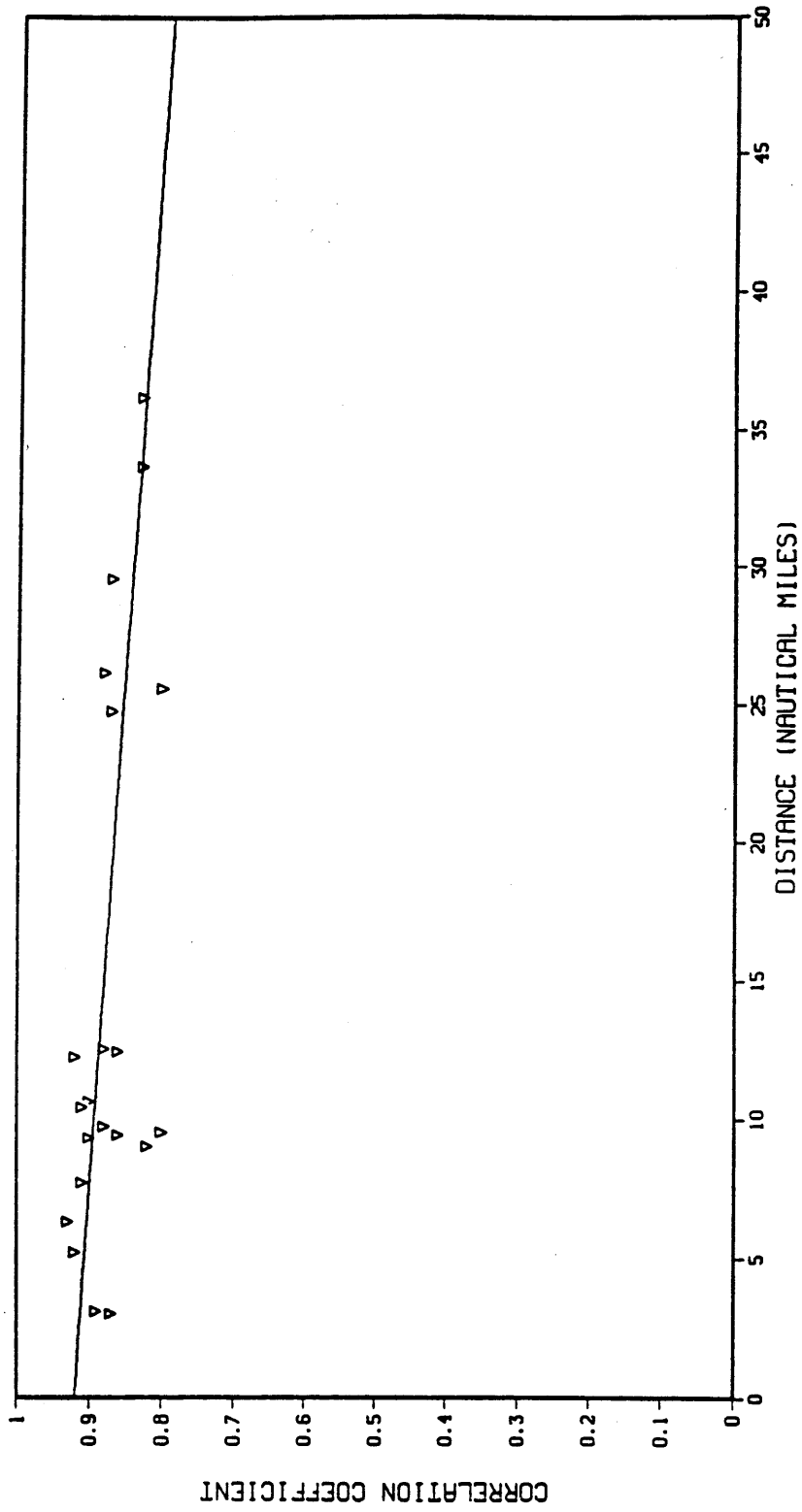


Figure 4,39 Correlation Function - May 1

Table 4.17

Statistics for Interpolated Regression
Pseudo-Observed Estimates

<u>Upper Area</u>	<u>Feb 1</u>	<u>Mar 1</u>	<u>Apr 1</u>	<u>May 1</u>
Average Error (mm)	0.1	0.3	0.2	-0.2
Absolute Max. Error (mm)	158.6	128.6	99.1	159.4
Avg. Absolute Error (mm)	46.7	43.3	41.3	51.5
RMS Error (mm)	61.9	54.5	52.3	67.7
Bias (%)	0.0	0.1	0.0	0.0
Correlation Coefficient	.879	.921	.949	.937
<u>Lower Area</u>				
Average Error (mm)	-0.3	0.1	0.6	2.6
Absolute Max. Error (mm)	54.7	61.3	74.1	59.5
Avg. Absolute Error (mm)	24.3	24.6	24.0	19.1
RMS Error (mm)	30.0	29.1	31.2	25.4
Bias (%)	-0.2	0.0	0.4	5.9
Correlation Coefficient	.911	.939	.954	.869

Table 4.18
Streamflow Error Statistics - Updated with Interpolation
- Other Months

<u>Daily</u>	Updating Through			
	<u>Feb 1</u>	<u>Mar 1</u>	<u>Apr 1</u>	<u>May 1</u>
Avg. Absolute Error (cmsd)	4.78	4.63	4.50	4.50
RMS Error (cmsd)	9.10	8.72	8.44	8.40
Correlation Coefficient	.952	.956	.958	.959
<u>Monthly</u>				
Avg. Absolute Error (mm)	4.93	4.70	4.48	4.39
RMS Error (mm)	8.58	7.86	7.36	7.32
<u>Seasonal (April-September)</u>				
Average Error (10^6m^3)	-0.7	0.6	2.0	0.4
Absolute Max. Error (10^6m^3)	189.0	149.0	131.2	126.7
Avg. Absolute Error (10^6m^3)	50.4	41.9	37.9	38.6
RMS Error (10^6m^3)	66.4	56.7	49.5	50.4
Bias (%)	-0.1	0.1	0.3	0.1
Correlation Coefficient	.961	.969	.975	.974

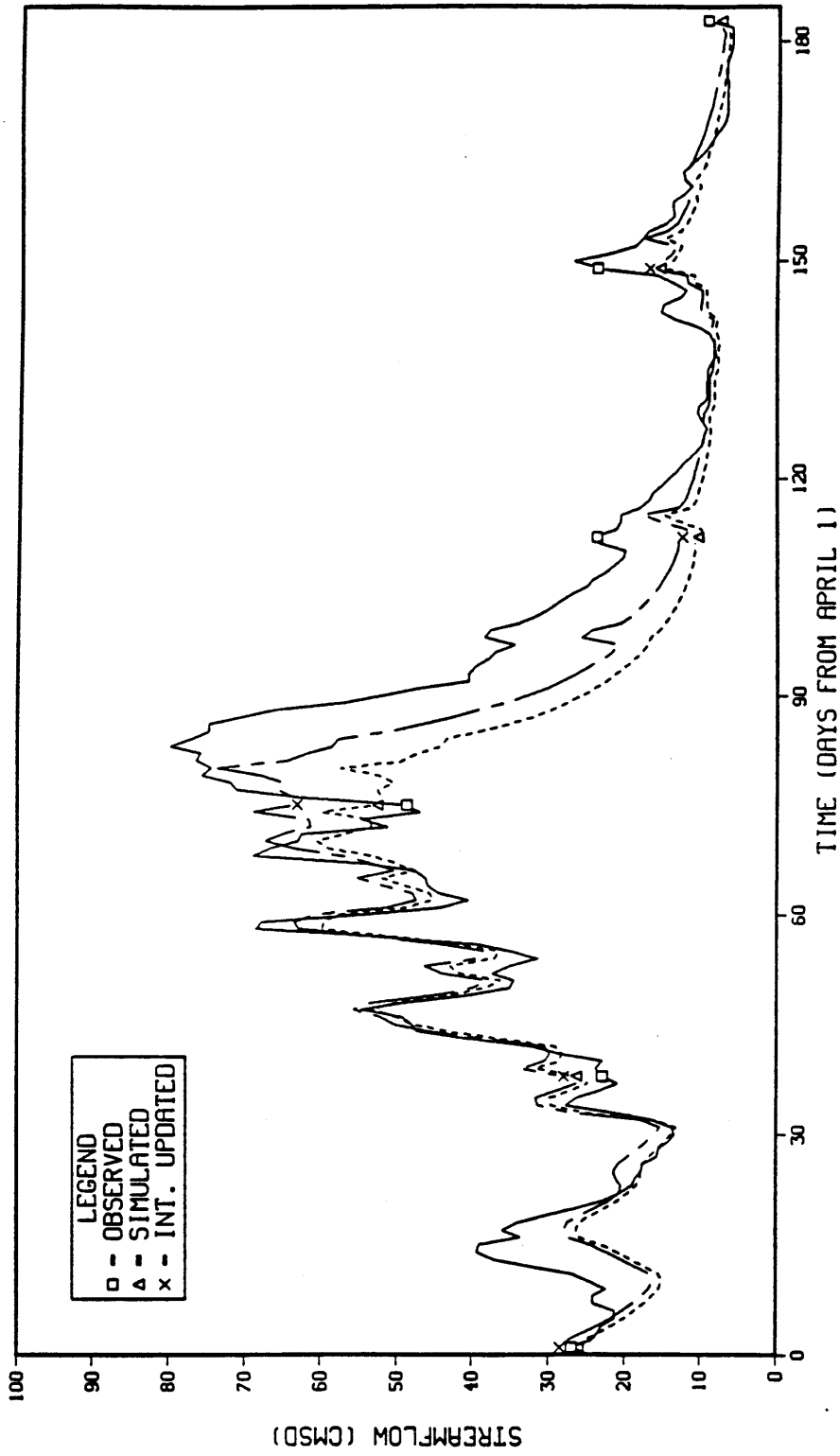


Figure 4.40 1971 Hydrographs (Interpolation Updated - all months)

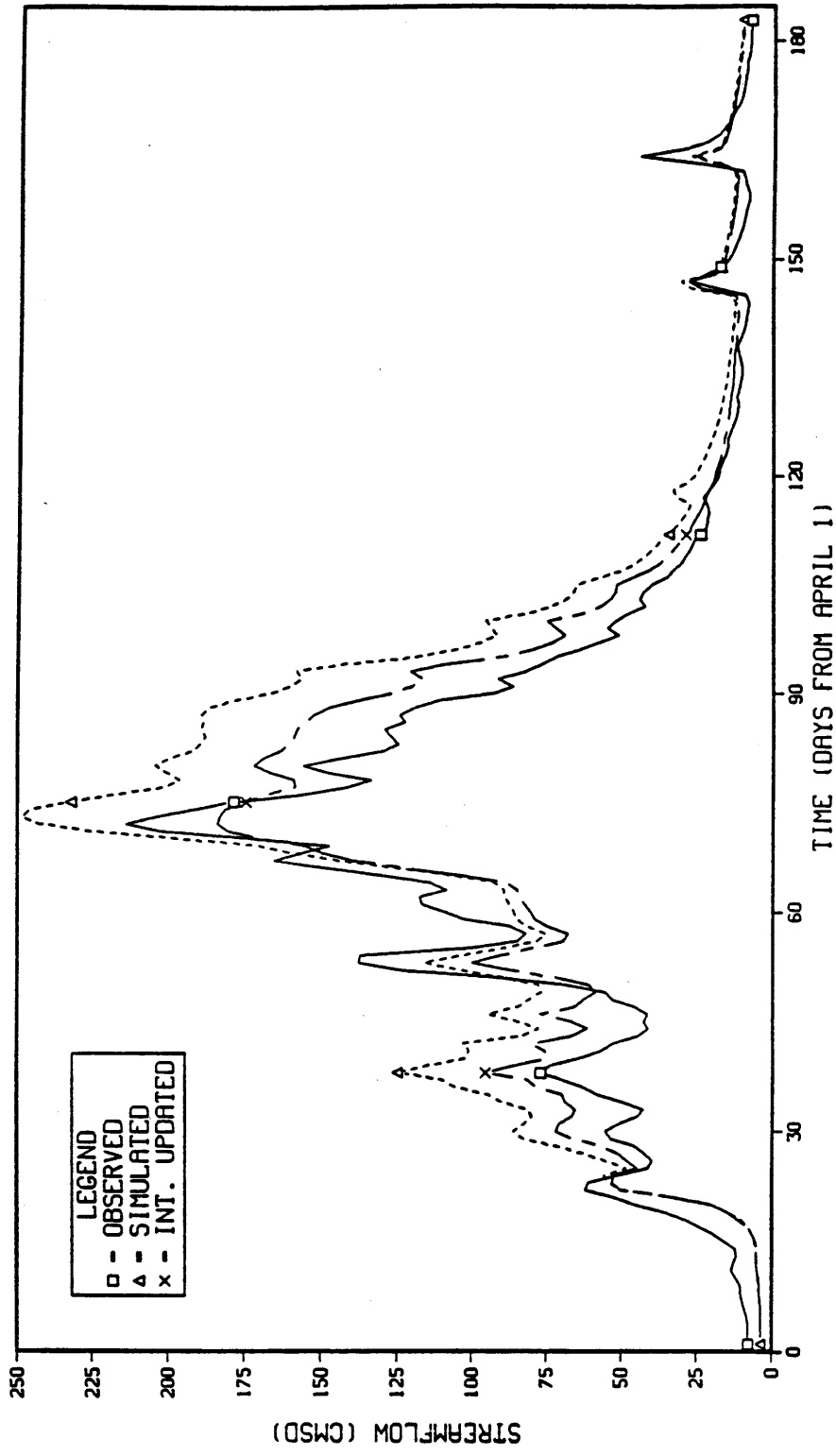


Figure 4.41 1980 Hydrographs (Interpolation Updated - all months)

and regression equations were developed between the pseudo-observed values and the areal estimates. This procedure was used to develop observations for the first of each month, February to May, to use in updating. Updating with these observations produced significant improvements in the streamflow simulation. The results improved as additional observations were used for updating through April, but updating with the May observations did not significantly affect the results.

Two techniques were developed for estimating the mean snow-water-equivalent field. The first technique adjusts the field of October through April precipitation using an elevation relationship. This technique was successfully demonstrated for April 1. The second technique modeled snowmelt in zones of similar snowmelt characteristics. Monthly accounting of snow-water-equivalent was performed at the grid points and averaged over 35 years to produce estimates of the mean snow-water-equivalent fields for the first of each month, February to May.

Summary

A procedure for updating the states of a conceptual snow model has been developed and tested on the Animas Basin near Durango, Colorado. Two approaches were successfully tested for relating the snow course observations to the model states. Both approaches use an estimate of the optimal model state that is conditioned on the historical seasonal streamflow. The first approach is based strictly on regression, whereas the second approach uses optimal interpolation to estimate snow-water-equivalent throughout the basin. Both techniques produced significant improvements in daily, monthly, and seasonal streamflow simulation.

Chapter 5

SUMMARY, CONCLUSIONS, AND RECOMMENDATIONS

Summary

A methodology has been presented for updating the states of a conceptual snow model using observations of point snow-water-equivalent. An extended Kalman filter was used to combine estimates of model states from a nonlinear snow model simulation with estimates from observations based on their relative uncertainties. The filter is able to propagate reasonable estimates of the state error covariance matrix for five model states: frozen-water-equivalent, liquid-water-equivalent, negative heat storage, temperature index, and areal extent of snow cover. Two approaches were presented for relating the observations to the model water-equivalent states. Both approaches rely on estimates of the optimal model states, which were derived by conditioning the model water-equivalent states on historical seasonal streamflow. The first approach is based on regression, whereas the second approach uses optimal interpolation to estimate the snow-water-equivalent field. Updating with either approach produced significant improvements in streamflow simulation. The regression approach produced slightly better results, but the interpolation approach offers important advantages.

Conclusions

A nonlinear conceptual snow model was successfully put into state-space form. State-space equations were written for the frozen-water-equivalent, liquid-water-equivalent, negative heat storage, temperature index, and areal extent of snow cover states. When an extended Kalman filter was applied to the model, it propagated reasonable estimates of the state error covariance matrix. More importantly, when the filter was used to update the model states using estimates of the states from point snow-water-equivalent observations, significant improvements in streamflow simulation were realized.

A technique was developed for making estimates of the true model states, which are unobservable. The technique is based on estimating pseudo-observed model states by conditioning them on seasonal streamflow volume, which is observable. These estimates were then used to relate the observations to the model states and to estimate the model system error. The results from the Animas Basin indicated that the technique led to reasonable estimates for Q and R. The updating improved the seasonal streamflow statistics, but not at the expense of the shorter time interval simulation.

Two approaches were demonstrated for relating the observations to the model states. The first approach was based strictly on regression. Good relationships were developed between the pseudo-observed model state estimates and the snow course observations for each month, February through May. Updating with observations derived from

these relationships produced significant improvements in streamflow simulation. The RMS error in April through September streamflow was reduced 21 percent by updating only on February 1. The streamflow simulation improved each month as additional observations were used to update the model states. Although a good relationship was obtained between the May 1 pseudo-observed values and the snow course observations, the incremental improvements achieved by updating with May 1 observations were small. Updating only on April 1 produced results almost as good as those produced when updates were made for February 1, March 1, and April 1. This is not surprising, however, since the April 1 observation contains most of the information from earlier snow-water-equivalent observations.

The second approach to developing a relationship between the pseudo-observed values and the snow course observations used spatial interpolation. Both the regression approach and the spatial interpolation approach estimate the pseudo-observed value as a linear combination of the observations. Although the regression approach is based on estimating the coefficients by minimizing the sum of the squared error, the interpolation approach outperformed the regression approach in the verification test based on the same criterion. If a shorter period of record had been used, the sample error would have been larger and this effect could have been even more dramatic. The interpolation approach results were slightly better than the regression approach results when the model was only updated April 1, but the spatial interpolation results with monthly updates are slightly inferior to the results obtained with the regression approach, despite the fact that the spatial interpolation provided better estimates of the pseudo-observed values. The fact that the results using the spatial interpolation are only slightly inferior is an important result. The advantages to the interpolation approach are that it is conceptually appealing, provides estimates of the entire snow-water-equivalent field, does not necessarily require a long historical record for all of the observations, and is adaptable to a changing network. In addition, the interpolation approach provides a framework that might be useful in network design.

The spatial interpolation approach did not work as well for May 1 as it did for other months. Although the stations used in the interpolation were highly correlated with one another, they are apparently not entirely representative of the rest of the basin. After April 1, significant melt occurs in many parts of the basin. Six of the snow courses had observations of zero snow-water-equivalent for May 1 in eight or more of the years. By May 1, snowmelt has significantly complicated the snow-water-equivalent field, and apparently, the use of standardized deviates was not as successful in removing the resulting heterogeneity in May 1 snow-water-equivalent.

Application of the spatial interpolation approach requires an estimate of the mean snow-water-equivalent field. The snow model was applied to zones containing grid points with similar snowmelt characteristics. Monthly snow-water-equivalent accounting was performed at each grid point and averaged over the historical record to provide estimates of the monthly mean snow-water-equivalent field. Limited

verification indicated that the spatial melt results were reasonable. Some of the differences in the results between the lumped model and the spatial model may be due to the areal depletion curve used in the lumped model. On a lumped basis, the areal depletion curve can adjust for errors in the melt rates.

Tests of the updating methodology on the Animas Basin showed dramatic improvements in daily, monthly, and seasonal streamflow simulation. The improvements in the seasonal statistics were particularly noteworthy, because of their magnitude and the importance of seasonal forecasts to water management. Updating with April 1 snow-water-equivalent data reduced the maximum error, the average error, and the RMS error in seasonal volume simulation for the Animas Basin by 35 to 45 percent. Once the methodology has been incorporated into an operational forecasting system, it should produce significant improvements in streamflow forecast accuracy. Enormous benefits would be realized from improved forecasts that allow for more efficient use of scarce water resources.

Recommendations for Future Research

A methodology has been presented for updating the states of a conceptual snow model using point observations of snow-water-equivalent. The structure of the methodology will allow other data to be incorporated, such as line observations of snow-water-equivalent which are available for the upper midwest and parts of the west. Further research is required, however, to extend the interpolation approach to handle additional sample geometries.

The extended Kalman filter, developed as part of this research, can accept data types other than snow-water-equivalent, provided these data can be related to the model states through the measurement equation. Areal extent of snow cover from satellite observations is one such data type. Areal extent of snow cover does not provide information early in the forecast season, since basins are usually completely covered with snow. Once bare ground appears, however, areal extent of snow cover observations provide information about the rate of snowmelt production from a basin, as well as information about the amount of water-equivalent remaining. Updating with areal extent of snow cover should improve the volume and timing of streamflow simulation. Some work will be required, however, to relate the areal extent of snow cover observations to the areal extent of snow cover state, since the model state takes other factors into account, such as the changing average basin melt rate.

Discharge observations are another source of information about the snow model states, once melt begins. State-space versions of the Sacramento soil-moisture accounting model are available. Kalman filters have been used with the Sacramento model for updating states and for parameter estimation. It may be possible to develop one filter that contains both models, or it may be more efficient to connect separate filters through a feedback loop. The snow model filter also provides uncertainty information about the snow model states, which could be important in estimating the uncertainty of streamflow forecasts.

Several areas of research could improve the spatial interpolation approach. The correlation plots showed considerable scatter around the correlation functions. Some of the scatter is due to sampling error, but much more needs to be learned about the spatial correlation of snow-water-equivalent in the mountains. If more of this variability could be explained, it would improve the performance of the interpolation procedure. The spatial snowmelt analysis was successful, but much could be done to fine tune its performance. It may be feasible to apply the snow model in a distributed manner in real-time to provide a simulated water-equivalent field that could be merged with observations.

Several filter issues should also be addressed. One of the filter assumptions is that the observations are independent. Successive observations of snow-water-equivalent are probably not independent, especially when it is necessary to update at a shorter time interval than the monthly interval used here. A procedure for dealing with correlated observations would probably be needed in such cases. There are also operational issues, such as efficiency, that might be considered. Several of the states did not seem sensitive to changes in filter parameters. Could they be excluded from the filter without adversely affecting the water-equivalent states? Could the frozen-water-equivalent and liquid-water-equivalent states be combined, so that only one variance needed to be propagated?

The updating procedure was tested on the Animas Basin, and significant improvements in streamflow simulation were demonstrated. The procedure should be tested on additional basins to see if similar improvements can be obtained in areas where the quality of the data network and model calibration may be different.

APPENDIX

State-Space Equation Derivatives

This appendix contains the derivatives of the state-space equations defined in Chapter 4. These derivatives are the elements of the A and B matrices used in Equation (4.13). The derivatives of the snowmelt, free water, and heat exchange equations are defined separately in order to simplify the derivatives of the state-space equations. This appendix uses the notation and symbols introduced in Chapter 4.

Snowmelt

During Non-rain Period --

$$\partial M / \partial x_1 = L_{01} \quad (\text{A.1})$$

$$\partial M / \partial x_2 = 0. \quad (\text{A.2})$$

$$\partial M / \partial x_3 = 0. \quad (\text{A.3})$$

$$\partial M / \partial x_4 = 0. \quad (\text{A.4})$$

$$\begin{aligned} \partial M / \partial x_5 = & [M_f (T_a - p_s) M_{01} + .0125 P_x (1 - F_s) T_a \\ & \cdot (1 - K_{01})] (1 - L_{01}) - L_{01} G_m \end{aligned} \quad (\text{A.5})$$

$$\begin{aligned} \partial M / \partial u_1 = & .0125 (1 - F_s) T_a (1 - K_{01}) x_5 (1 - L_{01}) \\ & + L_{01} F_s p_2 \end{aligned} \quad (\text{A.6})$$

$$\begin{aligned} \partial M / \partial u_2 = & [M_f M_{01} + .0125 P_x (1 - F_s) (1 - K_{01})] \\ & \cdot x_5 (1 - L_{01}) \end{aligned} \quad (\text{A.7})$$

During Rain Period --

$$\partial M / \partial x_1 = L_{01} \quad (\text{A.8})$$

$$\partial M / \partial x_2 = 0. \quad (\text{A.9})$$

$$\partial M / \partial x_3 = 0. \quad (\text{A.10})$$

$$\partial M / \partial x_4 = 0. \quad (\text{A.11})$$

$$\begin{aligned} \partial M / \partial x_5 = & [\sigma ([.01 (T_a + 273)]^4 - 55.55) \\ & + p_4 (2.10291 \cdot 10^9 \cdot e^{-4278.63 / (T_a + 242.792)} - 51.935) \\ & + .004845 P_a p_4 T_a + .0125 P_x (1 - F_s) T_a (1 - K_{01})] \\ & \cdot (1 - L_{01}) - L_{01} G_m \end{aligned} \quad (\text{A.12})$$

$$\begin{aligned} \partial M / \partial u_1 = & .0125 (1 - F_s) T_a (1 - K_{01}) x_5 (1 - L_{01}) \\ & + L_{01} F_s p_2 \end{aligned} \quad (\text{A.13})$$

$$\begin{aligned} \partial M / \partial u_2 = & [.04 \sigma [.01 (T_a + 273)]^3 + 8.9977574 \cdot 10^{12} \\ & \cdot \frac{e^{-4278.63 / (T_a + 242.792)}}{(T_a + 242.792)^2 p_4} + .004845 P_a p_4 \\ & + .0125 P_x (1 - F_s) (1 - K_{01})] x_5 (1 - L_{01}) \end{aligned} \quad (\text{A.14})$$

Free Water

$$\partial W / \partial x_1 = \partial M / \partial x_1 \quad (\text{A.15})$$

$$\partial W / \partial x_2 = \partial M / \partial x_2 \quad (\text{A.16})$$

$$\partial W / \partial x_3 = \partial M / \partial x_3 \quad (\text{A.17})$$

$$\partial W / \partial x_4 = \partial M / \partial x_4 \quad (\text{A.18})$$

$$\partial W / \partial x_5 = \partial M / \partial x_5 + P_x (1 - F_s) \quad (\text{A.19})$$

$$\partial W / \partial u_1 = \partial M / \partial u_1 + x_5 (1 - F_s) \quad (\text{A.20})$$

$$\partial W / \partial u_2 = \partial M / \partial u_2 \quad (\text{A.21})$$

Heat Exchange

$$\partial H / \partial x_1 = 0. \quad (\text{A.22})$$

$$\partial H / \partial x_2 = -N_{01} \quad (\text{A.23})$$

$$\partial H / \partial x_3 = 0. \quad (\text{A.24})$$

$$\partial H / \partial x_4 = \frac{M_f}{p_s} p_s x_5 (1 - N_{01}) (1 - H_{01}) \quad (\text{A.25})$$

$$\partial H / \partial x_5 = \frac{M_f}{p_s} p_s [x_4 (1 - H_{01}) + T_a (H_{01} - K_{01})] \cdot (1 - N_{01}) \quad (\text{A.26})$$

$$\partial H / \partial u_1 = - \frac{F_s p_2 T_a K_{01}}{160.} \quad (\text{A.27})$$

$$\frac{\partial H}{\partial u_2} = \frac{M_f}{p_5} p_8 x_5 (1 - N_{01}) (H_{01} - K_{01})$$

$$- \frac{P_x F_s p_2 K_{01}}{160.} \quad (\text{A.28})$$

Frozen Water-Equivalent --

$$\frac{\partial f_1}{\partial x_1} = -\frac{\partial M}{\partial x_1} + (1 - J_{01}) \frac{\partial W}{\partial x_1} + J_{01} \frac{\partial H}{\partial x_1} \quad (\text{A.29})$$

$$\frac{\partial f_1}{\partial x_2} = -\frac{\partial M}{\partial x_2} + (1 - J_{01}) \frac{\partial W}{\partial x_2} + J_{01} \frac{\partial H}{\partial x_2} + J_{01} \quad (\text{A.30})$$

$$\frac{\partial f_1}{\partial x_3} = -\frac{\partial M}{\partial x_3} + (1 - J_{01}) \frac{\partial W}{\partial x_3} + J_{01} \frac{\partial H}{\partial x_3} \quad (\text{A.31})$$

$$\frac{\partial f_1}{\partial x_4} = -\frac{\partial M}{\partial x_4} + (1 - J_{01}) \frac{\partial W}{\partial x_4} + J_{01} \frac{\partial H}{\partial x_4} \quad (\text{A.32})$$

$$\frac{\partial f_1}{\partial x_5} = -G_m - \frac{\partial M}{\partial x_5} + (1 - J_{01}) \frac{\partial W}{\partial x_5} + J_{01} \frac{\partial H}{\partial x_5} \quad (\text{A.33})$$

$$\frac{\partial f_1}{\partial u_1} = F_s p_2 - \frac{\partial M}{\partial u_1} + (1 - J_{01}) \frac{\partial W}{\partial u_1} + J_{01} \frac{\partial H}{\partial u_1} \quad (\text{A.34})$$

$$\frac{\partial f_1}{\partial u_2} = -\frac{\partial M}{\partial u_2} + (1 - J_{01}) \frac{\partial W}{\partial u_2} + J_{01} \frac{\partial H}{\partial u_2} \quad (\text{A.35})$$

Negative Heat Storage --

$$\begin{aligned} \partial f_2 / \partial x_1 &= (\partial H / \partial x_1 - \partial W / \partial x_1) (1 - J_{01}) (1 - F_{01}) \\ &+ 0.33 F_{01} (1. + \partial f_1 / \partial x_1) \end{aligned} \quad (\text{A.36})$$

$$\begin{aligned} \partial f_2 / \partial x_2 &= [(\partial H / \partial x_2 - \partial W / \partial x_2) (1 - J_{01}) - J_{01}] \\ &\cdot (1 - F_{01}) + F_{01} (0.33 \partial f_1 / \partial x_2 - 1.) \end{aligned} \quad (\text{A.37})$$

$$\begin{aligned} \partial f_2 / \partial x_3 &= (\partial H / \partial x_3 - \partial W / \partial x_3) (1 - J_{01}) (1 - F_{01}) \\ &+ 0.33 F_{01} \partial f_1 / \partial x_3 \end{aligned} \quad (\text{A.38})$$

$$\begin{aligned} \partial f_2 / \partial x_4 &= (\partial H / \partial x_4 - \partial W / \partial x_4) (1 - J_{01}) (1 - F_{01}) \\ &+ 0.33 F_{01} \partial f_1 / \partial x_4 \end{aligned} \quad (\text{A.39})$$

$$\begin{aligned} \partial f_2 / \partial x_5 &= (\partial H / \partial x_5 - \partial W / \partial x_5) (1 - J_{01}) (1 - F_{01}) \\ &+ 0.33 F_{01} \partial f_1 / \partial x_5 \end{aligned} \quad (\text{A.40})$$

$$\begin{aligned} \partial f_2 / \partial u_1 &= (\partial H / \partial u_1 - \partial W / \partial u_1) (1 - J_{01}) (1 - F_{01}) \\ &+ 0.33 F_{01} \partial f_1 / \partial u_1 \end{aligned} \quad (\text{A.41})$$

$$\begin{aligned} \partial f_2 / \partial u_2 &= (\partial H / \partial u_2 - \partial W / \partial u_2) (1 - J_{01}) (1 - F_{01}) \\ &+ 0.33 F_{01} \partial f_1 / \partial u_2 \end{aligned} \quad (\text{A.42})$$

Liquid Water-Equivalent --

$$\begin{aligned} \partial f_3 / \partial x_1 = & \frac{I_{01} x_3 G_m x_5}{x_1} + (\partial W / \partial x_1 - \partial H / \partial x_1) J_{01} I_{01} \\ & + (1 - I_{01}) p_{10} (1. + \partial f_1 / \partial x_1) \end{aligned} \quad (A.43)$$

$$\begin{aligned} \partial f_3 / \partial x_2 = & J_{01} I_{01} (\partial W / \partial x_2 - 1. - \partial H / \partial x_2) \\ & + (1 - I_{01}) p_{10} \partial f_1 / \partial x_2 \end{aligned} \quad (A.44)$$

$$\begin{aligned} \partial f_3 / \partial x_3 = & - \frac{I_{01} G_m x_5}{x_1} + J_{01} I_{01} (\partial W / \partial x_3 - \partial H / \partial x_3) \\ & + (1 - I_{01}) (p_{10} \partial f_1 / \partial x_3 - 1.) \end{aligned} \quad (A.45)$$

$$\begin{aligned} \partial f_3 / \partial x_4 = & J_{01} I_{01} (\partial W / \partial x_4 - \partial H / \partial x_4) \\ & + (1 - I_{01}) p_{10} \partial f_1 / \partial x_4 \end{aligned} \quad (A.46)$$

$$\begin{aligned} \partial f_3 / \partial x_5 = & - \frac{I_{01} x_3 G_m}{x_5} + J_{01} I_{01} (\partial W / \partial x_5 - \partial H / \partial x_5) \\ & + (1 - I_{01}) p_{10} \partial f_1 / \partial x_5 \end{aligned} \quad (A.47)$$

$$\begin{aligned} \partial f_3 / \partial u_1 = & J_{01} I_{01} (\partial W / \partial u_1 - \partial H / \partial u_1) \\ & + (1 - I_{01}) p_{10} \partial f_1 / \partial u_1 \end{aligned} \quad (A.48)$$

$$\begin{aligned} \partial f_3 / \partial u_2 = & J_{01} I_{01} (\partial W / \partial u_2 - \partial H / \partial u_2) \\ & + (1 - I_{01}) p_{10} \partial f_1 / \partial u_2 \end{aligned} \quad (A.49)$$

Temperature Index --

$$\partial f_4 / \partial x_1 = 0. \quad (\text{A.50})$$

$$\partial f_4 / \partial x_2 = 0. \quad (\text{A.51})$$

$$\partial f_4 / \partial x_3 = 0. \quad (\text{A.52})$$

$$\partial f_4 / \partial x_4 = [-H_{01} + p_7 (H_{01} - 1)] (1 - G_{01}) G_{01} \quad (\text{A.53})$$

$$\partial f_4 / \partial x_5 = 0. \quad (\text{A.54})$$

$$\partial f_4 / \partial u_1 = 0. \quad (\text{A.55})$$

$$\partial f_4 / \partial u_2 = [H_{01} K_{01} - p_7 (H_{01} - 1)] (1 - G_{01}) \quad (\text{A.56})$$

Areal Extent of Snow Cover --

Case 1 ($T_w \geq A_I$) snow cover is above the areal depletion curve --

$$\partial f_5 / \partial x_1 = 0. \quad (\text{A.57})$$

$$\partial f_5 / \partial x_2 = 0. \quad (\text{A.58})$$

$$\partial f_5 / \partial x_3 = 0. \quad (\text{A.59})$$

$$\partial f_5 / \partial x_4 = 0. \quad (\text{A.60})$$

$$\partial f_5 / \partial x_5 = -1. \quad (\text{A.61})$$

$$\partial f_5 / \partial u_1 = 0. \quad (\text{A.62})$$

$$\partial f_5 / \partial u_2 = 0. \quad (\text{A.63})$$

Case 2 ($T_w \leq S_D$) snow cover is following the areal depletion curve --

$$\partial f_5 / \partial x_1 = C_1 (\partial f_1 / \partial x_1 + \partial f_3 / \partial x_1) \quad (\text{A.64})$$

$$\partial f_5 / \partial x_2 = C_1 (\partial f_1 / \partial x_2 + \partial f_3 / \partial x_2) \quad (\text{A.65})$$

$$\partial f_5 / \partial x_3 = C_1 (\partial f_1 / \partial x_3 + \partial f_3 / \partial x_3) \quad (\text{A.66})$$

$$\partial f_5 / \partial x_4 = C_1 (\partial f_1 / \partial x_4 + \partial f_3 / \partial x_4) \quad (\text{A.67})$$

$$\partial f_5 / \partial x_5 = C_1 (\partial f_1 / \partial x_5 + \partial f_3 / \partial x_5) \quad (\text{A.68})$$

$$\partial f_5 / \partial u_1 = C_1 (\partial f_1 / \partial u_1 + \partial f_3 / \partial u_1) \quad (\text{A.69})$$

$$\partial f_5 / \partial u_2 = C_1 (\partial f_1 / \partial u_2 + \partial f_3 / \partial u_2) \quad (\text{A.70})$$

where, C_1 = average rate of change over the time period in areal extent of snow cover with respect to total water-equivalent.

Case 3 ($T_w > S_b$) and ($T_w \geq S_w$) snow cover is 100% because of new snow --

$$\partial f_5 / \partial x_1 = C_1 (\partial f_1 / \partial x_1 + \partial f_3 / \partial x_1) \quad (\text{A.71})$$

$$\partial f_5 / \partial x_2 = C_1 (\partial f_1 / \partial x_2 + \partial f_3 / \partial x_2) \quad (\text{A.72})$$

$$\partial f_5 / \partial x_3 = C_1 (\partial f_1 / \partial x_3 + \partial f_3 / \partial x_3) \quad (\text{A.73})$$

$$\partial f_5 / \partial x_4 = C_1 (\partial f_1 / \partial x_4 + \partial f_3 / \partial x_4) \quad (\text{A.74})$$

$$\partial f_5 / \partial x_5 = C_1 (\partial f_1 / \partial x_5 + \partial f_3 / \partial x_5) \quad (\text{A.75})$$

$$\partial f_5 / \partial u_1 = C_1 (\partial f_1 / \partial u_1 + \partial f_3 / \partial u_1) \quad (\text{A.76})$$

$$\partial f_5 / \partial u_2 = C_1 (\partial f_1 / \partial u_2 + \partial f_3 / \partial u_2) \quad (\text{A.77})$$

where, C_1 = average rate of change over the time period in areal extent of snow cover with respect to total water-equivalent.

Case 4 ($T_w > S_b$) and ($T_w < S_w$) snow cover is on the new snow line --

$$\partial f_5 / \partial x_1 = C_1 (\partial f_1 / \partial x_1 + \partial f_3 / \partial x_1) \quad (\text{A.78})$$

$$\partial f_5 / \partial x_2 = C_1 (\partial f_1 / \partial x_2 + \partial f_3 / \partial x_2) \quad (\text{A.79})$$

$$\partial f_5 / \partial x_3 = C_1 (\partial f_1 / \partial x_3 + \partial f_3 / \partial x_3) \quad (\text{A.80})$$

$$\partial f_5 / \partial x_4 = C_1 (\partial f_1 / \partial x_4 + \partial f_3 / \partial x_4) \quad (\text{A.81})$$

$$\partial f_5 / \partial x_5 = C_1 (\partial f_1 / \partial x_5 + \partial f_3 / \partial x_5) \quad (\text{A.82})$$

$$\partial f_5 / \partial u_1 = C_1 (\partial f_1 / \partial u_1 + \partial f_3 / \partial u_1) \quad (\text{A.83})$$

$$\partial f_5 / \partial u_2 = C_1 (\partial f_1 / \partial u_2 + \partial f_3 / \partial u_2) \quad (\text{A.84})$$

where, C_1 = average rate of change over the time period in areal extent of snow cover with respect to total water-equivalent.

REFERENCES

- Anderson, E.A., National Weather Service River Forecast System - Snow Accumulation and Ablation Model, NOAA Technical Memorandum, NWS, HYDRO-17, Silver Spring, Maryland, 1973.
- Anderson, E.A., A Point Energy and Mass Balance Model of a Snow Cover, NOAA Technical Report NWS 19, Silver Spring, Maryland, 1976.
- Anderson, E.A., "Techniques for Predicting Snow Cover Runoff," International Symposia on the Role of Snow and Ice in Hydrology, Symposium on Measurement and Forecasting, IAHS, Pub. 107, Vol. 2, p. 840-861, 1972.
- Barton, M., "SNOTEL: Wave of the Present," U.S. Dept. of Agriculture, Soil Conservation Service, Portland, Oregon, 1977.
- Bastin, G., G. Lorent, C. Duque, and M. Gevers, "Optimal Estimation of the Average Areal Rainfall and Optimal Selection of Rain Gauge Locations," Water Resources Research, Vo. 20, No. 4, p. 463-470, 1984.
- Bergman, M.J., and J.W. Delleur, "Kalman Filter Estimation and Prediction of Daily Stream Flows: I. Review, Algorithm, and Simulation Experiments," Water Resources Bulletin, Vol. 21, No. 5, p. 815-825, 1985.
- Bergstrom, S., "The Development of a Snow Routine for HBV-2 Model," Nordic Hydrology, Vol. 6, No. 2., 1975.
- Bolzern, P., M. Ferrario, and G. Fronza, "Adaptive Real-Time Forecast of River Flow-Rates From Rainfall Data," Journal of Hydrology, Vol. 47, p. 251-267, 1980.
- Bras, R.L., and I. Rodriguez-Iturbe, "Network Design for the Estimation of Areal Mean of Rainfall Events," Water Resources Research, Vo. 12, No. 6, p. 1185-1195, 1976a.
- Bras, R.L., and I. Rodriguez-Iturbe, "Rainfall Network Design for Runoff Prediction," Water Resources Research, Vol. 12, No. 6, p. 1197-1208, 1976b.
- Bras, R.L., and I. Rodriguez-Iturbe, Random Functions and Hydrology, Addison-Wesley, Reading, Massachusetts, 1985.
- Brazil, L.E., "Multilevel Calibration Strategy for Complex Hydrologic Simulation Models," PhD Dissertation, Colorado State University, Fort Collins, Colorado, 1988.
- Burn, D.H., and E.A. McBean, "River Flow Forecasting Model for Sturgeon River," Journal of Hydraulic Engineering, Vol. 111, No. 2, p. 316-333, 1985.

- Burnash, R.J.C., L.R. Ferral, and R.A. McGuire, "A Generalized Streamflow Simulation System, Joint Federal-State River Forecast Center," Sacramento, California, 1973.
- Carroll, T.R., "A Procedure to Incorporate Snow Course Data Into the National Weather Service River Forecast System," Proceedings of Modeling of Snow Cover Runoff, U.S. Army Cold Regions Research and Engineering Laboratory, Hanover, New Hampshire, p. 351-358, 1978.
- Carroll, T.R., and E.L. Peck, "Advantages of Conceptual Models for Northern Research Basins Studies," Presented at Third Symposium - Workshop conducted by the IHP Regional Working Group on Northern Research Basins, Quebec City, Canada, 1979.
- Carroll, T.R., and R.D. Marshall, "Cost-Benefit Analysis of Airborne Gamma Radiation Snow Water Equivalent Measurements Made Before the February 1985 Fort Wayne Flood," Presented at the Sixth Conference on Hydrometeorology, American Meteorological Society, Indianapolis, Indiana, 1985a.
- Carroll, T.R., R.M. Vogel, and R.L. Gauthier, "Operational Airborne Snow Water Equivalent and Soil Moisture Measurements Used in Water Supply and Snowmelt Flood Forecasting," Fifth Remote Sensing Symposium, Remote Sensing Applications for Water Resources Management, Ann Arbor, Michigan, 1985b.
- Carroll, T.R., and M.W. Allen, "National Remote Sensing Hydrology Program, User's Guide, Version 3.0," National Weather Service, NOAA, Minneapolis, Minnesota, 1988.
- Castruccio, P., H. Louts, D. Lloyd, P. Newman, Applications Systems Verification and Transfer Project, Volume VII: Cost/Benefit Analysis for the ASVT on Operational Applications of Satellite Snow-Cover Observations, NASA Technical Paper 1828, Goddard Space Flight Center, NASA, Greenbelt, Maryland, 1981.
- Charbonneau, R., J.P. Fortin, and G. Morin, "The CEQUEAU Model: Description and Examples of its Use in Problems Related to Water Resources Management," Hydrological Sciences Bulletin, Vol. 22, No. 1, p. 193-302, 1977.
- Chiu, C.L. (Editor), "Applications of Kalman Filter to Hydrology, Hydraulics and Water Resources," Proceedings of American Geophysical Union Chapman Conference, Pittsburgh, Pennsylvania, 1978.
- Chua, S.H., and R.L. Bras, "Optimal Estimators of Mean Areal Precipitation in Regions of Orographic Influence," Journal of Hydrology, Vol. 57, No. 1/2, p. 23-48, 1982.
- Codd, A.R., and R.A. Work, "Establishing Snow Survey Networks and Snow Courses for Water Supply Forecasting," Proceedings of Western Snow Conference, Portland, Oregon, p. 6-13, 1955.

- Colbeck, S.C., E.A. Anderson, V.C. Bissell, A.G. Crook, D.H. Male, C.W. Slaughter, and D.R. Wiesnet, "Snow Accumulation, Distribution, Melt, and Runoff," EOS, Transactions, American Geophysical Union, Vol. 60, No. 21, p. 464-471, 1979.
- Cooper, D.M., and E.F. Wood, "Identification of Multivariate Time Series and Multivariate Input-Output Models," Water Resources Research, Vol. 18, No. 4, p. 937-946, 1982.
- Corps of Engineers, "Snow Hydrology, Summary Report of the Snow Investigations," North Pacific Division, Portland, Oregon, 1956.
- Creutin, J.D., and C. Obled, "Objective Analyses and Mapping Techniques for Rainfall Fields: An Objective Comparison," Water Resources Research, Vol. 18, No. 2, p. 413-431, 1982.
- Curtis, D.C., and J.C. Schaake, Jr., "The NWS Extended Streamflow Prediction Technique," Presented at the Engineering Foundation Conference: Water Conservation - Needs and Implementing Strategies, Rindge, New Hampshire, 1979.
- Davis, R.E., "Objective Mapping by Least Squares Fitting," Journal of Geophysical Research, Vol. 90, No. C3, p. 4773-4777, 1985.
- Day, G.N., "Extended Streamflow Forecasting Using NWSRFS," Journal of Water Resources Planning and Management, Vol. 111, No. 2, p. 157-170, 1985.
- Eggleston, K.O., E.K. Israelsen, J.P. Riley, Hybrid Computer Simulation of the Accumulation and Melt Processes in a Snowpack, Utah State University Report, PRWG65-1, 1971.
- Federal Interagency Committee, "Report of the Interagency Committee on Wilderness Hydrometeorological Data Collection," in draft.
- Fortin, J.P., J.P. Villeneuve, A. Guilbot, and B. Seguin, "Development of a Modular Hydrological Forecasting Model Based on Remotely Sensed Data, for Interactive Utilization on a Microcomputer," Hydrologic Applications of Space Technology, IAHS, Publication No. 160, p. 307-319, 1986.
- Gambolati, G., and G. Volpi, "A Conceptual Deterministic Analysis of the Kriging Technique in Hydrology," Water Resources Research, Vol. 15, No. 3, p. 625-629, 1979.
- Gandin, L.S., "Objective Analysis of Meteorological Fields," Israel Program for Scientific Translations, Jerusalem, 1965.
- Garnier, B.J., and A. Ohmura, "A Method of Calculating the Direct Shortwave Radiation Income of Slopes," Journal of Applied Meteorology, Vol. 7, p. 796-800, 1968.
- Gelb, A., J.F. Kasper, Jr., R.A. Nash, Jr., C.F. Price, and A.A. Sutherland, Jr., Applied Optimal Estimation, The MIT Press, Cambridge, Massachusetts, 1974.

- Georgakakos, K.P., H. Rajaram, and S.G. Li, On Improved Operational Hydrologic Forecasting of Streamflows, Iowa Institute of Hydraulic Research, Report No. 325, Iowa City, Iowa, 1988.
- Gupta, V.K., and S. Sorooshian, "The Automatic Calibration of Conceptual Catchment Models Using Derivative-Based Optimization Algorithms," Water Resources Research, Vol. 21, No. 4, p. 473-485, 1985.
- Hall, D.K., J.L. Foster, and A.T.C. Chang, "Nimbus-7 SMMR Polarization Responses to Snow Depth in the Mid-Western U.S.," Nordic Hydrology, Vol. 15, p. 1-8, 1984.
- Hannaford, J.F., R.L. Hall, and A.J. Brown, "Application of Snow Covered Area to Runoff Forecasting in the Southern Sierra Nevada," Proceedings of Western Snow Conference, p. 56-67, 1979.
- Hino, M., "Runoff Forecasts by Linear Predictive Filter," Journal of Hydraulics, Vol. 96, No. HY3, p. 681-707, 1970.
- Hino, M., "On-Line Prediction of Hydrologic System," Proceedings of the 15th Congress of the International Association for Hydraulic Research, Istanbul, Vol. 4, Ankara, Turkey: State Hydraulics Printing House, p. 121-129, 1973.
- Huber, A.L., "A Comparison of Several Snow Accumulation and Ablation Algorithms Used in Watershed Modeling," Proceedings of Western Snow Conference, Vancouver, Washington, p. 76-88, 1983.
- Huber, A.L., "Water Supply Forecasting in Real-Time," Water Resources Bulletin, Vol. 20, No.2, p. 167-171, 1984.
- Jazwinski, A.H., Stochastic Processes and Filtering Theory, Academic Press, New York, New York, 1970.
- Johnson, E.R., E.L. Peck, and T.N. Keefer, Combining Remotely Sensed and Other Measurements for Hydrologic Areal Averages, NASA Report, NASA-CR-170457, Greenbelt, Maryland, 1982.
- Kalman, R.E., "A New Approach to Linear Filtering and Prediction Problems," Journal of Basic Engineering, Vol. 82D, p. 35-45, 1960.
- Kalman, R.E., and R.S. Bucy, "New Results in Linear Filtering and Prediction Theory," Journal of Basic Engineering, Vol. 83D, p. 95-108, 1961.
- Kitanidis, P.K., and R.L. Bras, "Real-Time Forecasting With a Conceptual Hydrologic Model, 1. Analysis of Uncertainty," Water Resources Research, Vol. 16, No. 6, p. 1025-1033, 1980a.
- Kitanidis, P.K., and R.L. Bras, "Real-Time Forecasting With a Conceptual Hydrologic Model, 2. Applications and Results," Water Resources Research, Vol. 16, No. 6, p. 1034-1044, 1980b.

- Kohler, M.A., "Water Supply Forecasting Developments, 1951-1956," Proceedings of Western Snow Conference, Santa Barbara, California, p. 62-68, 1957.
- Krajewski, W.F., "Cokriging Radar-Rainfall and Rain Gage Data," Journal of Geophysical Research, Vol. 92, No. D8, p. 9571-9580, 1987.
- Kuusisto, E., Snow Accumulation and Snowmelt in Finland, Water Research Institute, National Board of Waters, No. 55, Helsinki, Finland, 1984.
- Larson, L.W., and E.L. Peck, "Accuracy of Precipitation Measurements for Hydrologic Modeling," Water Resources Research, Vol. 10, No. 4, p. 857-863, 1974.
- Lawson, D.W., and S.Y. Shiau, "Data Requirements and Reference Documents for the Sacramento Watershed Modelling System," Inland Waters Directorate, Environment Canada, 1977.
- Leavesley, G.H., "A Mountain Watershed Simulation Model," Proceedings of Modeling of Snow Cover Runoff, U.S. Army Cold Regions Research and Engineering Laboratory, Hanover, New Hampshire, p. 379-386, 1978.
- Lenton, R.L., and I. Rodriguez-Iturbe, "A Multidimensional Model for the Synthesis of Processes of Areal Rainfall Averages," Water Resources Research, Vol. 13, No. 3, p. 605-612, 1977a.
- Lenton, R.L., and I. Rodriguez-Iturbe, "Rainfall Network Systems Analysis: The Optimal Estimation of Total Area Storm Depth," Water Resources Research, Vol. 13, No. 5, p. 825-836, 1977b.
- Lettenmaier, D.P., and S.J. Burges, "Use of State Estimation Techniques in Water Resource System Modeling," Water Resources Bulletin, Vol. 12, No. 1, p. 83-99, 1976.
- Leu, Cheng-Hua, "Evaluation of Spatially-Distributed Snowpack Estimation Using Pattern Recognition," PhD Dissertation, Utah State University Library, Logan, Utah, 1988.
- Linsley, R.K., "A Simple Procedure for the Day-to-Day Forecasting of Runoff from Snowmelt," Transactions American Geophysical Union, Vol. 24, Part 3, p. 62-67, 1943.
- Linsley, R.K., M.A. Kohler, and J.L.H. Paulhus, Hydrology for Engineers, McGraw-Hill, New York, New York, 1975.
- Martinec, J., "Snowmelt-Runoff Model for Streamflow Forecasts," Nordic Hydrology, Vol. 6, p. 145-154, 1975.
- Matheron, G., "The Theory of Regionalized Variables and Its Applications," Cahiers du Centre de Morphologie Mathematique, Ecole des Mines, Fontainebleau, France, 1971.

- McCuen, R.H., and W.M. Snyder, Hydrologic Modeling, Statistical Methods and Applications, Prentice-Hall, Englewood Cliffs, New Jersey, 1986.
- Mejia, J.M., and I. Rodriguez-Iturbe, "On the Synthesis of Random Field Sampling From the Spectrum: An Application to the Generation of Hydrologic Spatial Processes," Water Resources Research, Vol. 10, No. 4, p. 705-711, 1974.
- Mizumura, K., and Chao-Lin Chiu, "Prediction of Combined Snowmelt and Rainfall Runoff," Journal of Hydraulic Engineering, Vol. 111, No. 2, p. 179-193, 1985.
- Monro, J.C., Direct Search Optimization in Mathematical Modeling and a Watershed Model Application, NOAA Technical Memorandum, NWS, HYDRO-12, Silver Spring, Maryland, 1971.
- Morris, and Godfrey, "The European Hydrological System Snow Routine," Proceedings of Modeling of Snow Cover Runoff, U.S. Army Cold Regions Research and Engineering Laboratory, Hanover, New Hampshire, p. 269-278, 1978.
- National Weather Service, "NWS River Forecast System User's Manual," U.S. Dept. of Commerce, NOAA, NWS, Silver Spring, Maryland.
- Nielsen, S.A., and E. Hansen, "Numerical Simulation of the Rainfall-Runoff-Process on a Daily Basis," Nordic Hydrology, Vol. 4, p. 171-190, 1973.
- O'Connell, P.E. (Editor), "Real-Time Hydrological Forecasting and Control," Proceedings 1st International Workshop, Institute of Hydrology, Wallingford, England, 1980.
- O'Connell, P.E., and R.T. Clarke, "Adaptive Hydrological Forecasting - a Review," Hydrological Sciences - Bulletin, Vol. 26, No. 2, p. 179-205, 1981.
- Palmer, P.L., "The SCS Snow Survey Water Supply Forecasting Program: Current Operations and Future Directions," Proceedings of Western Snow Conference, Kalispell, Montana, p. 43-51, 1988.
- Peck, E.L. and J.C. Schaake, "Network Design for Water Supply Forecasting in the West," Water Resources Bulletin, in press.
- Peck, E.L., and M.J. Brown, "An Approach to the Development of Isohyetal Maps for Mountainous Areas," Journal of Geophysical Research, Vol. 67, No. 2, p. 681-694, 1962.
- Peck, E.L., and E.A. Anderson, "Operational Use of Snow Accumulation and Ablation Model in the United States," Presented at the Snow Accumulation and Ablation Model Symposium, Northern Research Basin Symposium-Workshop, Fairbanks, Alaska, 1977.

- Peck, E.L., E.R. Johnson, and T.N. Keefer, Creating a Bridge Between Remote Sensing and Hydrologic Models, NASA Report, NASA-CR-170517, Greenbelt, Maryland, 1983.
- Peterson, N.R., and A.J. Brown, "Accuracy of Snow Measurements," Proceedings of Western Snow Conference, Coronado, California, 1975.
- Quick, M.C., and A. Pipes, "U.B.C. Watershed Model," Hydrological Sciences - Bulletin, Vol. 22, No. 1, p. 153-161, 1977.
- Rango, A., "Progress in Snow Hydrology Remote Sensing Research," IEEE Transactions on Geoscience and Remote Sensing, Vol. GE-24, No. 1, p. 47-53, 1986.
- Ripley, B.D., Spatial Statistics, John Wiley & Sons, New York, New York, 1981.
- Rodriguez-Iturbe, I., and J.M. Mejia, "The Design of Rainfall Networks in Time and Space," Water Resources Research, Vol. 10, No. 4, p. 713-728, 1974a.
- Rodriguez-Iturbe, I. and J.M. Mejia, "On the Transformation of Point Rainfall to Areal Rainfall," Water Resources Research, Vol. 10, No. 4, p. 729-736, 1974b.
- Schaake, J.C., and E.L. Peck, "Analysis of Water Supply Forecast Accuracy," Proceedings of Western Snow Conference, Boulder, Colorado, 1985.
- Schaake, J.C., and E.L. Peck, "Hydrometeorological Network Analysis for Mountainous Areas," NOAA, NWS, Silver Spring, Maryland, 1986.
- Schaefer, G.L., and B.A. Shafer, "A Critical Analysis of Five Years of SNOTEL Performance in the Rocky Mountains," Proceedings of the International Symposium on Hydrometeorology, Denver, Colorado, 1982.
- Shafer, B.A., "SNOTEL, U.S. Dept. of Agriculture," Soil Conservation Service, Portland, Oregon, 1981.
- Sittner, W.T., and K.M. Krouse, Improvement of Hydrologic Simulation by Utilizing Observed Discharge as an Indirect Input/ Computed Hydrograph Adjustment Technique - CHAT, NOAA Technical Memorandum, NWS, HYDRO-38, Silver Spring, Maryland, 1979.
- Smith, J.A., and A.F. Karr, "Parameter Estimation for a Model of Space-Time Rainfall," Water Resources Research, Vol. 21, No. 8, p. 1251-1257, 1985.
- State of California, Snow Survey Measurements Through 1970, Department of Water Resources, Bulletin No. 129-70, 1971.

- Speers, D., D. Kuehl, and V. Schermerhorn, "Development of the Operational Snow Band SSARR Model," Proceedings of Modeling of Snow Cover Runoff, U.S. Army Cold Regions Research and Engineering Laboratory, Hanover, New Hampshire, p. 369-378, 1978.
- Sugawara, M., I. Watanabe, E. Ozaki, and Y. Katsuyama, Tank Model with Snow Component, Research Notes of the National Research Center for Disaster Prevention, No. 65, National Research Center for Disaster Prevention, Science and Technology Agency, Japan, 1984.
- Szollosi-Nagy, A., "An Adaptive Identification and Prediction Algorithm for the Real-Time Forecasting of Hydrologic Time Series," Hydrological Science Bulletin, Vol. 21, No. 3, p. 163-176, 1976.
- Tabios III, G.Q., and J.D. Salas, "A Comparative Analysis of Techniques for Spatial Interpolation of Precipitation," Water Resources Bulletin, Vol. 21, No. 3, p. 365-380, 1985.
- Tangborn, W.V., "A Model to Predict Short-Term Snowmelt Runoff Using Synoptic Observations of Streamflow, Temperature, and Precipitation," Proceedings of Modeling of Snow Cover Runoff, U.S. Army Cold Regions Research and Engineering Laboratory, Hanover, New Hampshire, p. 414-426, 1978.
- Thiessen, A.H., "Precipitation Averages for Large Areas," Monthly Weather Review, Vol. 39, No. 7, p. 1082-1084, 1911.
- Todini, E., and D. Bouillot, "A Rainfall-Runoff Kalman Filter Model," In: System Simulation in Water Resources, G.C. Vansteenkiste, ed., Amsterdam: North Holland, 1975.
- Turcan, J., "Empirical-Regressive Forecasting Runoff Model," Proceedings of Conference VUVH, Bratislava, 1981.
- Twedt, T.M., J.C. Schaake, Jr., and E.L. Peck, "National Weather Service Extended Streamflow Prediction," Proceedings of Western Snow Conference, Albuquerque, New Mexico, 1977.
- U.S. Army Corps of Engineers, "Program Description and User Manual for SSARR Model," Portland, Oregon, 1972.
- Willen, D.W., C.A. Shumway, and J.E. Reid, "Simulation of Daily Snow Water Equivalent and Melt," Proceedings of Western Snow Conference, Billings, Montana, p. 1-8, 1971.
- Wood, E.F., and A. Szollosi-Nagy, "An Adaptive Algorithm for Analyzing Short-Term Structural and Parameter Changes in Hydrologic Prediction Models," Water Resources Research, Vol. 14, No. 4, p. 577-581, 1978.

World Meteorological Organization, Intercomparison of Conceptual Models Used in Operational Hydrologic Forecasting, WMO, Operational Hydrology Report No. 7, Geneva, Switzerland, 1975.

World Meteorological Organization, Intercomparison of Models of Snowmelt Runoff, WMO, Operational Hydrology Report No. 23, Geneva, Switzerland, 1986.

- NWS 18 Joint Probability Method of Tide Frequency Analysis Applied to Apalachicola Bay and St. George Sound, Florida. Francis P. Ho and Vance A. Myers, November 1975, 43 p. (PB-251123)
- NWS 19 A Point Energy and Mass Balance Model of a Snow Cover. Eric Anderson, February 1976, 150 p. (PB-254651)
- NWS 20 Precipitable Water Over the United States, Volume 1: Monthly Means. George A. Lott, November 1976, 173 p. (PB-264219)
- NWS 20 Precipitable Water Over the United States, Volume II: Semimonthly Maxima. Francis P. Ho and John T. Riedel, July 1979, 359 p. (PB-300870)
- NWS 21 Interduration Precipitation Relations for Storms - Southeast States. Ralph H. Frederick, March 1979, 66 p. (PB-297192)
- NWS 22 The Nested Grid Model. Norman A. Phillips, April 1979, 89 p. (PB-299046)
- NWS 23 Meteorological Criteria for Standard Project Hurricane and Probable Maximum Hurricane and Probable Maximum Hurricane Windfields, Gulf and East Coasts of the United States. Richard W. Schwerdt, Francis P. Ho, and Roger R. Watkins, September 1979, 348 p. (PB-80 117997)
- NWS 24 A Methodology for Point-to-Area Rainfall Frequency Ratios. Vance A. Myers and Raymond M. Zehr, February 1980, 180 p. (PB80 180102)
- NWS 25 Comparison of Generalized Estimates of Probable Maximum Precipitation With Greatest Observed Rainfalls. John T. Riedel and Louis C. Schreiner, March 1980, 75 p. (PB80 191463)
- NWS 26 Frequency and Motion of Atlantic Tropical Cyclones. Charles J. Neumann and Michael J. Pryslak, March 1981, 64 p. (PB81 247256)
- NWS 27 Interduration Precipitation Relations for Storms-- Western United States. Ralph H. Frederick, John F. Miller, Francis P. Richards, and Richard W. Schwerdt, September 1981, 158 p. (PB82 230517)
- NWS 28 GEM: A Statistical Weather Forecasting Procedure. Robert G. Miller, November 1981, 103 p.
- NWS 29 Analysis of Elements of the Marine Environment for the Atlantic Remote Sensing Land Ocean Experiment (ARSLOE) -- An Atlas for October 22 through October 27, 1980. Lawrence D. Burroughs, May 1982, 116 p. (PB82 251281)
- NWS 30 The NMC Spectral Model. Joseph G. Sela, May 1982, 38 p. (PB83 115 113)
- NWS 31 A Monthly Averaged Climatology of Sea Surface Temperature. Richard W. Reynolds, June 1982, 37 p. (PB83 115469)
- NWS 32 Pertinent Meteorological and Hurricane Tide Data for Hurricane Carla. Francis P. Ho and John F. Miller, August 1982, 111 p. (PB83 118240)
- NWS 33 Evaporation Atlas for the Contiguous 48 United States. Richard K. Farnsworth, Edwin S. Thompson, and Eugene L. Peck, June 1982, 26 p.
- NWS 34 Mean Monthly, Seasonal, and Annual Pan Evaporation for the United States. Richard K. Farnsworth and Edwin S. Thompson, December 1982, 85 p. (PB83 161729)
- NWS 35 Pertinent Meteorological Data for Hurricane Allen of 1980. Francis P. Ho and John F. Miller, September 1983, 73 p. (PB 272 112)
- NWS 36 Water Available for Runoff for 1 to 15 Days Duration and Return Periods of 2 to 100 Years for Selected Agricultural Regions in the Northwest United States. Frank P. Richards, John F. Miller, Edward A. Zurndorfer, and Norma S. Foat, April 1983, 59 p. (PB84 120591)
- NWS 37 The National Weather Service Hurricane Probability Program. Robert C. Sheets, April 1984, 70 p. (PB84 182757)
- NWS 38 Hurricane Climatology for the Atlantic and Gulf Coasts of the United States. Francis P. Ho, James C. Su, Karen L. Hanevich, Rebecca J. Smith, and Frank P. Richards, April 1987, 195 p.
- NWS 39 Monthly Relative Frequencies of Precipitation for the United States for 6-, 12-, and 24-H Periods. John S. Jensenius, Jr., and Mary C. Erickson, September 1987, 262 p.
- NWS 40 An Eight-Year Climatology of Meteorological and SBUV Ozone Data. Ronald M. Nagatani, Alvin J. Miller, Keith W. Johnson, and Melvyn E. Gelman. March 1988, 123 pp.

(Continued from last page)

NWS 41 A Precipitation Climatology of Five-Day Sequences. Edward S. Epstein. October 1988, 160 pp.

NWS 42 Multilevel Calibration Strategy for Complex Hydrologic Simulation Models. Larry E. Brazil, February 1989, 196 pp.

NWS 43 A Methodology for Updating a Conceptual Snow Model With Snow Measurements. Gerald N. Day, March 1990, 133 pp.

NOAA SCIENTIFIC AND TECHNICAL PUBLICATIONS

The National Oceanic and Atmospheric Administration was established as part of the Department of Commerce on October 3, 1970. The Mission responsibilities of NOAA are to assess the socioeconomic impact of natural and technological changes in the environment and to monitor and predict the state of the solid Earth, the oceans and their living resources, the atmosphere, and the space environment of the Earth.

The major components of NOAA regularly produce various types of scientific and technical information in the following kinds of publications:

PROFESSIONAL PAPERS - Important definitive research results, major techniques, and special investigations.

CONTRACT AND GRANT REPORTS - Reports prepared by contractors or grantees under NOAA sponsorship.

ATLAS - Presentation of analyzed data generally in the form of maps showing distribution of rainfall, chemical and physical conditions of oceans and atmosphere, distribution of fishes and marine mammals, ionospheric conditions, etc.

TECHNICAL SERVICE PUBLICATIONS - Reports containing data, observations, instructions, etc. A partial listing includes data serials; prediction and outlook periodicals; technical manuals, training papers, planning reports, and information serials; and miscellaneous technical publications.

TECHNICAL REPORTS - Journal quality with extensive details, mathematical developments, or data listings.

TECHNICAL MEMORANDUMS - Reports of preliminary, partial, or negative research or technology results, interim instructions, and the like.

